UNIVERSITÀ DEGLI STUDI DI MILANO

Suola di Dottorato in Fisica, Astrofisica e Fisica Applicata
Dipartimento di Fisica
Corso di Dottorato in Fisica, Astrofisica e Fisica Applicata
Ciclo XXV

Cosmological observations and backreaction

Supervisore: **Prof. Davide MAINO**
Co-supervisore: **Dott. Elisabetta MAJEROTTO**
Coordinatore: **Prof. Marco BERSANELLI**

Tesi di Dottorato di:
Matteo Chiesa

Anno accademico: 2013/2014

Commission of the final examination:

External Referee: Prof. Sabino MATARRESE

External Member: Prof. Stefano BORGANI

External Member: Prof. Will PERCIVAL

Final examination:

21^{st} March 2014
Universitá degli Studi di Milano, Dipartimento di Fisica, Milano, Italy

PACS:98.80.Jk
MIUR Sectors: FIS/05, FIS/02

...Il cielo stellato sopra di me,
la legge morale dentro di me.
(Immanuel Kant)

Contents

Introduction

The Universe on large scales appears homogeneous and isotropic. General Relativity provides a simple and clear description of the Universe in terms of a homogeneous and isotropic spacetime metric. This Friedmann-Lemaitre-Robertson-Walker geometry solves the field equations under general assumptions of maximal simmetry. The metric is non-static and its non-trivial dynamics is sourced by the energy content of the Universe. Since this model accounts for many observed phenomena and allows to use perturbation theory to describe small deviations from this background cosmology, one of the most striking challenges of current research is to clarify the actual energy content of the Universe in terms of matter, radiation and other cosmological fluids which enter the stress-energy tensor of the FLRW model. The apparent accelerated expansion observed from SN Ia [1, 2] contrasts such a simple view of our Universe: the deceleration parameter must be always positive for ordinary types of matter and radiation, so a new negative pressure fluid is needed to explain the acceleration. This fluid, called Dark Energy, should account for about 70% of the whole energy content of the Universe. (see for example [3, 4] and references therein)

Many different models have been built to describe the physical features of Dark Energy (see for example [11, 12, 13] for an useful review). The simplest one is based on a cosmological constant which enters Einstein equations, while other models assume some exotic new energy content such as a scalar field called quintessence. The apparent acceleration could also be described by a modification of the fundamental laws of physics on large scales such as general deviations on large scales of gravity. The debate between Dark Energy and Modified Gravity models as the best way of understanding the large scale features of the Universe is still open.

Recently Buchert [26] proposed to describe the cosmic acceleration as an effect of the backreaction of the local inhomogeneities. He suggested that the procedure of averaging the local inhomogeneties over finite spatial domains could explain the apparent accelerated expansion. Indeed the smoothing over a finite domain and its global dynamics are non-commutative operations which modify the Friedmann equations, allowing in principle for an apparent accelerated expasion without the need of postulating any new cosmological fluid (see [32] for an overview).

Models of backreaction were first constructed in the context of Newtonian gravity [26, 27]. Generalizations including a fully relativistic theory followed [28, 30, 31], focusing on the interpretation of the averaging problem in the context of General Relativity. In these models the spacetime metric plays a crucial role: the full metric which describes the non linear inhomogeneities and their gravitational effects is unknown, requiring to make strong assumptions on its form. On the other hand a perturbative approach could be used up to linear scales, starting from a homogeneous FLRW background.

Larena et al. [34] proposed a way of testing a backreaction model based on a template metric whose constant time slices are FLRW-like. The FLRW curvature parameter is assumed to be time-dependent in order to encode the effect of backreaction. Under these assumptions, in [34] the authors perform a likelihood analysis of the scaling solution to the backreaction problem, providing likelihood confidence contours of the present matter density parameter of the Universe ($\Omega_m^{D_0}$) and the scaling exponent n. The likelihood function is built from supernovae of the SuperNova Legacy Survey (SNLS) [9] and CMB data from the three-year release of the Wilkinson Microwave Anysotropy Probe ($WMAP$) [41] and it is compared to a standard FLRW model with a quintessence field of constant equation of state modelling Dark Energy.

Here we assume the same background metric and test the backreaction model upgrading data sets from actual measurements. We also introduce a new testing technique based on angular diameter distances measured from SZ cluster catalogs. We derive the theoretical angular diameter distance for each cluster of the catalog of Bonamente et al. [24] and then perform a likelihood analysis comparing the theoretical value to the measured one. We look at constraints in the parameter plane $\Omega_m^{D_0} - w$, providing likelihood contours for the Dark Energy parameter w which is associated to the scaling exponent n as it is proposed in [34].

We also derive the theoretical predictions of the distance modulus from the template metric proposed in [34] and compare them to two SN Ia data catalogs, providing confidence contours for $\Omega_m^{D_0} - w$. We first use the SuperNova Legacy Survey (SNLS) catalog, obtaining results consistent with [34] and then the data release from the Supernova Cosmology Project *Union2.1* presented in [7].

We finally make predictions from different sets of CMB data provided by the nine-year release of the Wilkinson Microwave Anisotropy Probe ($WMAP$) [43] and by the *Planck* Mission [44]. We focus on contours given by the CMB shift parameters and separately by the position of the peaks and dips of the TT-power spectrum of the CMB. We analyzed the data published in the section 4.6.1 of [43], which provides a direct measurement of the shift parameters l_A, R and z^*. Then we fit the TT-power spectrum of the CMB and found the position of the first three peaks and the first dip. We separately fit the $WMAP$ data and the *Planck* ones, giving two different sets of positions.

We show constraints separately and then we compute the joint likelihood both for a standard flat FRW Universe filled with Dark Energy of constant equation of state and for the the backreacted model based on Buchert's averaging scheme. We find that SN Ia data confirm the prediction shown in Fig.2 of [34] of a slightly denser Universe if backreaction is considered, but recent CMB data alone seem to suggest the opposite behaviour. The apparent inconsistency has been already noticed in [53] as a consequence of the new relation among the scale factor and the redshift due to the template metric: the geodesic equation is slightly changed since the curvature parameter is time dependent and consequently the path of photons is modified with respect to the standard FRW Universe. In [53] no further detail is explored. We try to go on studying tyhe incosistency in terms of how the theoretical modelling of CMB mathces with the backreaction scheme. We find that the incosistency may be explained in terms of rescaling boundary conditions today on the size of the Universe, but the theoretical approach encounters difficulties when checked against data since relevant parameter like the redshift of recombination are computed by fitting formulae which were constructed on assuming standard cosmology with standard boundary conditions.

For completeness we perform the full likelihood analysis discussing how the basic definitions of CMB observables, like the shift parameters or the fundamental multipole,should change and we argue that ignoring the apparent incosistency is not relevant if old data sets are used, since uncertainties are too big. On the contrary we find that more precise current data are able to cast light on this quite subtle problem.

Chapter 1

The homogeneous Universe

The Universe is homogeneous. This sentence is a clear example of the logical path often followed in Physics. We assume some simplifying hypothesis in order to deal with complicated phenomena. In Physics complex topics must be reduced to simpler schemes we can treat with mathematical tools. What topic is harder than the whole Universe? How can we apply physical methods to the Universe? In principle Physics itself is the reduction of the Universe to simpler sectors of human knowledge.

Making assumptions can be quite expensive: any hypothesis is also a simplification. So, making assumptions means loosing some aspects of Nature and choosing what we can describe with mathematics and what we are not able to understand completely.

The homogeneity explains clearly this fascinating aspect of the scientific method. We can raise our eyes, look at the sky above us and see the contrast between the vacuum around us the Earth under us... the Universe does not seem homogeneous. On the other hand, if we look at very large scales, where galaxies can be treated as mathematical points, their distribution suggests an intrinsic homogeneity of the mass density in the observable Universe.

Here we sum up the basic tools that are used to deal with the *zero order* description of the observable Universe, which is based on homogeneity, isotropy and equilibrium. Under these preliminary assumptions mathematics provides a basic scheme which is known as the *Standard Model of Cosmology*. Topics reviewed here are treated in a wide litera-

ture. Throughout our discussion we follow [58, 59, 63, 60].

1.1 The Cosmological Principle

The Cosmological Principle is the basis of the current Standard Model of Cosmology. It sums up many assumptions on the basic symmetries underlying our description of the Universe and our conception of space.

1.1.1 Homogeneity

Assuming that the Universe is homogeneous on large scales means that the mass density field ρ does not depend on the space coordinate $\vec{x}$. Usually we write

$$\rho(\vec{x}, t) \equiv \rho(t) \tag{1.1}$$

but this statement is only the last consequence of homogeneity. Homogeneity has far deep consequences that we remember here.

Let us define a function $f(\vec{x})$ of the $3D$ vector $\vec{x}$. If we apply a global traslation (driven by a fixed vector $\vec{a}$) of the reference frame, we can look how the function $f(\vec{x})$ changes

$$f(\vec{x}) \to f(\vec{y}) = f(\vec{x} + \vec{a}) = f(\vec{x}) + \vec{a} \cdot \vec{\nabla} f(\vec{x}) + O(a^2) \tag{1.2}$$

the last equality following from the Taylor expansion under the hypothesis that the traslation vector $\vec{a}$ is small.

The first equality holds for any vector $\vec{a}$, the second one holds only for an *infinitesimal* traslation. If the function $f(\vec{x})$ is describing a scalar quantity, it gives a real (or a complex) number as its output. We can simply state that the space is homogeneous in the point $\vec{x}$ if our measurements of a scalar quantity do not change if we slightly move from $\vec{x}$ to $\vec{x} + \vec{a}$, for **any** arbitrarly small vector $\vec{a}$. In other words the space is homogeneous if scalar functions are invariant under infinitesimal traslations.

It is easy to demonstrate that if $f(\vec{x})$ is invariant under infinitesimal traslations, then

$$f(\vec{x}) = f(\vec{x}) + \vec{a} \cdot \vec{\nabla} f(\vec{x}) + O(a^2) \tag{1.3}$$

must hold $\forall \vec{a}$, so

$$\vec{a} \cdot \vec{\nabla} f(\vec{x}) + O(a^2) = 0 \tag{1.4}$$

and the gradient must be orthogonal to the whole space, forcing $\vec{\nabla} f(\vec{x}) = 0$. This shows that homogeneity requires that scalars must be constant in any sufficently small neighbourhood of $\vec{x}$.

Local homogeneity has another longstanding consequence. Let us suppose that the scalar function we are looking at is the Lagrangian describing some local physical process. Under infinitesimal traslations the Lagrangian changes as

$$L(x) \to L(x) + \delta L \tag{1.5}$$

where δL is $O(\vec{a})$. Since the Lagrangian is unphysical, we are not interested in forcing $\delta L = 0$, because we cannot measure the value assumed by the Lagrangian, but we are only interested in understanding how δL changes the Euler-Lagrange equations, which drive the physics of the process. If the space is homogeneous δL should enter the Euler-Lagrange equations without changing the physics of the process.

In order to understand what happens we recall the principle of least action, which states that the classical action is stationary along the trajectories given by the forces involved in any physical process. So

$$\delta S = \delta \int L(q, \dot{q}) dt = 0 \tag{1.6}$$

for a given Lagrangian of the generalized coordinates q and velocities $\dot{q}$. Expanding the variation

$$\int_{t_i}^{t_f} \left(\frac{\partial L}{\partial \dot{q}} \delta \dot{q} + \frac{\partial L}{\partial q} \delta q \right) dt = 0 \tag{1.7}$$

in terms of an infinitesimal coordinate shift δq, the integration of the first term by parts gives

$$\int_{t_i}^{t_f} \frac{d}{dt} \left(\frac{\partial L}{\partial \dot{q}} \delta q \right) dt + \int_{t_i}^{t_f} \left(\frac{\partial L}{\partial q} - \frac{d}{dt} \frac{\partial L}{\partial \dot{q}} \right) \delta q dt = 0 \tag{1.8}$$

The second term is trivially annihilated by the Euler-Lagrange equations, while the first term is a surface term. We can ensure that the surface term vanishes imposing

$$\frac{d}{dt}\left(\frac{\partial L}{\partial \dot{q}}\delta q\right) = 0 \tag{1.9}$$

that is a conservation law. If the variation of the Lagrangian is given by our infinitesimal traslation, the conserved quantity is the standard conjugate momentum to the generalized coordinate

$$\vec{p} = \frac{\partial L}{\partial \vec{q}} \tag{1.10}$$

since $\delta\vec{q} = \vec{a}$ is constant. This is one of the simplest application of Noether's Theorem, stating that the invariance of the Lagrangian under transformations of a given continuous group implies a conservation law. In our case homogeneity is linked to the invariance under a very specific class of coordinate transformations and is treated as a fundamental symmetry of space whose main consequence is the conservation of the linear momentum. Finally, if the space is homogeneous in every point, then scalars do not depend on the position vector and the linear momentum is conserved along the trajectories follwed by partcles, whatever generalized coordinate frame we choose.

1.1.2 Isotropy

Isotropy can be treated in the same way and has important consequences too. Intuitively space is isotropic around a given point $\vec{x}_0$ if there is no way of choosing a preferred direction in space. In other words physical phenomena are always the same whatever their orientation in space is. If we are fixed in $\vec{x}_0$, *looking around us without finding any preferred direction* means that physical observables are invariant under rotations centered in $\vec{x}_0$, reagardless of the direction $\vec{n}$ of the rotation axis.

It is well known that the transformation

$$\vec{x} \to R\vec{x} \tag{1.11}$$

defines a general rotation centered in $\vec{x} = 0$ if and only if the matrix R is orthogonal. The matrix R can be expanded in power series of infinitesimal

rotations around the coordinate axes, using the exponential map between the rotation group and the corresponding Lie algebra. The generators are the three components of the angular momentum, referred to $\vec{x} = 0$. In general, for any rotation $R(\alpha, \vec{n})$ of angle α around the direction $\vec{n}$ we can write

$$R(\alpha, \vec{n}) = e^{i\alpha\vec{n}\cdot\vec{L}} \tag{1.12}$$

(the i factor is conventional) and up to first order in α, it follows

$$R(\alpha, \vec{n}) = 1 + i\alpha\vec{n} \cdot \vec{L} + O(\alpha^2) \tag{1.13}$$

The angular momentum should be understood as a vector of linear operators. This simply implies that a scalar function $f(\vec{x})$ is invariant under rotations if

$$f(\vec{x}) = f(\vec{Rx}) \tag{1.14}$$

which requires to write the small vector

$$\delta\vec{x} = (R(\alpha, \vec{n}) - 1)\vec{x} \tag{1.15}$$

in a suitable way, rememberring that the operator $R(\alpha, \vec{n}) - 1$ is written in terms of its representation matrices. It is well known that Eq. 1.14 is non-trivial, since the function $f(\vec{x})$ may transform in different ways. The most general transformation rule ensures that

$$f(R\vec{x}) = D(R)^\dagger f(\vec{x}) D(R) \tag{1.16}$$

where $D(R)$ is the representation matrix of the rotation. Expanding $D(R)$ accordingly to Eq. 1.13 we find

$$(1 + i\alpha D(\vec{n} \cdot \vec{L}))^\dagger f(1 + i\alpha D(\vec{n} \cdot \vec{L})) = f \tag{1.17}$$

where $D(\vec{n}\cdot\vec{L})$ is the representation matrix of the projection of the angular momentum on the direction $\vec{n}$. Since the angular momentum is observable $D(\vec{n}\cdot\vec{L})$ must be self-adjoint and the invariance condition becomes the well known *commutation rule*

$$\alpha[f, D(\vec{n} \cdot \vec{L})] = 0 \tag{1.18}$$

up to first order in α. We can simplify this condition assuming that $\vec{n}$ is the z-axes and then the problem of finding functions commuting with the angular momentum is reduced to the simpler problem of diagonalizing $\vec{L}$. The diagonalization is usually carried out in terms of the squared modulus L^2 and the z-component of the angular momentum L_z, leading to the well known result that the eigenfunctions are spherical harmonics.

Finally the application of Noether's theorem provides that the invariance under rotations of the lagrangian implies the conservation law of the angular momentum, because it is the infinitesimal generator of the rotation group.

We are interested in showing how homogeneity and isotropy around a given point x_0 combine in the Cosmological Principle. Preliminarly we can demonstrate

Global isotropy 1.1.1 *If the space is isotropic in a given point x_0 and homogeneous, then it is isotropic in every point.*

Proof. Let us assume that $f(x)$ is invariant under traslations and rotations around x_0. We will show that $f(x)$ is invariant under rotations around any other point too. We need to make a composition of a rotation around x_0 and a traslation. Rotations and traslations are elements of the Euclidean group and we can derive the combined action of their generators from the commutation rules

$$[P_i, P_j] = 0 \tag{1.19}$$
$$[L_i, P_j] = i\epsilon_{ijk} P_k \tag{1.20}$$
$$[L_i, L_j] = i\epsilon_{ijk} L_k \tag{1.21}$$

where P_i is the generator of the traslation along the i-th axis and L_j is the component of the angular momentum around the j-th one. By isotropy and homogeneity $[f, L_i] = 0$ and $[f, P_i] = 0$ must hold. We are interested in computing $[f, L_i P_j]$ because $L_i P_j$ defines an infintesimal rotation after an infinitesimal traslation. Then

$$[f, L_i P_j] = L_i [f, P_j] + [f, P_i] P_j = 0 \tag{1.22}$$

The second equality follows from isotropy and homogeneity.

Showing that $[f, P_j L_i] = 0$ is trivial and follows directly from the commuting P_j and L_i.

Homogeneity and isotropy are basic features of the Standard Model of Cosmology and enter the description of the Universe giving strict prescriptions on the symmetries spacetime must exihibit.

1.1.3 Basic principles

Since it is clear that the mass density is not homogeneous on small scales, the features we assume in constructing the Standard Model are summed up in a *working prescription* that is called **Cosmological Principle** for historical reasons.

Cosmological Principle 1.1.1 *At sufficently large scales the Universe is homogeneous and isotropic.*

It is clear that the problem underlying the application of the Cosmological Principle is the precise definition of the scales that can be considered sufficently large for treating the mass density as constant. From prime principles we should neither treat the mass field as a continuous medium, since matter is clustered and a smooth differentiable function do not work well for representing a clumpy structure. From this simple considerations follows that the first requirement for treating the universe as homogeneous is considering galaxies as mathematical points, so we can assume that scales larger than 100 Mpc fit the general idea underlying the Cosmological Principle. On smaller scale the working prescription begins to fail and inhomogeneities of the density require to follow new assumptions.

The Cosmological Principle has a phylosophical meaning too. It is considered as an independent formulation of the Copernican Principle in the context of Cosmology. The Copernican principle states that no observer is preferred and laws of Physics are the same whatever point in the Universe we choose for checking them with observations. Although the Copernican Principle seems very similar to the Cosmological Principle, it add a completely new logical element to our research related to how the scientific method applies in Cosmology. Indeed the scientific method requires that any theory should be checked against experience and any experiment

should be reproduced independently, changing place, time, people... This important prescription is intrinsically violated by cosmological observations, since we are always looking at the same Universe from the same point of view. The well known *fair sample hypothesis* solves the problem of extracting cosmological information from observations of a smaller volume of the Universe, but changing the volume we are looking at does not mean *changing the Universe* or changing the point of view. Since we are not able to deal with the problem of looking at many Universes, which would be also a hard logical problem, we relax the prescriptions of the scientific method only on this topic, but we need to specify a preliminary hypothesis that clearly states that we are not able to change the observation point too. This logical topic is independent of stating that at sufficently large scales we can treat the Universe as homogeneous and isotropic. But we should be careful that the Copernican Principle ensures only that we should agree about physical laws with someone living on a far away galaxy, it does not remove the dependence of our point of view on being exactly in the Milky Way. In other words, we cannot forget that the realization of the Universe we are looking at is exactly as it is, containig our point of view exactly here and not elsewhere. This aspect defines quite well the boundary of the logical path underlying the application of the scientific method to Cosmology. The Copernican and the Cosmological Principles give us the working prescriptions, provided that they could be limited by an Antropic view of Physics.

1.2 Friedmann-Robertson-Walker metric

Although gravity is very weak, it is overwhelming in the Universe. If we measure the relative intensity of known forces comparing their coupling constants, we will find a well defined hierarchy

$$\alpha_{strong} \sim 1 \tag{1.23}$$

$$\alpha_{em} \sim \frac{1}{137} \tag{1.24}$$

$$\alpha_{weak} \sim 10^{-13} \tag{1.25}$$

$$\alpha_{gravity} \sim 10^{-38} \tag{1.26}$$

Gravitational force is by far the weakest, but galaxies, stars and astrophysical phenomena are often driven by gravity alone.

The Equivalence Principle underlying our present view of gravity allows for a metric description of the gravitational field. General Relativity has been constructed on such a powerful tool and provides highly non linear field equations linking the metric to the energy content of spacetime itself. We are dealing with two independent aspects of the description of the Universe. We can describe the action of gravity by assigning a metric tensor to spacetime, whose curvature provides the paths of freely falling observers. Then, we can give a link between the form of the metric and the mass-energy content of spacetime by solving Einstein equations. The former aspect is independent of the latter and this independence has suggested many *Modified Gravity* models in recent times based on metric theories supporting modified Einstein equations.

1.2.1 Isotropic observers

We are interested in finding a general form for the metric of the Universe. We assume that the Universe is represented by a $4D$ Riemaniann manifold, which exhibits symmetries related to our simplifying assumptions of homogeneity and isotropy. We remember that a n dimensional manifold is a set M *which locally looks like* $\mathbf{R}^n$. Looking like $\mathbf{R}^n$ means that we are able to find a maximal atlas for M. An atlas is a collection $A(U_\alpha, \phi_\alpha)$ of C^∞ invertible maps ϕ_α from open domains $U_\alpha \in M$ to open sets in $\mathbf{R}^n$, covering M. The domains U_α are linked smoothly and the maps ϕ_α and ϕ_β are compatible. In other words

1. $\bigcup_\alpha U_\alpha = M$
2. $\forall \alpha, \beta \quad U_\alpha \cap U_\beta \to \phi_\alpha \circ \phi_\beta^{-1}(\phi_\alpha(U_\alpha) \circ \phi_\beta(U_\beta)) = \phi_\beta(U_\alpha \cap U_\beta)$

The manifold is Riemaniann if we can define a point dependent 2-form $g_{\mu\nu}(x)$ which defines the inner product of two arbitrary vectors of the tangent space $T_p(M)$ in the point p. It is usually called *metric tensor*, because it is involved in computing distances upon the manifold. The elementary distance is written as

$$ds^2 = g_{\mu\nu} dx^\mu dx^\nu \tag{1.27}$$

and it takes a simpler form if $g_{\mu\nu}$ exihibits some symmetries. First of all, we can syncronize clocks, setting g_{00} to a constant value. We arbitrarly choose the convention $g_{00} = -1$. Since the manifold is describing the Universe, the metric tensor is Minkoskian and must have an odd number of negative eigenvalues. We arbitrarly set the time coordinate corresponding to the negative eigenvalue and the space coordinates to the positive ones. Then we add symmetries. The spacetime must represent an homogeneous and isotropic 3D space, but clearly the whole metric do not represent a four dimensional homogeneous and isotropic spacetime, since the time coordinate clearly sets a preferred direction.

So, let us assume that an isotropic observer exists. The isotropic observer follows a worldline in the spacetime and at each given time it must see an isotropic space. This immediately gives a strong relation on the metric: if isotropic observer are fixed in space , than the tangent τ^μ to their worldline must be orthogonal to the constant-time space slices, because if it were not, then the projection of τ^μ on the slice selects a preferred direction in space, violating isotropy. This simply proves that homogeneous space slices must be always orthogonal to the worldlines of isotropic observers. If isotropic observers are fixed in space, their four-velocity must be $u^\mu = (1, 0, 0, 0)$, and then the metric must satisfy

$$g_{0i} = g_{i0} = 0 \tag{1.28}$$

in order to annihilate the projection of u^μ onto any space slice. This choice of coordinates is well known and we usually refer to them as comoving coordinates.

1.2.2 Maximal symmetry

Up to now we used homogeneity and isotropy for simplifying the general form of the metric without giving a precise definition.

Homogeneity 1.2.1 *A space (M, g) defined by a manifold M with given metric tensor $g_{\mu\nu}$ is called* ***homogeneous*** *if a one-parameter family of space-like hyper-surfaces Σ_t that foliate spacetime exists such that $\forall t$, chosen two arbitrary points $p, q \in \Sigma_t$, an isometry ϕ_t of $g_{\mu\nu}$ exists satisfying $\phi_t(p) = q$.*

This definition remembers invariance under traslations, since we can look at the isometry ϕ_t as a traslation on a non flat space.

The definition of isotropic spaces is a little bit harder:

Isotropy 1.2.1 *A space (M, g) defined by a manifold M with given metric tensor $g_{\mu\nu}$ is* ***isotropic*** *about a point p if there is a congruence of time-like geodesics through p with tangents τ such that $\forall v_1, v_2$ orthogonal to τ an isometry ψ exists satisfying $\psi(v_1) = v_2$.*

This definition states that the observer in p can freely rotate space vectors among one another, which corresponds to a generalization of rotational invariance to curved spaces.

Any isometry acts on the metric leaving the metric tensor invariant by definition

$$\phi_t g = g \tag{1.29}$$

which corresponds to the annihilation of the Lie derivative of the metric

$$L_V g_{\mu\nu} = 0 \tag{1.30}$$

along the direction defined by the vector V which infinitesimally generates ϕ. The vector V is called *Killing vector* and it satisfies

$$\nabla_\mu V_\nu + \nabla_\nu V_\mu = 0 \tag{1.31}$$

where the covariant derivative operator ∇_μ generalizes the standard derivative to

$$\nabla_\mu V_\nu = \partial_\mu V_\nu - \Gamma^\alpha_{\mu\nu} V_\alpha \tag{1.32}$$

involving the Christoffel's symbols $\Gamma^\alpha_{\mu\nu}$. The symbols are not tensors, because they do not covariantly transform under coordinate transformations, but define a connection on the spacetime. In General Relativity the connection is usually torsion-free (Levi-Civita connection)

$$\Gamma^\alpha_{\mu\nu} = \Gamma^\alpha_{\nu\mu} \tag{1.33}$$

because non-null torsions have longstanding consequences in how particles of different spin couple to gravity. The Γs can be written in terms of standard derivatives of the metric:

$$\Gamma^{\alpha}_{\mu\nu} = \frac{1}{2} g^{\alpha\beta}(\partial_\mu g_{\alpha\nu} + \partial_\nu g_{\mu\alpha} - \partial_\alpha g_{\mu\nu}) \tag{1.34}$$

Any space of dimension n having exactly $n(n+1)/2$ Killing vectors is said *maximally symmetric*. The isometry group of the constant-time hypersurfaces must be the Euclidean group E^3, which has exactly 6 generators, corresponding to three independent traslations and three independent rotations. Since the constant-time hypersurfaces are three-dimensional and have exactly 6 Killing vectors, then they are maximally symmetric subspaces of the whole spacetime.

So, the space part of the line element

$$ds^2 = -dt^2 + ds_s^2 = -dt^2 + g_{ij}(t,u)du^i du^j \tag{1.35}$$

must be rewritten in a suitable way. Invariance under rotations suggests to use spherical coordinates instead of standard cartesian ones. For the Minkowski spacetime we can write

$$ds_M^2 = \eta_{\mu\nu} dx^\mu dx^\nu = -dt^2 + dr^2 + r^2 d\Omega^2 \tag{1.36}$$

where the last equality holds in spherical coordinates. $d\Omega^2$ is the spherical line element on the 2-sphere S^2 and is defined as

$$d\Omega^2 = d\theta^2 + \sin^2(\theta) d\phi^2 \tag{1.37}$$

We have written the metric of the homogeneous and isotropic Universe rememberring that our metric is block-diagonal, since the time coordinate is not mixed with space coordinates. Then the most general ansatz for the metric is

$$ds^2 = -dt^2 + a(t)^2 \gamma_{ij}(u) du^i du^j \tag{1.38}$$

provided that γ_{ij} is the metric of a static maximally symmetric space invariant under the Euclidean group. The structure of the line element shows that the space slices are static three-dimensional spaces, while the whole four-dimensional manifold is neither static nor stationary. The free

function $a(t)$ is the scale factor and shows that the space slices are dynamical objects. Since it multiplies distances on a given space slice, it gives an estimate of the size of the space slice itself. If the scale factor is non-constant, space slices have a non trivial dynamics and change their physical size, telling us that the Standard Model of Cosmology predicts an expanding Universe. Hubble found that far away galaxies seem to escape from us with velocities proportional to their distances, which is a clear check that assumptions underlying the metric treatment of the homogeneous and isotropic Universe work. The time dependence of the space part of the metric factors out and involves an unique function because we assumed isotropy. If we allow a generalization

$$a(t) \to a_{ij}(t) \tag{1.39}$$

different directions would scale in a different way, violating isotropy. We can in principle skip this problem restricting the tensor $a_{ij}(t)$ only to the subclass showing only one eigenvalue with a three dimensional eigenspace, but care is required. In this case the three principal axes of $a_{ij}(t)$ scale in the same way, saving isotropy. On the other hand the diagonalization procedure may involve a time dependent rotation $R(t)_{ij}$ and this would clearly be a violation of the Copernican Principle, because we would be able to distinguish the observer that rotates in time accordingly to the rotation matrix that makes isotropy safe. All other observers that do not follow the rotation matrix would not agree in observing an isotropic expansion.

Eq. 1.38 suggests the main property of comoving observers. If a comoving observer satisfies

$$\frac{du^i}{dt} = 0 \tag{1.40}$$

then it is not fixed, but it follows the cosmic expansion being fixed on the space slice. Neglecting peculiar velocities any far away galaxy can be considered as a comoving observer. Comoving observers seem to escape from one another with increasing velocities. This interesting feature is a consequence of the Copernican Principle, since there is no centre for the cosmic expansion. Fixing a comoving observer, the set of all other comoving observers forms the Hubble flow, which is the main proof of

cosmic expansion. In terms of General Relativity this aspect is obvious, because comoving observers cannot be fixed with respect to one another. Indeed a comoving observer is fixed with respect to the constant-time space slice it belongs to, but it cannot be in causal contact with any other observer on the same space slice, since their distance is necessarily space-like ($dt = 0$). Then any comoving observer can be in causal contact only with comoving observers lying in the intersection between its past light-cone and a space slice. The two observers measure distances in different way (due to different values of $a(t)$) and this reflects in a *variation in time of distances*, i.e. a velocity.

Finally we write the metric of the space slices in spherical coordinates. The Riemann tensor of maximally symmetric Euclidean spaces satisfies

$$R_{ijkm} = k(\gamma_{ik}\gamma_{jm} - \gamma_{im}\gamma_{jk}) \tag{1.41}$$

where k is a given constant. This form of the Riemann curvature tensor is a consequence of isotropy. Let us raise two indexes of the Riemann tensor with γ^{ij}: we find

$$R_{ij}^{lm}(x) = \gamma^{la}\gamma^{mb}R_{ijab}(x) \tag{1.42}$$

which is a linear map between the space of the two-forms at x into itself. Due to the symmetry property of the Riemann tensor

$$R_{ijab} = R_{abij} \tag{1.43}$$

this map must be symmetric, which ensures that it must be diagonalized by a suitable basis of orthogonal eigenvectors. If the eigenvalues corresponding to different eigenvectors were distinct, then we would be able to find a geometrical prescription for picking up a well defined two-form, which means we would be able to extract a vector at x, violating isotropy. So, it must follow that

$$R_{ij}^{ab} = \lambda(\delta_i^a\delta_j^b - \delta_i^b\delta_j^a) \tag{1.44}$$

for a given proportionality constant λ. Lowering the indexes simply gives Eq. 1.41 and contracting the indexes identifies λ with the curvature.

The corresponding Ricci tensor is then

$$R_{ij} = 2k\gamma_{ij} \tag{1.45}$$

and the Ricci scalar is simply $R = 6k$. The physical meaning of the constant k is explained by this equation: it is the constant Gaussian curvature of the constant-time space slices of the Universe.

1.2.3 The metric

For finding the final form of the metric we remember that if the metric is maximally symmetric, then it must also be spherically symmetric, then we can write the general ansatz

$$ds^2 = -dt^2 + a^2(t)\left(e^{2\beta(r)}dr^2 + r^2 d\Omega^2\right) \tag{1.46}$$

for an unknown function $\beta(r)$. We can compute the Ricci tensor of the space slices

$$\begin{aligned} R_{rr} &= \frac{2}{r}\partial_r\beta & (1.47)\\ R_{\theta\theta} &= e^{-2\beta}(r\partial_r\beta - 1) + 1 & (1.48)\\ R_{\phi\phi} &= R_{\theta\theta}\sin^2(\theta) & (1.49) \end{aligned}$$

and find a differential equation for the function $\beta(r)$ by imposing Eq. 1.45. We immediately find

$$\partial_r\beta = kre^{2\beta} \tag{1.50}$$

which gives

$$\beta(r) = -\frac{1}{2}(1 - 2kr^2) \tag{1.51}$$

Then the metric becomes

$$ds^2 = -dt^2 + a^2(t)\left(\frac{dr^2}{1 - kr^2} + r^2 d\Omega^2\right) \tag{1.52}$$

which is well known as **Friedmann-Robertson-Walker** metric. The line element shows an extra symmetry: it is invariant under the scaling

$$k \rightarrow \frac{k}{|k|} \tag{1.53}$$

$$r \rightarrow r\sqrt{|k|} \tag{1.54}$$

$$a \rightarrow \frac{a}{\sqrt{|k|}} \tag{1.55}$$

which tells that only the sign of the curvature is relevant. This scaling symmetry changes intrinsically the definition of the radial coordinate r, which becomes dimensionless, due to the non-trivial dimensions of the gaussian curvature k. The relevant aspect is given by the required scaling of the factor $a(t)$ in passing to dimensionless distances. This suggests an interpretation: scaling distances is equivalent to rescale the size of the whole Universe at a given epoch, which exactly corresponds to fix a value for the factor $a(t)$, for example, today. So, this symmetry ensures that we can always fix $a = 1$ today without loss of generality.

The general topological structure of the spacetime $\mathbf{M}$ is

$$\mathbf{M} = \mathbf{R} \times \mathbf{H} \tag{1.56}$$

where $\mathbf{H}$ is a globally hyperbolic space. The topological structure shows our construction of the spacetime as a direct product of the time line and an internal curved slice. The globally hyperbolic space $\mathbf{H}$ has three different topological structures depending on the sign of the curvature k. If $k = 0$ the slice is flat, so it must have the topology of the euclidean space $\mathbf{R}^3$, if $k > 0$ it has the topology of a three dimensional sphere, otherwise it is topologically equivalent to a three dimensional hyperboloid.

There are many equivalent forms for the FRW metric. Generally the structure

$$ds^2 = -dt^2 + a^2(t)(dr^2 + S^2(r)d\Omega^2) \tag{1.57}$$

is used. This form suggest an ambiguity in the coordinate distance r. We have defined

$$S_k(x) = \begin{cases} \frac{1}{\sqrt{|k|}} \sin(x\sqrt{|k|}) & \text{if} \quad k < 1 \\ x \quad \text{if} \quad k = 1 \\ \frac{1}{\sqrt{k}} \sinh(x\sqrt{k}) & \text{if} \quad k > 1 \end{cases} \tag{1.58}$$

and we see that $S_k(r)$ plays here the role r plays in Eq. 1.52. The substitution $r \to S_k(r)$ recovers the standard form 1.52.

1.3 Geodesics

The Friedmann-Robertson-Walker metric (from now on FRW) describes the homogeneous and isotropic Universe well. The curvature of the spacetime has a direct physical meaning being related to the action of the gravitational field. The Equivalence Principle relates freely falling observers into the gravitational field with the local curvature of the spacetime manifold, prescripting that they has to follow a geodesic path. This is a straightforward consequence of the assumption that they are *freely falling* into the gravitational field and one of the building blocks of General Relativity. Geodesic motion is the most important feature of a metric theory of gravity and, in principle, we can modify Einstein's field equations without changing the fundamental assumptions that observers follow geodesics.

Let us consider a comoving observer in the Universe. Since it is freely falling, its acceleration along the path must vanish. We know that in flat space this condition means that an observer follows straight lines with constant velocity vector, but inside a general manifold the path may be more complicated. We face the problem writing

$$D_u u^\mu = 0 \tag{1.59}$$

where u^μ is the four-velocity and D_u is the total differential along the observer's path. We have stated no more than that the directional derivative of the four velocity along the path must vanish, but in terms of geometrical objects this translates in a strict property of the tangent vector u^μ to the path followed by the observer. It is parallel-transported along the path itself and this property defines a geodesic. Fixing λ that suitably parameterizes the path, we can write

$$\frac{dx^\mu}{d\lambda} = u^\mu \tag{1.60}$$

and develop the absolute differential on the local basis defined by u^μ itself. This gives

$$u^\nu \nabla_\nu u^\mu = 0 \tag{1.61}$$

provided that the operators ∇_ν are consistently the covariant derivatives. Inserting Eq. 1.32 gives the **geodesic equation**

$$\frac{d^2x^\mu}{d\lambda^2} + \Gamma^\mu_{\alpha\beta}\frac{dx^\alpha}{d\lambda}\frac{dx^\beta}{d\lambda} = 0 \tag{1.62}$$

In order to describe the geodesic motion in the Universe, we need to compute the connection for the FRW metric. The computation is straightforward: the only non vanishing symbols are

$$\begin{aligned}
\Gamma^0_{rr} &= \frac{\dot{a}a}{1-kr^2} && (1.63)\\
\Gamma^0_{\theta\theta} &= \dot{a}ar^2 && (1.64)\\
\Gamma^0_{\phi\phi} &= \dot{a}ar^2\sin^2(\theta) && (1.65)\\
\Gamma^i_{0j} &= \delta^i_j\frac{\dot{a}}{a} && (1.66)\\
\Gamma^r_{rr} &= \frac{kr}{1-kr^2} && (1.67)\\
\Gamma^r_{\theta\theta} &= -r(1-kr^2) && (1.68)\\
\Gamma^r_{\phi\phi} &= -r(1-kr^2)\sin^2(\theta) && (1.69)\\
\Gamma^\theta_{r\theta} &= \frac{1}{r} && (1.70)\\
\Gamma^\theta_{\phi\phi} &= -\sin(\theta)\cos(\theta) && (1.71)\\
\Gamma^\phi_{r\phi} &= \frac{1}{r} && (1.72)\\
\Gamma^\phi_{\theta\phi} &= \cot(\theta) && (1.73)\\
& && (1.74)
\end{aligned}$$

Now we can use the geodesic motion for deriving an useful relation between the scale factor and the energy of a particle following geodesics into the FRW geometry. The four-momentum of a massive particle

$$p^\mu = mu^\mu = m\frac{dx^\mu}{d\lambda} \tag{1.75}$$

gives an implicit definition of the parameter λ. We can write

$$\frac{d}{d\lambda} = \frac{dx^\alpha}{d\lambda}\frac{d}{dx^\alpha} = \frac{p^\alpha}{m}\partial_\alpha \tag{1.76}$$

using the chain rule. The components of the four momentum are $p^0 = E$ and $p^i = \vec{p}^i$, so

$$\frac{d}{d\lambda} = \frac{E}{m}\partial_t + \frac{a^2(t)}{m}\vec{p}\cdot\vec{\nabla} \tag{1.77}$$

where $\vec{p}\cdot\vec{\nabla} = \gamma_{ij}p^i\partial^j$ is the scalar product in the three dimensional slice with metric γ_{ij}. The modulus of the four momentum is defined by the mass of the particles, so we can write

$$-m^2 = g_{\mu\nu}p^\mu p^\nu = -E^2 + a^2(t)\gamma_{ij}p^i p^j \tag{1.78}$$

which provides a relation for rewriting the geodesic equation. Indeed the time component of

$$(E\partial_t + a^2(t)\vec{p}\cdot\vec{\nabla})p^\mu + \Gamma^\mu_{\alpha\beta}p^\alpha p^\beta = 0 \tag{1.79}$$

is a differential equation for the energy of the particle:

$$(E\partial_t + a^2(t)\vec{p}\cdot\vec{\nabla})E + \Gamma^0_{ij}p^i p^j \tag{1.80}$$

Inserting the only non vanishing Christoffel's symbols and remembering that they satisfy the relation

$$\Gamma^0_{ij} = \dot{a}a\gamma_{ij} = \frac{\dot{a}}{a}g_{ij} \tag{1.81}$$

the geodesic equation becomes

$$(E\partial_t + a^2(t)\vec{p}\vec{\nabla})E + \frac{\dot{a}}{a}(E^2 - m^2) = 0 \tag{1.82}$$

If we consider the particle as a comoving observer, since $\vec{p} = 0$, we find

$$E\partial_t E + \frac{\dot{a}}{a}(E^2 - m^2) = 0 \tag{1.83}$$

which is solved in terms of E^2, giving

$$\int_{E_0^2}^{E^2(t)} \frac{d(E^2)}{E^2 - m^2} = -2 \int_{a_0}^{a(t)} \frac{da}{a} \tag{1.84}$$

The solution is

$$E(t) = \sqrt{\frac{a_0^2}{a(t)^2}(E_0^2 - m^2) + m^2} \tag{1.85}$$

where we set boundary conditions at a given time t_0 such that $E(t_0) = E_0$ and $a(t_0) = a_0$.

For massless particles the computation is similar. We can find the solution taking the limit $m/E \to 0$ in the solution, finding

$$E(t) = E_0 \frac{a_0}{a(t)} \tag{1.86}$$

which tells that the energy of a photon is rescaled by the cosmic expansion. Then the wavelength of a quantum of the electromagnetic field satisfies (we set $E(t) = h\nu$)

$$\lambda(t) = \lambda_0 \frac{a(t)}{a_0} \tag{1.87}$$

which explains the redshift of the spectral lines of distant galaxies. If we assume t_0 as today and $a(t) < a_0$, we immediately find that $\lambda(t) < \lambda_0$. This shows that at present time we measure wavelengths that are redshifted by a factor that is strictly related to the size of the Universe at the emission time.

1.4 Energy

This simple derivation shows the role the scale factor plays in the dynamics of the Universe. The FRW metric describes the geometry of the Universe, but we need to link the free parameter $a(t)$ to the energy content of the Universe, since the geometry (which describes the gravitational field) is strictly related to mass and energy density.

1.4.1 Field equations

We apply Einstein field equations

$$R_{\mu\nu} - \frac{1}{2} g_{\mu\nu} R = 8\pi G T_{\mu\nu} \tag{1.88}$$

assuming that the metric is FRW. The stress-energy tensor is completely unknown and we need to make assumptions on the energy content on the Universe in order to write $T_{\mu\nu}$. Computing the Ricci tensor

$$R_{\mu\nu} = \partial_\alpha \Gamma^\alpha_{\mu\nu} - \partial_\nu \Gamma^\alpha_{\mu\alpha} + \Gamma^\alpha_{\alpha\beta}\Gamma^\beta_{\mu\nu} - \Gamma^\alpha_{\beta\mu}\Gamma^\beta_{\nu\alpha} \tag{1.89}$$

is straightforward. The only non vanishing components are diagonal:

$$\begin{aligned} R_{00} &= -3\frac{\ddot{a}}{a} && (1.90)\\ R_{rr} &= \frac{\ddot{a}a + 2\dot{a}^2 + 2k}{1 - kr^2} && (1.91)\\ R_{\theta\theta} &= (\ddot{a}a + 2\dot{a}^2 + 2k)r^2 && (1.92)\\ R_{\phi\phi} &= (\ddot{a}a + 2\dot{a}^2 + 2k)r^2 \sin^2(\theta) && (1.93) \end{aligned}$$

The Ricci scalar is

$$R = R_{\mu\nu} g^{\mu\nu} = \frac{6}{a^2}(\ddot{a}a + \dot{a}^2 + k). \tag{1.94}$$

We have explicitly computed the left-hand side of Einstein field equations, now we have to deal with the stress-energy tensor. The Universe is not empty, so we model the energy content of the Universe as a superposition of perfect fluids. There are different definitions for the tensor $T^{\mu\nu}$ of a perfect fluid, but they are equivalent for our computation. We remember Weinberg's definition (see [63]) of a perfect fluid as a fluid which is isotropic in its rest frame. This definition matches well with our view of the expanding Universe as homogeneous and isotropic, since the gravitational field exerted by an isotropic source is isotropic too: the metric itself reflects the symmetry properties of its source.

1.4.2 Stress-energy tensor

The general defintion of the stress-energy tensor is written in terms of functional derivatives

$$T^{\mu\nu} = \frac{2}{\sqrt{-\det(g)}} \frac{\delta S}{\delta g_{\mu\nu}} \tag{1.95}$$

where S is the action of the fluid and $g_{\mu\nu}$ the metric. This definition allows for treating the electromagnetic field and any quantum field as perfect fluids, provided we know the action. First of all we need to generalize the action principle to a curved spacetime. The action must be written in an invariant form

$$S[\phi] = \int_M L(\phi, d\phi, \det(g)^{-1}) \sqrt{-\det(g)} d^4x \tag{1.96}$$

where M is the spacetime manifold and $\sqrt{-\det(g)}d^4x$ is the invariant measure. We wrote explicitly the dependence of the lagrangian on the fields and their derivatives, provided that we must be careful on the covariant formulation of the differential operators. The principle of least action can be written as

$$\left.\frac{d}{d\lambda}\right|_{\lambda=0} S(\phi + \lambda h) = 0 \tag{1.97}$$

where λ is a real parameter and h is an arbitrary variation of the fields ϕ vanishing on the boundary ∂M of the manifold.

Expanding the variation leads to

$$0 = \int_M \left(h\frac{\delta L}{\delta \phi} + \frac{\delta L}{\delta(d\phi)} \delta(d\phi) \right) \sqrt{-\det(g)} d^4x \tag{1.98}$$

The derivative operators may not commute due to the curved geometry, but we have to remember that $\delta\phi = \lambda h$ is not a derivative function, so we can still write $\delta(d\phi) = \lambda dh$. The computation then is straightforward

$$0 = \int_M \left(h\frac{\delta L}{\delta \phi} - hDiv\left(\frac{\delta L}{\delta(d\phi)}\right) \right) \sqrt{-\det(g)} d^4x + \quad b.t. \tag{1.99}$$

where $b.t.$ is the boundary term

$$\int_M d\left(h\frac{\delta L}{\delta(d\phi)}\right)\sqrt{-\det(g)}d^4x = 0 \tag{1.100}$$

which can be transformed into an integral on the boundary ∂M by virtue of the divergence theorem. This integral vanishes since h vanish on the boundary by definition. We have found the generalization of the Euler-lagrange equations for curved manifold

$$\frac{\delta L}{\delta\phi} - Div\left(\frac{\delta L}{\delta(d\phi)}\right) \tag{1.101}$$

provided that the differential operators must be written covariantly. Computing the general form of the stress energy tensor from the action is now an easy task:

$$T^{\mu\nu} = 2\frac{\delta L}{\delta g_{\mu\nu}} - g^{\mu\nu}L \tag{1.102}$$

Now we have moved the problem of finding the energy momentum tensor for the cosmological fluids to the problem of writing a lagrangian density for the content of the Universe. If we consider the fluid at rest, then each element of the perfect fluid is a comoving observer and we can construct the lagrangian treating each fluid element in analogy with particles. For a particle of mass m, the action is given by

$$S = m\int ds = m\int d^4x \int d\lambda\sqrt{g_{\mu\nu}u^\mu u^\nu}\delta^{(4)}(x - x(\lambda)) \tag{1.103}$$

where λ parameterizes the worldline follwed by the particle. The term $\sqrt{-\det(g)}$ coming from the integration measure cancels out because the Dirac delta function must be divided by the same term, since it behaves like a density. We can generalize this action to a countinuous field of density $\rho(x)$ substituting $m\delta^{(4)}(x - x(\lambda))$ with the density field:

$$S = \int \rho(x)\sqrt{g_{\mu\nu}u^\mu u^\nu}d^4x \tag{1.104}$$

The stress-energy tensor of the fluid requires contributions coming from the pressure exerted by the fluid itself. In order to write this contribution, we construct a tensor $p^{\alpha\beta}$ whose components account for the

pressure exerted by a force f^α on a surface orthogonal to the direction n^β. Since the perfect fluid is isotropic in its rest frame, the pressure field must exihibit the symmetries of the spacetime, so we assume that

$$p^{\alpha\beta} = pg^{\alpha\beta} \tag{1.105}$$

where p is a real scalar. We must be careful in handling $p^{\alpha\beta}$ since we measure pressures on the three-dimensional slice of the spacetime at a fixed time, so we have to project the pressure tensor on the space slices of the FRW metric in order to find the right contribution to the stress-energy tensor. This is an easy task, because the tensor

$$h_{\mu\nu} = g_{\mu\nu} + u_\mu u_\nu \tag{1.106}$$

is a projector on the hyphersurfaces orthogonal to u^μ. Since the element of the fluid are comoving observers $h_{\mu\nu}$ projects correctly. So, we have to add a new contribution to the Lagrangian

$$\Pi = g_{\mu\nu}\Pi^{\mu\nu} = g_{\mu\nu}h^{\mu\alpha}h^{\nu\beta}p_{\alpha\beta} \tag{1.107}$$

which accounts for the pressure stresses. If the pressure tensor is proportional to the metric the computation is straightforward

$$\Pi^{\mu\nu} = (g^{\mu\nu} + u^\mu u^\nu)p \tag{1.108}$$

and

$$\Pi = 3p \tag{1.109}$$

The action then reads

$$S = \int \left(\rho \frac{\sqrt{g_{\mu\nu}u^\mu u^\nu}}{\sqrt{-\det(g)}} + \Pi \right) \sqrt{-\det(g)} d^4x \tag{1.110}$$

and the stress energy tensor for a perfect fluid becomes

$$T^{\mu\nu} = \rho u^\mu u^\nu + \Pi^{\mu\nu} = (\rho + p)u^\mu u^\nu + pg^{\mu\nu} \tag{1.111}$$

1.5 Friedmann equations

The stress-energy tensor of the perfect fluid allows for finding a differential equation linking the scale factor to the energy content of the Universe. The 00 component of the Einstein field equations gives

$$-3\frac{\ddot{a}}{a} + \frac{3}{a^2}(\ddot{a}a + 2\dot{a}^2 + 2k) = 8\pi G\rho \tag{1.112}$$

which is the first Friedmann equation

$$H^2 + \frac{k}{a^2} = \frac{8}{3}\pi G\rho \tag{1.113}$$

where we have explicitly written the Hubble parameter $H = \frac{\dot{a}}{a}$. The remaining components of the Einstein's equations are equivalent and give

$$-2\frac{\ddot{a}}{a} - H^2 - \frac{k}{a^2} = 8\pi G p \tag{1.114}$$

Substituting H^2 with Eq. 1.113, we find the second Friedmann equation

$$\frac{\ddot{a}}{a} = -\frac{4}{3}\pi G(\rho + 3p) \tag{1.115}$$

Friedmann equations link the scale factor to the pressure and the density of the cosmological fluid filling the Universe. In order to solve the equations we need to specify at least one of the sources. In general we solve the equations rememberring that we can always write an equation of state for a perfect fluid, linking the pressure and the density

$$p \equiv p(\rho) \tag{1.116}$$

The equation of state works as a boundary condition for the Friedmann equations and has an important physical role, since it models the cosmological fluid. We are able to test the validity of the model making comparisons between the predicted dynamics of the scale factor and the observed cosmological expansion.

Looking at the the sky we see that matter is clustered in objects of very different sizes. Acting on all scales, gravity forms planets, stars, galaxies and bigger objects, such as clusters of galaxies and superclusters. These

objects are sources of radiation due to the high energies involved. So, the most simple model for the cosmological fluid requires to account for matter and radiation. Matter is characterized by

$$p_{matter} = 0 \tag{1.117}$$

while the equation of state for radiation is

$$p_{rad} = \frac{1}{3}\rho \tag{1.118}$$

Some care is needed: matter is defined as a pressureless fluid (often called *dust*) because the velocities involved in exerting pressure for a perfect gas are negligible with respect to relativistic scales. We know that for a perfect Maxwellian gas the pressure exerted by the gas is

$$p_{gas} = \frac{1}{3}\rho\bar{v^2} \tag{1.119}$$

where $\bar{v^2}$ is the mean square velocity of the particles. The pressure is negligible only in a relativistic framework if $v << c$, so the matter fluid acconts for all non-relativistic species of particles in the Universe. The pressure of radiation is easily computed by the general theory of the electromagnetic field. The radiation fluid accounts for photons and all relativistic massive particles.

Solving Friedmann equations under simple hypothesis is an easy task, provided we know an equation giving the evolution of the density and pressure of the cosmological fluid in terms of the scale factor. Noether's theorem guarantees that the stress energy tensor carries a conserved current: the underlying symmetries of the theory are the isometries of the spacetime. We can write

$$\nabla_\nu T^{\nu\mu} = 0 \tag{1.120}$$

as a consequence of Noether's theorem. Expanding the $\mu = 0$ component we find

$$\partial_\nu T^{\nu 0} + \Gamma^\nu_{\nu\alpha} T^{\alpha 0} + \Gamma^0_{\nu\alpha} T^{\nu\beta} = 0 \tag{1.121}$$

Inserting the Christoffel's symbols gives the continuity equation

$$\partial_t \rho + 3H(\rho + p(\rho)) = 0 \tag{1.122}$$

which can be easily solved for simple cosmological fluid like dust or radiation. The solutions are straightforward:

$$\rho_m(a) = \rho_m^{(0)} \frac{a_0^3}{a^3} \tag{1.123}$$

$$\rho_r(a) = \rho_r^{(0)} \frac{a_0^4}{a^4} \tag{1.124}$$

The continuity equation suggests to treat comsological fluids in a common way. If we assume a linear equation of state

$$p(\rho) = w\rho \tag{1.125}$$

where w is a proportionality constant, the solution of the continuity equation is obvious

$$\rho_f(a) = \rho_f^{(0)} \left(\frac{a_0}{a}\right)^{3(1+w)} \tag{1.126}$$

giving a general rule for the time evolution of the density. In cosmology many comsological fluids were introduced for giving explanations to observed phenomena, depending on the value of w. Here we remember the main ones:

- Dust: $w = 0$
- Radiation: $w = \frac{1}{3}$
- Cosmological constant: $w = -1$
- Dark Energy: any $w < -\frac{1}{3}$

Dark Energy and the cosmological constant were introduced for explaining the present accelerated expansion and we will discuss them later.

Now we are able to solve Friedmann equations and find the evolution in time of the scale factor under quite simple assumptions. We define the critical density ρ_c as

$$\rho_c = \frac{3H_0^2}{8\pi G} \tag{1.127}$$

and the cosmological parameters as

$$\Omega_i = \frac{\rho_i}{\rho_c} \tag{1.128}$$

The critical density is the value of the total density that flattens the Universe at the given time t_0. We can assume that t_0 is exactly today for simplicity, since we are making measurements at this cosmic time. Correspondingly the cosmological parameters measure how the energy is divided among its components during cosmic evolution. Indeed for many fluids we find

$$H^2 = \frac{8\pi G}{3}\sum_i \rho_i - \frac{k}{a^2} \tag{1.129}$$

and inserting the definition of the cosmological parameters at the present time we find

$$1 = \sum_i \Omega_i - \frac{k}{a_0^2 H_0^2} \tag{1.130}$$

showing that the first Friedmann equation corresponds to the conservation of the total energy in the universe. If the Universe is flat ($k = 0$), then the balancing condition is $\sum_i \Omega_i = 1$, otherwise any deviation from this balancig condition is a proof of the curved geometry of the space slices of the FRW spacetime. We are also able to define a curvature cosmological parameter in analogy with the standard definition:

$$\Omega_k = -\frac{k}{a_0^2 H_0^2} \tag{1.131}$$

which allows for writing the energy conservation in the simple form

$$\sum_i \Omega_i = 1 \tag{1.132}$$

provided that the curvature is treated as a cosmological fluid. This correspondence should be handled with care, since the physical meaning of

treating curvature as a cosmological fluid is given by General Relativity: the non-flat geometry of the spacetime slices can be treated mathematically as an extra energy term which enters the conservation of energy, like curving spacetime requires energy. No other analogies exist between the curvature term and other cosmological fluids sourcing gravity, because we are not able, for instance, to well define the pressure or the w parameter for the curvature.

The first Friedmann equation can be written in terms of cosmological parameters. We can write explicitly the different parameters corresponding to different cosmological fluids, like

$$H^2 = H_0^2 \left(\Omega_m a^{-3} + \Omega_r a^{-4} + \Omega_{DE} a^{-3(1+w_{DE})} + \Omega_k a^{-2} \right) \tag{1.133}$$

where we separately accounted for matter (Ω_m), radiation (Ω_r), Dark Energy (Ω_{DE}) and the curvature (Ω_k). This form of the first Friedmann equation is very useful in cosmology, since measuring the Ωs from observations tells how the energy content of the Universe is distributed between its components at any stage of its history and how the dynamics of the scale factor is then affected. We should look at this equation as the fundamental relation. Different values of the Ωs imply different physical effects, so it is well known that a given set of values for the Ωs defines a *Cosmology*. We can test the Cosmology trying to constrain the cosmological parameters against observations of physical phenomena highly affected by their values. We will discuss how to deal with observations later, here we simply remember the easiest solutions for the Friedmann equations.

For dust only we find

$$H^2 = \frac{8\pi G\rho}{3} \left(1 + [(\sum_i \Omega_i)^{-1} - 1] \frac{a}{a_0} \right) \tag{1.134}$$

inserting k from Eq. 1.130. The non-trivial solution requires the parametrization of a and t in terms of a suitable parameter η. For an open Universe ($\sum_i \omega_i < 1$) the solution is

$$a(\eta) = \frac{a_0}{2|1-(\sum_i \Omega_i)^{-1}|}(\cosh(\eta)-1) \tag{1.135}$$

$$t(\eta) = \frac{a_0\sqrt{|k|}}{2|1-(\sum_i \Omega_i)^{-1}|}(\sinh(\eta)-\eta) \tag{1.136}$$

The solution for the closed universe ($\sum_i \omega_i > 1$) is easily found applying Wick's rotation

$$\eta \rightarrow i\eta \tag{1.137}$$

$$\sqrt{|k|} \rightarrow i\sqrt{k} \tag{1.138}$$

due to the symmetry properties of hyperbolic functions. The coefficients change suitably and the final solution is

$$a(\eta) = -\frac{a_0}{2|1-(\sum_i \Omega_i)^{-1}|}(\cos(\eta)-1) \tag{1.139}$$

$$t(\eta) = -\frac{a_0\sqrt{|k|}}{2|1-(\sum_i \Omega_i)^{-1}|}(\sin(\eta)-\eta) \tag{1.140}$$

The flat case is well known for historical reasons, since the corresponding spacetime is the Einstein-de-Sitter Universe (EdS). The general integral is

$$\int_{a(t)}^{a_0} \sqrt{a}da = \int_t^{t_0} \sqrt{\frac{8\pi G\rho_0}{3}a_0^3} \tag{1.141}$$

which gives

$$\frac{a(t)}{a_0} = \left(1-\frac{3}{2}\sqrt{\frac{8\pi G\rho_0}{3}}(t_0-t)\right)^{\frac{2}{3}} \tag{1.142}$$

and

$$H = \frac{\sqrt{\frac{8\pi G\rho_0}{3}}}{1-\frac{3}{2}\sqrt{\frac{8\pi G\rho_0}{3}}(t_0-t)} \tag{1.143}$$

The initial time t_0 is the present age of the Universe and corresponds to today, ρ_0 is the present value of the density. Since the integrand function is monothonic, necessarily $a(t) < a_0$. The exact value of t_0 is not crucial, since the main result is

$$a(t) \sim t^{\frac{2}{3}} \tag{1.144}$$

which ensures that an EdS Universe expands forever. Since $a(t)$ is monothonic and non-negative, we should be careful of what happens if $a(t) \to 0$. The density becomes infinte and the metric shows a true singularity. We can find the age of the Universe following this simple path: we set the origin of the time coordinate at the Big Bang singularity, such that $a(t = 0) = 0$. Consequently

$$t_0 = \frac{2}{3}\sqrt{\frac{3}{8\pi G\rho_0}} \tag{1.145}$$

which simplifies the solution:

$$a(t) = a_0 \left(\frac{3}{2}\sqrt{\frac{8\pi G\rho_0}{3}}t\right)^{\frac{2}{3}} \tag{1.146}$$

Finally we remember that

$$H_0^2 = \frac{8\pi G\rho_0}{3} \tag{1.147}$$

which gives

$$a(t) = a_0 \left(\frac{3}{2}H_0 t\right)^{\frac{2}{3}} \tag{1.148}$$

The constant a_0 is still a free parameter, corresponding to a degree of freedom we have not set yet. Usually the size of the Universe is referred to today and it is arbitrarly chosen $a_0 = 1$ for further simplicity.

1.6 Redshift

We have already shown that photons travelling along geodesics of the FRW geometry change their frequency as a consequence of the non-trivial

dynamics of the Universe. Here we briefly explain this redshift. Let us consider two comoving observers, the source S of a photon and the observer O. they follow two distinct geodesics in the FRW geometry and are linked by the null path followed by the photon. The four-momentum of the photon satisfies $k^\mu k_\mu = 0$ and $k^0 = E$ as usual. Since for comoving observers $u^\mu = (1, 0, 0, 0)$, we can pick up the energy of the photon computing the inner product $k^\mu u_\mu$. The redshift z of a photon is defined as

$$1 + z = \frac{(k^\mu u_\mu)_S}{(k^\nu u_\nu)_O} \tag{1.149}$$

in order to have $z = 0$ if the observer and the source coincide. In order to compute the inner products, we use a powerful lemma:

Lemma 1.6.1 *Let (M, g) be a Riemannian manifold with metric tensor $g_{\mu\nu}$, let τ^μ be the tangent vector to a given geodesic curve Γ of M and ξ^μ be a Killing vector for the metric $g_{\mu\nu}$. Then the inner product $\tau^\mu \xi_\mu$ is constant along Γ.*

Proof: It is only a matter of direct calculation. If λ parameterizes the geodesic, then we need to compute

$$\frac{d}{d\lambda}(\tau^\mu \xi_\mu) = \xi_\mu \frac{d\tau^\mu}{d\lambda} + \tau^\mu \frac{d\xi_\mu}{d\lambda} \tag{1.150}$$

The former derivative can be simplified by the geodesic equation:

$$\frac{d\tau^\mu}{d\lambda} = -\Gamma^\mu_{\alpha\beta} \tau^\alpha \tau^\beta \tag{1.151}$$

the latter one by the Killing equation

$$\nabla_\mu \xi_\nu + \nabla_\nu \xi_\mu = 0 \tag{1.152}$$

which implies $(\forall a^\mu)$

$$a^\mu a^\nu \partial_\mu \xi_\nu = \Gamma^\alpha_{\mu\nu} \xi_\alpha a^\mu a^\nu \tag{1.153}$$

by virtue of the symmetry properties of the Christoffel's symbols. It follows

$$\tau^\mu \frac{d\xi_\mu}{d\lambda} = \tau^\mu \tau^\alpha \partial_\alpha \xi_\mu = \Gamma^\alpha_{\mu\nu} \xi_\alpha \tau^\mu \tau^\nu \tag{1.154}$$

This demonstrates that the derivative along the geodesic is trivial.

We assumed that the space slices Σ_t of the FRW spacetime are homogeneous and isotropic. Maximal symmetry ensures that we can always find a Killing vector in Σ_t which generates the isometry group of Σ_t. Then since

$$k^\mu (g_{\mu\nu} + u_\mu u_\nu) \xi^\nu \tag{1.155}$$

is constant and k^μ is a null vector, the projection of k^μ on u^μ must be constant too. This trick allows for substituting u^μ with ξ^μ in the computation of the redshift. Since the Killing vector is not normalized we need in principle to deal with

$$1 + z = \frac{(u^\mu \xi_\mu)_S}{(u^\nu \xi_\nu)_O} \sqrt{\frac{(\xi^2)_O}{(\xi^2)_S}} \tag{1.156}$$

The first ratio is trivial due to the application of the lemma. The ratio involving the norm ξ^2 requires some care. We look at the derivative of ξ^2 along a geodesic of a comoving observer. Since $u^\mu = (1, 0, 0, 0)$, we find

$$\frac{d}{d\lambda} \xi^2 = \frac{d}{dt} (g_{\mu\nu} \xi^\mu \xi^\nu) \tag{1.157}$$

Computing the time derivative requires some care. The Killing vectors of the FRW spacetime generate isometries of the three-dimensional hypersurfaces of constant time. These hypersurfaces are always orthogonal to u^μ and to the time direction. This simply implies that $\xi^0 = 0$, because Killing vectors generating isometries of the constant-time hypersurfaces cannot mix two distinct slices. Then we can simplify the computation rememberring that

$$\frac{d}{d\lambda} \xi^2 = \dot{g}_{ij} \xi^i \xi^j = 2H \xi^2 \tag{1.158}$$

where the last equality follows from inserting the FRW metric. The time derivative do not act on the contravariant vectors since

$$\dot{\xi^i} = \dot{g}^{ij}\xi_j + g^{ij}\dot{\xi}_j = -2H\xi^i + 2H\xi^i = 0 \tag{1.159}$$

Then it is clear that

$$\frac{(\xi^2)_O}{(\xi^2)_S} = \frac{a_O^2}{a_S^2} \tag{1.160}$$

which leads to

$$1 + z = \frac{a_O}{a_S} \tag{1.161}$$

This well-known relation between the scale factor and the redshift is a direct consequence of maximal symmetry and can be easily broken.

1.7 Distances

Observing the sky requires clear definitions of distances. We have to be careful in defining distances in the FRW spacetime, since we have to mind the fundamental prescriptions underlying General Relativity. In cosmology we make measurements based on light rays. Photons from distant galaxies carry cosmological informations primarly as redshift: we know from standard quantum mechanics the wavelength corresponding to a given atomic transition and we are able to measure its redshift on the spectrum of a distant galaxy. This procedure links a redshift measurement with a distance and the last ingredient we need is a formula for relating the distance to the underlying cosmology.

1.7.1 Comoving distance

Since photons coming from a distant galaxy follow null radial geodesics, we can write

$$0 = ds^2 = -dt^2 + a^2(t)\frac{dr^2}{1 - kr^2} \tag{1.162}$$

which gives a differential equation for the coordinate distance r. It follows

$$\int_t^{t_0} \frac{dx}{a(x)} = \int_r^0 \frac{dr}{\sqrt{1 - kr^2}} \tag{1.163}$$

We assume that the size of the Universe today is a_0 and the corresponding coordinate distance is $r = 0$, since we want to compute distances from us. Direct integration gives

$$S_k(r) = \int_a^{a_0} \frac{da}{a^2 H(a)} \tag{1.164}$$

where the function $S_k(x)$ is defined in 1.58. Then, it follows

$$r = S_k^{-1}\left(\int_a^{a_0} \frac{dx}{x^2 H(x)}\right) \tag{1.165}$$

which relates the coordinate distance r with the cosmology. In terms of redshift we equivalently write

$$r = S_k^{-1}\left(\int_0^{z} \frac{dz'}{H(z')}\right). \tag{1.166}$$

There are many ways of defining distances starting from Eq. 1.166 (see [57] for more details). Usually we separate the present value of the Hubble parameter from its definition

$$H(z) = H_0 E(z) \tag{1.167}$$

and we rewrite Eq. 1.166 suitably:

$$r = D_H \int_0^{z} \frac{dz'}{E(z')} \tag{1.168}$$

The Hubble distance D_H is simply

$$D_H = \frac{c}{H_0} = 3000\mathrm{h}^{-1}\mathrm{Mpc} \tag{1.169}$$

where we made explicit the speed of light in order not to misunderstand distances and times. In natural units $c = 1$ and the Hubble distance corresponds to the Hubble time

$$t_H = \frac{1}{H_0} = 3.09 \times 10^{17}\mathrm{h}^{-1}\mathrm{s} \tag{1.170}$$

The comoving distance clearly depends on the curvature of the space slices through the function $S_k(x)$. The radial propagation of photons in

the FRW specitime affects the way we measure cosmological distances and we must be careful that the curvature enters the Hubble function too.

1.7.2 Angular diamater distance

In order to compute separations in the sky we have to deal with stransverse sizes, provided that we cannot disregard the effects of curvature. In a plane geometry we can easily compute the length of a circular arc knowing the radius of the circle and the angle subtended by the arc:

$$l = r\theta \tag{1.171}$$

A generalization should work for the FRW spacetime, since space slices are maximally symmetric. We look at the path followed by a photon travelling between two points at the same coordinate r:

$$ds^2 = -dt^2 + a^2(t) r^2 d\Omega^2 \tag{1.172}$$

Without lack of generality, we can always rotate the spherical coordinates in order to set the endpoints of the light path at the same coordinate ϕ, leaving the trivial equation

$$\frac{dt}{a(t)} = r d\theta \tag{1.173}$$

This equation shows that the standard relation in Eq. 1.171 still holds for the FRW spacetime, provided that $d\theta$ is a small angular separation subtended by two distant objects at the observer. The length $rd\theta$ is clearly a comoving transverse size, since it is not affected by the cosmological expansion. In order to define a physical *angular diameter distance* we only need to multiply the comoving transverse size by the corresponding scale factor, leaving

$$D_A = a S_k^{-1} \left(\int_a^{a_0} \frac{dx}{x^2 H(x)} \right) \tag{1.174}$$

or

$$D_A = \frac{1}{1+z} S_k^{-1} \left(\int_0^{z} \frac{dz'}{H(z')} \right) \tag{1.175}$$

in terms of redshift.

1.8 Luminosity distance and reciprocity

We have found equations giving coordinate distances in terms of the Hubble parameter. In standard optics the luminosity L of a source and the flux at a distance r are linked by

$$F = \frac{L}{4\pi r^2} \tag{1.176}$$

where r is the radius a sphere surrounding the source and F is the flux through the surface of the sphere. This formula simply defines the flux as the radiant energy going through a closed surface. We can reverse this point of view stating that a measure of the flux and a measure of the luminosity allow for computing the distance r of an observer looking at the source. In cosmology we have to deal with curved space, so we need to generalize this formula, defining a *luminosity distance* D_L in analogy:

$$D_L = \sqrt{\frac{L}{4\pi F}} \tag{1.177}$$

The luminosity distance D_L may be in principle very different from the coordinate radius r due to the curvature of the space slices and the non-trivial dynamics of the spacetime. In order to find a definition for the luminosity distance, we will follow the path that Etherington suggested in 1936 and that was also developed by Ellis et al. (see [61, 62])

1.8.1 Geometric optics

First of all we need to assume an underlying model for the propagation of light on a curved manifold. Maxwell's equations in vacuum read

$$\nabla_\mu F^{\mu\nu} = 0 \tag{1.178}$$
$$\nabla_{[\mu} F_{\alpha\beta]} = 0 \tag{1.179}$$

where the square brakets stands for the full symmetrization of the indexes. The first set of equations define the dynamics of the electromagnetic field, the second set contains constraints, like the Gauss law.

The field strength $F_{\mu\nu}$ is defined in terms of the four-potential A^μ as

$$F_{\mu\nu} = \nabla_\mu A_\nu - \nabla_\nu A_\mu \tag{1.180}$$

involving the connection coefficients. It is easy to see that

$$F_{\mu\nu} = \partial_\mu A_\nu - \partial_\nu A_\mu \tag{1.181}$$

because the Levi-Civita connection is torsion free and the Christoffel's symbols are symmetric in their lower indexes $\Gamma^\alpha_{\mu\nu} = \Gamma^\alpha_{\nu\mu}$. The four potential A_μ defines a 1-form on the manifold, which is *minimally coupled* to the geometry of the curved space. The minimal coupling of gauge fields A_μ is a general prescription in treating fundamental forces and simply corresponds to substitute the standard derivative operators with covariant ones, involving a non-trivial connection. In the context of gravity, the minimal coupling of the electromagnetic field with geometry is realized by the substitution

$$\partial_\mu \to \nabla_\mu \tag{1.182}$$

everywhere, provided that the connection is exactly the Levi-Civita induced by the metric tensor. We still know that the connection coefficients are exactly the Christoffel's symbols, so ∇_μ corresponds exactly to the covariant derivative defined in Eq. 1.32.

Since the field strength of the electromagnetic field is antisymmetric, it is immediate that

$$\nabla_{[\mu} F_{\alpha\beta]} = \partial_{[\mu} F_{\alpha\beta]} \tag{1.183}$$

showing that the minimal coupling leaves Maxwell's constraints invariant. On the other hand the general Maxwell's equation

$$\partial_\mu F^{\mu\nu} = J^\nu \tag{1.184}$$

cannot be invariant, because the density current J^ν is not invariant under the minimal coupling. Noether's theorem ensures that the component J^0 defines a conserved charge Q by the integral

$$Q = \int d^3x J^0(x) \tag{1.185}$$

which is a straightforward consequence of the continuity equation $\partial_\mu J^\mu = 0$. This equation is changed by the minimal coupling and consequently the definition of Q must change when a curved geometry is considered. It is easy to show that the minimal coupling acts on J^μ such that

$$J^\mu \to \frac{J^\mu}{\sqrt{-\det(g)}} \tag{1.186}$$

since $(g = \det(g))$

$$\nabla_\mu \left(\frac{J^\mu}{\sqrt{-g}} \right) = \frac{\partial_\mu J^\mu}{\sqrt{-g}} - \frac{J^\mu \partial_\mu \sqrt{-g}}{g} + \frac{\Gamma^\mu_{\mu\alpha} J^\alpha}{\sqrt{-g}} = 0 \tag{1.187}$$

The first term vanishes for the continuity equation and the last two are opposite because the general relation

$$\Gamma^\mu_{\mu\alpha} = \frac{1}{\sqrt{-g}} \partial_\alpha \sqrt{-g} \tag{1.188}$$

holds.

Maxwell's equations become

$$\nabla_\mu F^{\mu\nu} = \frac{J^\mu}{\sqrt{-\det(g)}} \tag{1.189}$$

Expanding the covariant derivative yelds

$$\partial_\mu F^{\mu\nu} + \Gamma^\mu_{\mu\alpha} F^{\alpha\nu} + \Gamma^\nu_{\mu\alpha} F^{\nu\alpha} = \frac{J^\nu}{\sqrt{-det(g)}} \tag{1.190}$$

The third term vanishes since the field strength is antisymmetric and the second term simplifies giving the general covariant form of Maxwell's equations on a curved geometry:

$$\frac{1}{\sqrt{-\det(g)}} \partial_\mu \left(\sqrt{-\det(g)} F^{\mu\nu} \right) = \frac{J^\nu}{\sqrt{-\det(g)}} \tag{1.191}$$

Solving Maxwell's equations is quite hard, so we can deal with the problem using *the geometric optics approximation*, which is based on a simple assumption: the wavelength of the electromagnetic field is much smaller that the curvature radius of the manifold.

We assume that the field strength can be written as

$$F^{\mu\nu} = A^{\mu\nu} e^{iS} \tag{1.192}$$

for a suitable complex tensor $A^{\mu\nu}$ and a phase S. This ansatz encodes the geometric optics approximation: let us model the gauge field A^{μ} as a real vector times a phase

$$A^{\mu} = f^{\mu} e^{iS} \tag{1.193}$$

Then the corresponding tensor $A^{\mu\nu}$ exists. It is

$$A^{\mu\nu} = \partial^{\mu} f^{\nu} - \partial^{\nu} f^{\mu} + i(f^{\nu}\partial^{\mu} S - f^{\mu}\partial^{\nu} S) \tag{1.194}$$

We assume that the derivatives of $A^{\mu\nu}$ are small ($O(\epsilon)$) and that the expansion

$$A^{\mu\nu} = B^{\mu\nu} + \epsilon C^{\mu\nu} + O(\epsilon^2) \tag{1.195}$$

holds for a suitable small parameter ϵ and a non-trivial $B^{\mu\nu}$.

Substituting into the first of Eq. 1.178 gives

$$A^{\mu\nu}\partial_{\mu}(e^{iS}) + e^{iS}\nabla_{\mu} A^{\mu\nu} = 0 \tag{1.196}$$

Inserting the series in ϵ for $A^{\mu\nu}$ provides two equations

$$\begin{aligned} B^{\mu\nu}\partial_{\mu} S &= 0 && (1.197)\\ \nabla_{\nu} B^{\mu\nu} + iC^{\mu\nu}\partial_{\nu} S &= 0 && (1.198) \end{aligned}$$

The tensors $B^{\mu\nu}$ and $C^{\mu\nu}$ satisfy symmetry constraints coming from the others Maxwell's equations:

$$\begin{aligned} (\partial_{[\mu} S) B_{\alpha\beta]} &= 0 && (1.199)\\ \nabla_{[\mu} B_{\alpha\beta]} &= -i\partial_{[\mu} C_{\alpha\beta]} && (1.200) \end{aligned}$$

Contracting the first constraint with $\partial^{\mu} S$ yelds immediately

$$\partial_{\mu} S \partial^{\mu} S = 0 \tag{1.201}$$

and the general definition of the stress-energy tensor for the electromagnetic field

$$T_{\mu\nu}^{(e.m.)} = F_{\mu\alpha}F_{\nu}^{\alpha} - \frac{1}{4}g_{\mu\nu}F^2 \tag{1.202}$$

leads to

$$\partial^{\mu}S\partial^{\nu}ST_{\mu\nu} = -\frac{1}{4}\partial_{\mu}S\partial^{\mu}S = 0 \tag{1.203}$$

which gives

$$T_{\mu\nu} = f\partial_{\mu}S\partial_{\nu}S + O(\epsilon) \tag{1.204}$$

for a given function f. The continuity equation $\nabla_{\mu}T^{\mu\nu} = 0$ becomes

$$\nabla_{\mu}\left(f\partial^{\mu}S\partial^{\nu}S\right) = 0 \tag{1.205}$$

In analogy with the standard theory of the electromagnetic field, we notice that the surfaces of constant $S(x)$ are regions of constant phase for the elctromagnetic waves propagating through the spacetime. The vector

$$k^{\mu} = \partial^{\mu}S \tag{1.206}$$

defines the direction of propagation of the wave front and satisfies

$$k^{\mu}k_{\mu} = 0 \qquad \nabla_{\mu}k_{\nu} + \nabla_{\nu}k_{\mu} = 0 \tag{1.207}$$

which immediately imply

$$k^{\mu}\nabla_{\mu}k^{\nu} = 0 \tag{1.208}$$

The last equation tells that k^{μ} is tangent to a set of lightlike geodesics. They are path followed by the photons of the electromagnetic radiation we are describing with the geometric optics approximations and can be identified as *rays* into the spacetime.

Now let us consider two comoving observers O_1 and O_2 which intersect a light ray emitted by a given source S. The generalization to non-comoving observers is quite long and is well reported in [62]. The observers intersecting ligth rays measure an intensity

$$I = T_{\mu\nu} u^\mu u^\nu = f(k_\alpha u^\alpha)^2 \tag{1.209}$$

through an infinitesimal area dA orthogonal to the rays. The variation is

$$dI = k^\mu \nabla_\mu I \tag{1.210}$$

which can be computed rememberring that $u^\mu = (1, 0, 0, 0)$ and that k^μ is lightlike. If we set a frame such that

$$k^\mu = (k^0, \chi, 0, 0) \tag{1.211}$$

the lightlike condition yelds

$$(k^0)^2 = \frac{a^2}{1 - kr^2} \chi^2 \tag{1.212}$$

for any polarization χ. The polarization is normalized by definition: $\chi^2 = 1$. It is easy to find that under our conventions

$$I = f(k^0)^2 \tag{1.213}$$

and consequently

$$dI = (k^0)^2 k^\mu \nabla_\mu f \tag{1.214}$$

since the operator $k^\mu \nabla_\mu$ annihilates k^0 as a consequence of the geodesics equation. Computing $k^\mu \nabla_\mu f$ is now an easy task, since

$$0 = \nabla_\mu (k^\mu f) = k^\mu \nabla_\mu f + f \nabla_\mu k^\mu \tag{1.215}$$

and so

$$dI = -(k^0)^2 f \nabla_\mu k^\mu \tag{1.216}$$

Then, the flux trough an area dA is constant along the rays, because

$$d^2 F = d(I dA) = -f(k^0)^2 \nabla_\mu k^\mu + f(k^0)^2 d^2 A = 0 \tag{1.217}$$

since $d^2 A = (\nabla_\mu k^\mu) dA$, by definition of derivative along the ray.

1.8.2 Reciprocity

We have shown that IdA is constant along a bundle of light rays. Now we are interested in finding the generalization to curved manifolds of the standard geometric relation linking the cross-sectional area dA with the distance and the solid angle $d\Omega$ subtended at the observer

$$dA = r^2 d\Omega \tag{1.218}$$

We consider a source S and an observer O. A bundle of light rays diverging from the observer substends $d\Omega_O$ at the observer and at some point at distance r_O it cuts a cross-sectional area dA_O. We define the same objects for the source, in analogy with the observer. Separately

$$dA_S = r_S^2 d\Omega_S \tag{1.219}$$

and

$$dA_O = r_O^2 d\Omega_O \tag{1.220}$$

hold.

We can find a relation among the two area distances r_O anmd r_S assuming that the bundle diverging from the source converges to the observer.

Reciprocity Theorem (Etheringthon) 1 *The area distances r_O and r_S satisfy*

$$r_S^2 = r_O^2 (1+z)^2 \tag{1.221}$$

provided that z is the redshift of the source.

Proof: If k_S^μ is the tangent vector to the outgoing bundle and k_O^μ is the tangent vector to the incoming one, necessarily at the observer $k_O^\mu = k_S^\mu$ on a common geodesic. Let λ and ρ affine parameters and p_S^μ and p_O^μ be connecting vectors for the related bundles. The following equations hold by definition:

$$k_S^\nu \nabla_\mu k_S^\mu = 0 \tag{1.222}$$
$$k_O^\nu \nabla_\nu k_O^\mu = 0 \tag{1.223}$$
$$k_S^\nu \nabla_\nu p_S^\mu = p_S^\nu \nabla_\nu k_S^\mu \tag{1.224}$$
$$k_O^\nu \nabla_\nu p_O^\mu = p_O^\nu \nabla_\nu k_O^\mu \tag{1.225}$$

These equations together are equivalent to the geodesic deviation equations, which reads

$$\frac{d^2 p_S^\mu}{d\lambda^2} + R^\mu_{\alpha\beta\gamma} k_S^\alpha p_S^\beta k_S^\gamma = 0 \tag{1.226}$$
$$\frac{d^2 p_O^\mu}{d\rho^2} + R^\mu_{\alpha\beta\gamma} k_O^\alpha p_O^\beta k_O^\gamma = 0 \tag{1.227}$$

Along the common geodesic, $R^\mu_{\alpha\beta\gamma} k_S^\alpha k_S^\gamma = R^\mu_{\alpha\beta\gamma} k_O^\alpha k_O^\gamma$, then we can write

$$p_O^\mu \frac{d^2 (p_\mu)_O}{d\rho^2} = p_S^\mu \frac{d^2 (p_\mu)_S}{d\lambda^2} \tag{1.228}$$

Therefore, on the common path

$$p_O^\mu \frac{d(p_\mu)_O}{d\rho} - p_S^\mu \frac{d(p_\mu)_S}{d\lambda} = A \tag{1.229}$$

for an arbitrary constant A. The constant is easily determined at the observer and gives

$$g_{\mu\nu} p_S^\mu p_O^\nu \big|_S + g_{\mu\nu} p_O^\mu p_S^\nu \big|_O = 0 \tag{1.230}$$

To find the connecting vectors we remember that p_S^μ is orthogonal to source four-velocity at the source and the the same relation holds for k_O^μ and the observer four-velocity at the observer.

We arbitrarly choose a pair of connecting vectors p_1^μ and p_2^μ among all the possible connecting vectors p_S^μ satisfying

$$\frac{dp_1^\mu}{d\lambda} \frac{dp_{\mu(2)}}{d\lambda}\bigg|_S = 0 \tag{1.231}$$

The angle among p_1^μ and p_2^μ at the observer is arbitrary. Changing the angle at the source changes the angle at the observer, so we can always find a pair of connecting vectors that satisfy

$$p_1^\mu p_{\mu(2)}\big|_O = 0 \tag{1.232}$$

too, rememberring that isotropy holds. For the same reasons we can find p_3^μ and p_4^μ among the connecting vectors p_O^μ satisfying

$$\begin{aligned}
p_{\mu(3)} \frac{dp_2^\mu}{d\lambda}\bigg|_S &= 0 && (1.233)\\
p_{\mu(4)} \frac{dp_1^\mu}{d\lambda}\bigg|_S &= 0 && (1.234)\\
p_{\mu(1)} \frac{dp_3^\mu}{d\rho}\bigg|_O &= 0 && (1.235)\\
p_{\mu(2)} \frac{dp_4^\mu}{d\rho}\bigg|_O &= 0 && (1.236)\\
p_3^\mu p_{\mu(4)}\big|_S &= 0 && (1.237)\\
\frac{dp_3^\mu}{d\rho}\frac{dp_{\mu(4)}}{d\rho}\bigg|_O &= 0 && (1.238)
\end{aligned}$$

These equations follows from our suitable choices of connecting vectors and allows for computing the soling angles $d\Omega_S$ and $d\Omega_O$. Indeed:

$$\begin{aligned}
dA_S &= p_1 p_2\big|_O && (1.239)\\
dA_O &= p_3 p_4\big|_S && (1.240)\\
d\Omega_S &= \frac{dp_1}{d\lambda}\frac{dp_2}{d\lambda}\bigg|_S && (1.241)\\
d\Omega_O &= \frac{dp_3}{d\rho}\frac{dp_4}{d\rho}\bigg|_O && (1.242)
\end{aligned}$$

Combining with Eq. 1.230 we simply find

$$d\Omega_S dA_O (k^\mu u_\mu)_S^2 = d\Omega_O dA_S (k^\mu u_\mu)_O^2 \tag{1.243}$$

which implies

$$r_S^2 = r_O^2(1+z)^2 \tag{1.244}$$

The Reciprocity Theorem is one of the most useful statement in observational cosmology. It simply generalizes the idea that two observers at rest with respect to each other see themeselves subtending the same solid angle, like in ordinary geometry. On the other hand, when relative motion is allowed the non-standard geometry modifies this symmetry. If the relative motion arises due to dynamical effects of the spacetime, the symmetry is broken by redshif effects. The crucial feature of this theorem is the generality of the underlying assumptions. Nowhere General Relativity enters the proof and only metricity is needed. This implies that reciprocity is strictly linked to our description of the spacetime as a Riemaniann manifold and it should work whatever theory of gravity we assume, provided that Riemaniann geometry is made safe. In principle, however, we should be careful to remember that the geometric optics approximation is working silently and the Reciprocity Theorem alone would be useless, because the source area distance r_S is not measurable. We need to define a measurable luminosity distance and building a consistent definition requires the geometric optics too.

In order to define the luminosity distance, we remember that we observe a flux from a distance source along some bundle of null rays which subtends a solid angle $d\Omega_S$ at the source and has a cross-sectional area dA_S at the observer. Locally around the source we can alway find a Lorentz transformation that makes the space Minkowskian, implying that we can compute the luminosity by integrating the local flux F_S on a sufficently small sphere, centered in the source, using euclidean geometry:

$$L = \int F_S dA = 4\pi F_S \tag{1.245}$$

We have implicitly assumed an isotropic emission of energy at the source.

From the geometric optics approximation we found that the combination FdA scales as $(1+z)^2$ along a bundle of null geodesics, so we can

apply the scaling in order to compute the luminosity by integrating the flux F on a far away surface. The scaling rule requires

$$(1+z)^2 F r_S^2 d\Omega_S = F_S d\Omega_S \tag{1.246}$$

which gives

$$F = \frac{L}{4\pi(1+z)^2 r_S^2} \tag{1.247}$$

after the integration over the spherical angles. The luminosity distance is then

$$D_L^2 = r_S^2 (1+z)^2 \tag{1.248}$$

Expanding r_O^2 with the reciprocity theorem we find

$$D_L^2 = D_A^2 (1+z)^4 \tag{1.249}$$

since we recognized that the observed area distance corresponds to the angular diameter distance by construction. This well-known relation is often used to test cosmology against data, since it gives a prescription for writing the luminosity distance in terms of the Hubble parameter $H(a)$.

Another useful relation arising from the geometric optics approximation is the *optical theorem*. If $I_\omega(O)$ and $I_\omega(S)$ are the intensities in the band ω at the observer and at the source respectively, from the Reciprocity Theorem it follows

$$I_\omega(O) = \frac{I_{(1+z)\omega}(S)}{(1+z)^3} \tag{1.250}$$

and the direct integration over all frequencies gives

$$\int I_\omega(O) d\omega = \int \frac{I_x(S)}{(1+z)^4} dx \tag{1.251}$$

where $x = (1+z)\omega$. Then the integrated intensities satisfy

$$I(O) = \frac{I(S)}{(1+z)^4} \tag{1.252}$$

The main consequences of this relation regard the Cosmic Microwave Background. Indeed the blackbody spectrum remains blackbody through cosmological expansion and the corresponding temperature scales as $(1+z)$, accordingly to the scaling law of photon energy in the FRW spacetime derived from the geodesic motion.

1.9 Dark Energy

Dark Energy is one of the widest field in current cosmological research, both on the observational and on the theoretical fields. We introduced Dark Energy (DE) as a postulated cosmological fluid characterized by a negative w. Physically the fluid is exerting a negative pressure, which may seem very strange. The physical interpretation of this strange assumption requires some care

1.9.1 Deceleration parameter

For the FRW spacetime, we can define a *deceleration parameter*

$$q_0 = -\frac{\ddot{a}a}{\dot{a}^2} = -\frac{\ddot{a}}{a}\frac{1}{H^2} \tag{1.253}$$

We can simplify the definition using both Friedmann equations:

$$q_0 = \frac{\rho + 3p}{2\rho - \frac{3k}{a^2}} \tag{1.254}$$

We see that the sign of q_0 depends strictly from the combination $\rho+3p$, because the denominator is always positive (being H^2). Rememberring that $p_i = w_i\rho_i$, we can generalize the definition to

$$q_0 = \frac{\sum_i \rho_i(1+3w_i)}{2\sum_i \rho_i - \frac{3k}{a_2}} \tag{1.255}$$

in the case of many cosmological fluids. It is easy to see that the numerator is always positive for ordinary matter and radiation, since w_i is positive. This proves that the Universe expansion is always decelerating if ordinary matter fills the Universe. This deduction is mathematically easy, but physically obviuos! The Universe is filled by matter and energy that exert

gravity. The gravitational field acts only as an attractive force and so matter and energy filling the Universe naturally evolve as collapsing. The spacetime is consequently dragged and the expansion must be decelerated. This interpretation seems easy, but General Relativity is working in full power. On the other hand, if at least one of the w_i satisfies $w_i \leq -1/3$, the deceleration parameter may vanish or become negative. Observations of nearby type Ia supernovae (SN Ia) has demonstrated that the observed Universe is undergoing a phase of accelerated expansion (see [1, 2, 3, 4] and references therein) which is in contrast with theoretical deductions from the Standard Model.

Introducing Dark Energy is a way of solving this problem. If we postulate that a cosmological fluid exists such that $w_{DE} < 0$ we are able to find a negative q_0. In order to handle the negative pressure, we remember that we may give an interpretation using the First Law of Thermodynamics. It is well known that we may write the First Law as

$$dE = \delta L + \delta Q \tag{1.256}$$

defining the total differential of the internal energy E as the sum of two contributions. On the other hand we can slightly change the definition reversing the sign of the elementary work δL writing

$$dE = \delta Q - \delta L \tag{1.257}$$

These definitions are mathematically different, but physically no difference arises and the two formulations of the First Law equally work well. They are clearly inconsistent with each other, but the only real problem in handling these definition is using a consistent notation if other physical laws are needed in computations. This ambiguity is the basic freedom of choosing arbitrarly whether positive works are those made **upon** the thermodynamical system or those made **by** the thermodynamical system. The apparent contraddiction is simply solved understanding that the two definitions are describing the same physical system behaving in the same way. If we mix the two descriptions we find an apparently inconsistency because a thermodynamical system described by the former definition of the First Law behaves exactly in the opposite way it should behave if all others physical laws are consisten with the latter formulation of the First law. Since in general we can write that

$$\delta L = pdV \tag{1.258}$$

we see that any ambiguity in defining the sign of the pressure reflects on the First Law exchanging the two definitions. It easy to argue that a negative pressure fluid can be seen as a fluid behaving in the opposite way standard fluids behave from a thermodynamical point of view. So we can look at DE as a fluid behaving opposite to ordinary matter and radiation. Since ordinary matter acts on the dynamical history of the FRW spacetime slowing down the expansion, DE accelerates it and easily we can imagine DE acting as a source of repulsive gravity.

1.9.2 Cosmological constant

The first attempts of introducing terms which acts as sources of repulsive gravity where made by Einstein. He was not convinced that General Relativity was not able to predict a static spacetime describing our Universe. Since static solutions where not allowed, Einstein modified the field equations adding an extra term

$$R_{\mu\nu} - \frac{1}{2} g_{\mu\nu} R + \Lambda g_{\mu\nu} = 8\pi G T_{\mu\nu} \tag{1.259}$$

where the constant Λ was called *Cosmological Constant*. The only generalization of the Einstein tensor $G_{\mu\nu} = R_{\mu\nu} - \frac{1}{2} g_{\mu\nu} R$ requires care. Taking the covariant derivative of both terms of the Einstein equations gives

$$\nabla^\mu G_{\mu\nu} = 8\pi G \nabla^\mu T_{\mu\nu} \tag{1.260}$$

The last term vanishes as a consequence of the continuity equation, and so the Einstein tensor must satisfy $\nabla^\mu G_{\mu\nu} = 0$. The combination

$$R_{\mu\nu} - \frac{1}{2} g_{\mu\nu} R \tag{1.261}$$

satisfy this strict condition for geometrical reasons only, as a consequence of Bianchi identities. Then, any consistent generalization should require to satisfy the constraint only for geometrical reasons based on the Bianchi identities. It is possible to demonstrate that the rank-2 tensors satisfying

$$\nabla_\mu T_{\alpha\beta} \tag{1.262}$$

are $g_{\mu\nu}$ and $R_{\mu\nu}$. Then, the only possible generalization of the Einstein tensor based only on the geometric properties of the spacetime is adding a term proportional to the metric.

If we move the cosmological constant on the r.h.s of Einstein equations, we find that generalizing the Einstein tensor is equivalent to add an extra term, proprtional to $g_{\mu\nu}$ to the stress-energy tensor of the perfect fluids filling the Universe. The new tensor is given by

$$T_{\mu\nu}^{new} = T_{\mu\nu} - \frac{\Lambda g_{\mu\nu}}{8\pi G} \tag{1.263}$$

Rememberring that the stress-energy tensor for the cosmological fluids is

$$T_{\mu\nu} = \rho u^{\mu} u^{\nu} + p g_{\mu\nu} \tag{1.264}$$

we see that the cosmological constant may be treated as cosmological fluid exerting a pressure $-\Lambda/(8\pi G)$. If Λ takes positive values, then the fluid exerts a negative pressure. This point of view suggested the idea of DE in analogy with the Cosmological Constant, but some care is required. The energy-momentum tensor of the Λ does not contain any term proportional to the density. This shows that the analogy with standard cosmological fluids is dangerous, sice the only way of annihilating $\rho u^{\mu} u^{\nu}$ seems to set $u^{\mu} = 0$. This singularity would break General Relativity and would prove that the fluid corresponding to the Cosmological Constant cannot be treated as a collection of comoving observers.

If we want to carry on the analogy, we need to find an equation of state for the fluid corresponding to Λ. The energy density ρ_{Λ} does not appear in the energy-momentum tensor of the Cosmological Constant, suggesting to follow a different way. We showed that any cosmological fluid exert a pressure which enter the lagrangian through the projection

$$\Pi^{\mu\nu} = h^{\mu\alpha} h^{\nu\beta} p_{\alpha\beta} \tag{1.265}$$

on the hypersurfaces orthogonal to the four-velocity u^{μ}. If we want to annihilate the kinetyic term into the stress-energy tensor, we can assume that the pressure of the fluid corresponding to Λ is simply

$$\Pi_{\Lambda}^{\mu\nu} = -\frac{\Lambda}{8\pi G} g^{\mu\nu} - \rho_{\Lambda} u^{\mu} u^{\nu} \tag{1.266}$$

where we have restored a non-null four-velocity u^μ for the fluid and its density ρ_Λ. In other words we want to solve the tensorial equation

$$\Pi_\Lambda^{\mu\nu} = h^{\mu\alpha}h^{\nu\beta}p_{\alpha\beta} \tag{1.267}$$

for the unknown $p_{\alpha\beta}$. We have already rememberred that the only structure of $p_{\alpha\beta}$ consistent with the symmetry properties of the spacetime is $p_{\alpha\beta} = pg_{\alpha\beta}$. This implies that the tensor $\Pi_\Lambda^{\mu\nu}$ of the vacuum (we can imagine that the Cosmological Constant as an intrinsic property of the geomtery of the spacetime) must have the standard form

$$\Pi_\lambda^{\mu\nu} = p(u^\mu u^\nu + g^{\mu\nu}) \tag{1.268}$$

Simple comparison with Eq. 1.266 provides the solution

$$p = -\frac{\Lambda}{8\pi G} \tag{1.269}$$

$$\rho_\Lambda = \frac{\Lambda}{8\pi G} \tag{1.270}$$

The relation between the energy density and the pressure of the vacuum is then

$$p_\lambda = -\rho_\Lambda \tag{1.271}$$

or equivalently

$$w_\Lambda = -1 \tag{1.272}$$

Taking the continuity equation $\nabla_\mu T^{\mu 0} = 0$, gives

$$\dot{\rho} + 3H(\rho + p) = 0 \tag{1.273}$$

for any cosmological fluid. In the case of the Cosmological Constant we see that $p + \rho = 0$ and the energy density ρ_Λ is constant in time.

The value of Λ can be measured from cosmological observations, while the density ρ_Λ can, in priniciple, be computed from prime principles as the vacuum expectation value of hamiltonian in a given quantum description of gravity. It is well known that this approach fails, since the predicted values

of the density ρ_Λ are ~ 120 order of magnitudes bigger than the value computed by measuring the cosmological parameter $\Omega_\Lambda = \rho_\lambda/\rho_c$. The longstanding problem of matching the cosmological prediction of λ with Quantum Field Theory is a crucial point in current research. Observations specify that some DE contribution should exist and the Λ is the best candidate.

1.9.3 Quintessence

Quintessence was introduced by Wetterich ([64]) for solving the fine-tuning problem of a very small Cosmological Constant. The crucial role is played by a suitable field, which describes Dark energy. Here we review how a canonical scalar field may play the role of DE, generalizing the Cosmological Constant. It is not necessary to quantize the field for computing the energy density of quintessence.

The lagrangian of a relativistic spin-0 scalar field ϕ on Minkowki spacetime is

$$L = \frac{1}{2}\partial_\mu\phi\partial^\mu\phi - \frac{1}{2}m^2\phi^2 \tag{1.274}$$

The corresponding Euler-Lagrange equation is the Klein-Gordon equation

$$\partial^\mu\partial_\mu\phi - m^2\phi^2 = 0 \tag{1.275}$$

which correctly describe the dynamics of a relativistic wave. We can generalize the $m^2\phi^2$ term, which corresponds to Yukawa's potential, to any function $V[\phi]$ describing any long-ranged behaviour of the field. Then, we can minimally couple the field to the metric tensor, generalizing the differential operators covariantly. The lagrangian becomes

$$L = \frac{g^{\mu\nu}}{2}\nabla_\mu\phi\nabla_\nu\phi - V[\phi] \tag{1.276}$$

provided that it is integrated over the measure $\sqrt{-\det(g)}d^4x$ in the action. Consequently the Euler-Lagrange equations become

$$\frac{1}{\sqrt{-\det(g)}}\partial_\mu(\sqrt{-\det(g)}g^{\mu\nu}\partial_\nu\phi) + \frac{\delta V}{\delta\phi} = 0 \tag{1.277}$$

which describe relativistic waves on a curved space.

The solution of the Klein-Gordon equation on a curved manifold is much easier if the metric is block diagonal, since a separable solution exists. In the case of the FRW metric we notice that the Klein-Gordon equations reduces to ($g = \det(g)$)

$$-\frac{1}{\sqrt{-g}}\partial_t(\sqrt{-g}\partial_t\phi) + \frac{1}{a^2}\nabla_r^2\phi + \frac{1}{a^2r^2}\nabla_{S^2}^2\phi + V'[\phi] = 0 \tag{1.278}$$

We defined

$$\nabla_r^2\phi = \frac{2}{r}\frac{d\phi}{dr} - 4kr\frac{d\phi}{dr} + (1-kr^2)\frac{d^2\phi}{dr^2} \tag{1.279}$$

$$\nabla_{S^2}^2\phi = \frac{1}{\sin(\theta)}\partial_\theta(\sin(\theta)\partial_\theta\phi) + \frac{1}{\sin^2(\theta)}\partial_\psi^2\phi \tag{1.280}$$

The additivity of the Laplacian allows a solution $\phi(t, r, \theta, \psi) = A(t)B(r)C(\theta, \psi)$ The operator $\nabla_{S^2}^2$ is the standard Laplacian on the 2-sphere S^2. We know that the SO(3) spherical harmonics $Y_{lm}(\theta, \phi)$ are solutions to the Laplace equation on the sphere, so the angular part of the quintessence field can be written as a superposition of spherical harmonics. The radial part of the Laplacian ∇_r^2 is clearly dependent on the FRW form of the metric. It is eay to see that if $k = 0$, then ∇_r^2 is the radial part of the Laplacian describing waves propagating inside a sphere and the whole spatial part of the Klein-Gordon equation reduces to the Helmoltz equation. For $k \neq 0$ the Sturm-liovulle problem

$$\frac{1}{r^2}\nabla_r^2 B(r) + \frac{l(l+1)}{r^2}B(r) + K^2B(r) = 0 \tag{1.281}$$

can be solved only if the case of a free field. Here $l(l+1)$ is the eigenvalue of the spherical harmonic Y_{lm} under the action of $\nabla_{S^2}^2$ and K^2 is the separation constant coming from the time sector of the Klein-Gordon equation. The time dependence is easily computed inserting the FRW metric and gives

$$-\frac{1}{\sqrt{-g}}\partial_t(\sqrt{-g}\partial_t\phi) = -\ddot{\phi} - 3H\dot{\phi} \tag{1.282}$$

The cosmic acceleration acts as a dragging term into the equation dumping the vawe amplitude.

A general solution is not easy, but assuming that the quintessence field is slowly varying in space

$$|\partial_i \phi| << \dot{\phi} \tag{1.283}$$

the Klein-Gordon equation takes the simple form

$$\ddot{\phi} + 3H\dot{\phi} + \frac{\delta V}{\delta \phi} = 0 \tag{1.284}$$

Computing the stress-energy tensor of the field is easy

$$T_{\mu\nu} = \nabla_\mu \phi \nabla_\nu \phi - \frac{1}{2} g_{\mu\nu} \nabla_\alpha \phi \nabla^\alpha \phi + V[\phi] g_{\mu\nu} \tag{1.285}$$

The pressure and the density of the field are the diagonal terms of the stress-energy tensor. Under our assumptions we find

$$\rho = \frac{1}{2}\dot{\phi}^2 + V[\phi] \tag{1.286}$$

$$p = \frac{1}{2}\dot{\phi}^2 - V[\phi] \tag{1.287}$$

If we look at the field as a fluid filling the Universe, we can define the corresponding equation of state and the w parameter

$$w = \frac{\frac{1}{2}\dot{\phi}^2 + V[\phi]}{\frac{1}{2}\dot{\phi}^2 - V[\phi]} \tag{1.288}$$

which takes values $-1 \leq w \leq 1$. For negative values the scalar field it behaves like a Dark Energy component, sourcing the cosmic acceleration. In principle any value in the interval may be reproduced by the scalar field, for a suitable form of the potential. Here we are not interested in further details, since no other consequences will be useful for our analysis of the backreaction model.

Chapter 2

CMB

The Cosmic Microwave Background Radiation (CMB or CMBR) was discovered in 1964 by Penzias and Wilson [65] . They discovered an almost homogeneous and isotropic emission in the microwave band all over the sky. The quite uniform emission of the background has a blackbody spectrum with temperature around 2.7 K. The present measured value of the temperature of the CMB [66] is

$$T_{CMB} = 2.72548 \pm 0.00057 \quad \text{K} \tag{2.1}$$

The CMB is considered as the most important fingerprint of the Big Bang, the primordial singularity corresponding to the $a \to 0$ limit of the FRW metric. Near the singularity the energy density of the cosmological fluids filling the early Universe become singular and, correspondingly, the temperature diverges. Assuming that the cosmological fluids are composed by particles in equilibrium, it seems easy to understand that the fundamental forces tend to unification. This fascinating aspect of the Hot Big Bang model faces longstanding theoretical problems due to the renormalization scheme of the coupling constants and the need of Supersymmetry. Here we are not interested in discussing these aspects, but we want to remember that the main consequence of unification is the possibility that at sufficently high energies particles may couple and exert forces that are completely suppressed at lower energies. The idea of Unification has been supported since the experimental evidence of the vector bosons $W^{\pm}$ and Z^0 (see [67] and references therein) showed that the weak force

and the electromagnetic force are consequences of symmetry breaking. At high energies the two forces are unified and while energy decreases the bigger symmetry among particles exerting electroweak interaction breaks down to smaller symmetries (see for instance [68, 69]). The breaking scale is fixed around 250 GeV, corresponding to the Higgs vacuum expetation value. The Higgs mechanism [70] works behind the symmetry breaking: the electroweak hypercharge symmetry $SU(2) \times U(1)_Y$ breaks down to the abelian electromagnetic symmetry $U(1)_{em}$ and four Goldstone bosons arise (there are as many Goldstone bosons as many broken generators of symmetry). Three of them (the three gauge bosons of the weak force) acquire a mass too, while the last field (the photon) remains massless. At lower energies we can only experiment two distinct sectors of the original theory, corresponding to the weak force and to the electromagnetic force separately.

Unification suggest the path for constructing a model for the CMB. If we are able to see the CMB, photons must be decoupled from matter, which means that the energy of the primordial Universe has already dropped down the decoupling treshold. The hot Universe cools due to expansion and the fields of elementary particles undergo spontaneous symmetry breaking. When photons decouple from ordinary matter the cross section of ordinary matter to photons has dropped down a critical treshold. The only remaining forces we experiment significantly are gravity and electromagnetic force, which must be considered in our picture of the primordial fluid we look at through CMB. Along our discussion we follow [71].

2.1 Photon-baryon fluid

We can model the primordial fluid as an equilibrium ensemble of matter and radiation. The present evidence of Dark Matter requires to divide the matter content of the fluid in a Dark component, which is completely decoupled from photons at any epoch, and a baryon component, which experiences electromagnetic interaction. The term *baryonic matter* does not refer to the elementary field content of the particles, but only to the non-trivial behavior with respect to the interaction with the gauge field A_μ, in contrast to Dark Matter. For this reason electrons and positrons

are considered as baryonic matter, altought they are leptons.

Dark Matter interacts with baryons gravitationally, while baryons are coupled to photons up to the decoupling epoch. After decoupling baryons and Dark Matter interacts gravitationally and enter the expansion history of the Universe as the standard matter component. For this reason we will review the physics of the photon-baryon fluid which is at the basis of our current observations of the CMB.

The photon-baryon fluid is dominated by electromagnetic processes. If the energy is sufficently high weak interactions may occur; otherwise, when the center of mass energy drops due to cosmic expansion, leptonic processes are suppressed, but the fluid is still thermally hot for ionizing atoms. We can model the fluid as an ensemble of electrons, photons, and ionized nuclei, which we can assume as free protons.

When matter and photons are coupled by high energy intercations pair production and photon production by pairs annihilation are allowed. Since the photon baryon fluid contains free electrons, Compton scattering of free photons is always allowed. While the energy drops, photon absorption and emission by ionized nuclei becomes important. Ionized nuclei can capture a photon and recombine with free electrons, forming a neutral atom. At the same time an energetic photon may scatter on a neutral atom and ionize the nucleus. This equilibrium process dominates the photon-baryon fluid near decoupling and ends when a huge fraction of matter has recombined. The mean free path of photons increases as recombination goes on and the process ends with decoupled photons.

2.1.1 Annihilations

Annihilations are common elementary processes. They are standard tree-level interactions in quantum field theories of fundamental forces. Leptonic particle-antiparticle annihilations are typical s-channel processes, such as Bhabha scattering, which is well described in Quantum ElectroDynamics (QED). If the annihilation is mediated by the weak interaction the charged current coupling allows the t-channel contribution too.

While the energy of the photon-baryon fluid drops due to cosmic expansion, annihilation cross sections drops too. For instance leptonic e^+e^- annihilations into leptons and weak processes, like Dark Matter annihilation into leptons or inverse β-decay involving protons, neutrons, neutrinos

and leptons progressively vanish. Here we will show how cross sections of elementary processes behave while energy is decreasing.

The tree-level annihilations involve two species annihilating into other two species. This four-point process affects the abundance of the species in the photon-baryon fluid. We assume that all the species involved are in equilibrium and the annihilation processes mantain the equilibrium while the Universe is sufficently hot. When the Universe cools, the annihilation rate drops and the reaction is freezed out, breaking the equilibrium and leaving a cosmological relic density of elementary particles that, in priciple, can tell us informations about the early Universe.

During the annihilation $1 + 2 \longleftrightarrow 3 + 4$ the time evolution of the number density of a given particle is driven by the Boltzmann equation

$$\frac{1}{a^3}\frac{d(na^3)}{dt} = \int \prod_{i=1}^{4} (dk_i)(2\pi)^4 \delta^{(4)}(k_1 + k_2 - k_3 - k_4) \times \\ [f_3 f_4 (1 \pm f_1)(1 \pm f_2) - f_1 f_2 (1 \pm f_3)(1 \pm f_4)] |\bar{\mathcal{M}}|^2 \tag{2.2}$$

We defined

$$(dk_i) = \frac{d^3 k_i}{(2\pi)^3 2E_{k_i}} \tag{2.3}$$

the Lorentz-invariant integration measure, where $E_{k_i}^2 = k_i^2 + m_i^2$. The delta function enforces the four-momentum conservation at the annihilation vertex, $|\bar{\mathcal{M}}|^2$ is the unpolarized average probability amplitude of the annihilation and f_i are the phase-space distribution functions of the involved particles. The S-matrix element $\mathcal{M}$ is averaged over the incoming spin states and summed over the outcoming ones. Fundamental interactions driving the annihilation processes enter the Boltzmann equation through the transition matrix $\mathcal{M}$.

The distribution functions under kinetic equilibrium are the well know Fermi-Dirac (for fermions) and Bose-Einstein (for bosons) functions

$$f(E) = \frac{1}{e^{\frac{E-\mu}{kT}} \pm 1} \tag{2.4}$$

up to a normalization constant. The + sign corresponds to Bose-Einstein distribution. The ensemble temperature T defines the reference energy kT,

provided that k is Boltzmann constant. This energy defines a critical scales at which quantum effects on the distribution become important, due to the quantum difference between fermions and bosons. If the exponential is overwhelming with respect to 1, as it is if $kT << E - \mu$, then $f(E)$ converges to the Boltzmann ditribution function and no deviation from the classical behavior can be probed, from a statistical point of view, due to quantum effects. Under this limit the fermion/boson diffference itself is completely negligible.

While the Universe expands the energies are bigger than the standard quantum kT and we neglect quantum effects on the distribution functions. The last factor in the Boltmann equation becomes

$$e^{\frac{E_1+E_2}{T}}\left(e^{\frac{\mu_3+\mu_4}{T}}-e^{\frac{\mu_1+\mu_2}{T}}\right) \tag{2.5}$$

where the chemical potentials are separated. Since

$$n_i = g_i e^{\frac{\mu_i}{T}}\int\frac{d^3k}{(2\pi)^3}e^{-\frac{E_i}{T}} \equiv n_i^0 e^{\frac{\mu_i}{T}} \tag{2.6}$$

(g_i is the statistical weight of the i-th particle, corresponding to the number of different spin states) we can simplify Boltzmann equation for annihilations such that

$$\frac{1}{a^3}\frac{d(a^3n)}{dt} = n_1^0 n_2^0\left(\frac{n_3n_4}{n_3^0n_4^0}-\frac{n_1n_2}{n_1^0n_2^0}\right)\langle\sigma v\rangle \tag{2.7}$$

provided that

$$\langle\sigma v\rangle = \frac{1}{n_1^0n_2^0}\int\prod_{i=1}^{4}(dk_i)e^{-\frac{E_1+E_2}{T}}(2\pi)^4\delta^{(4)}(k_1+k_2-k_3-k_4)|\bar{\mathcal{M}}|^2 \tag{2.8}$$

is the *thermally averaged cross section* of the process. The Boltzmann equation tells clearly that if $n_1n_2\langle\sigma v\rangle$ is larger than the expansion time H^{-1}, the left hand side is negligible and the only solution is the *Saha* equilibrium condition

$$\frac{n_1n_2}{n_1^0n_2^0} = \frac{n_3n_4}{n_3^0n_4^0} \tag{2.9}$$

corresponding to statistical equilibrium. Since $n_1 n_2 \langle \sigma v \rangle$ measures the efficency of the annihilation process, we see that highly efficent annihilations mantain equilibrium in the photon baryon fluid, as we assumed.

Here we will show that the thermally average cross section of annihilations drops significantly while the Universe expands and then equilibrium is broken. We look at interactions mediated by the weak force, like inverse β-decay, Dark Matter annihilation or proton-electron annihilation through W exchange. The inverse β-decay reaction is given by the crossing theorem from the standard neutron β-decay, reversing the electronic antineutrino final state into an ingoing neutrino:

$$n + \nu_e \longleftrightarrow p + e^- \tag{2.10}$$

The tree-level interaction follows the t-channel, due to charge selection rules, and a W^- gauge bosons is exchanged. The electron-proton annihilation mediated by the weak force is the opposite process $p + e^- \longleftrightarrow n + \nu_e$. It may seem that the two iteractions are exactly the same, but the latter one is mediated by the W^+.

We follow Peskin & Schroeder notations (see [72]) for computing the thermally averaged cross-section. Then, only for consistency, we assume that the Minkowski metric $\eta_{\mu\nu}$ is defined with reversed signs $\eta_{\mu\nu} = diag(1, -1, -1, -1)$. The Dirac gamma matrices satisfy the Clifford algebra

$$\{\gamma^\mu, \gamma^\nu\} \equiv \gamma^\mu \gamma^\nu + \gamma^\nu \gamma^\mu = 2\eta^{\mu\nu} \tag{2.11}$$

and their adjoint representation is given by $(\gamma^\mu)^\dagger = \gamma^0 \gamma^\mu \gamma^0$. The projectors onto definite helicity states (left-handed and right-handed spinors) are

$$P_L = \frac{1 - \gamma^5}{2} \qquad P_R = \frac{1 + \gamma^5}{2} \tag{2.12}$$

where $\gamma^5 = i\gamma^0\gamma^1\gamma^2\gamma^3$. Since P_L and P_R are projectors onto orthogonal states they satisfy $P_L P_R = P_R P_L = 0$ and the standard idempotency rule $P^2 = P$.

The fundamental spinors $u_\lambda(k)$ and $v_\lambda(k)$ satisfy the completeness relations

$$\sum_{\lambda} u_{\lambda}(k)\bar{u}_{\lambda}(k') = (\gamma^{\mu}k_{\mu} + m)\delta(k - k') \tag{2.13}$$

$$\sum_{\lambda} v_{\lambda}(k)\bar{v}_{\lambda}(k') = (-\gamma^{\mu}k_{\mu} + m)\delta(k - k') \tag{2.14}$$

provided that $\bar{u} = u^{\dagger}\gamma^{0}$ and $\bar{v} = v^{\dagger}\gamma^{0}$.

The propagator of the massive gauge bosons W^{+} and W^{-} is

$$\Delta_{\mu\nu}(q^2) = \frac{\eta_{\mu\nu} - \left(1 - \frac{1}{\xi}\right)\frac{q_{\mu}q_{\nu}}{q^2}}{q^2 - M_W^2 + i\epsilon} \tag{2.15}$$

where M_W is their rest mass and q^{μ} is the transferred four-momentum. We gauge fix assuming Feynman-t'Hooft condition $\xi = 1$, which corresponds to suppressing Fadeev-Popov ghost fields.

We simplify our rough calculations treating the neutron and the proton like structerless fermions, which corresponds to disregarding completely QCD prescriptions for hadron structure. Then, we treat protons and neutrons as leptons interacting weakly, like neutrinos. The coupling constant g of the charged current to leptons is given by the Glashow-Weinberg-Salam prescription

$$g = \frac{e}{\sin(\theta_W)} \tag{2.16}$$

where e is the electron charge and $\sin(\theta_W) \sim 0.22$ is the sine of the Weinberg rotation angle, responsible of the mass of the gauge bosons in the electroweak symmetry breaking mechanism.

For the computation of the transition amplitude we fix the center of mass frame. The incoming proton and electron interact leaving the outgoing neutron and neutrino. The momenta

$$p^{\mu} = (E, 0, 0, p) \qquad e^{\mu} = (p, 0, 0, p) \tag{2.17}$$

are the proton and electron four-momentum respectively in the center of mass frame. Conservation of the four-momentum in the interaction requires that neutron and neutrino momenta satisfy

$$n^\mu = (E, 0, p\sin(\theta), p\cos(\theta)) \qquad \nu^\mu = (p, 0, -p\sin(\theta), -p\cos(\theta)) \quad (2.18)$$

provided that θ is the angle between the outcoming direction of the neutron and the incoming direction of the proton. The energy E is given by $E^2 = p^2 + m^2$, where m is the proton mass. We assume the simplifying hypothesis that the neutron mass is exactly m and all other leptons are massless.

Than, the S-matrix element $\mathcal{M}$, at the tree level (only the t-channel contributes) in Glashow-Weinber-Salam theory is

$$\mathcal{M} = \left(\frac{ig}{\sqrt{2}}\right)^2 \bar{u}_p \gamma^\mu P_L u_n \frac{\eta_{\mu\alpha}}{q^2 - M_W^2} \bar{u}_\nu \gamma^\alpha P_L u_e \quad (2.19)$$

The unpolarized amplitude is given by averaging over the incoming helicity states and summing over the outgoing ones:

$$|\bar{\mathcal{M}}|^2 = \sum_{helicities} \mathcal{M}\mathcal{M}^* \quad (2.20)$$

It follows

$$\mathcal{M}^* = \left(\frac{-ig}{\sqrt{2}}\right)^2 \bar{u}_n \gamma^\mu P_R u_p \frac{\eta_{\mu\alpha}}{q^2 - M_W^2} \bar{u}_e \gamma^\alpha P_R u_\nu \quad (2.21)$$

When computing $|\bar{\mathcal{M}}|^2$ we can cycle the spinors and the gamma matrices, since a summation over spinor indexes is understood. Using the completeness relation for the fundamental spinors we find

$$\begin{aligned} |\bar{\mathcal{M}}|^2 = \frac{g^4}{16(q^2 - M_W^2)^2} Tr\left[\gamma^\alpha e_\alpha \gamma_\mu P_L \gamma^\beta \nu_\beta \gamma_\nu\right] \\ Tr\left[(\gamma^\alpha p_\alpha + m)\gamma^\nu P_L (\gamma^\beta n_\beta + m) P_R \gamma^\mu\right] \end{aligned} \quad (2.22)$$

The properties of the projectors P_L and P_R simplify the last trace and then

$$|\bar{\mathcal{M}}|^2 = \frac{g^4}{16(q^2 - M_W^2)^2} Tr\left[\gamma^\alpha e_\alpha \gamma_\mu P_L \gamma^\beta \nu_\beta \gamma_\nu\right] Tr\left[\gamma^\alpha p_\alpha \gamma^\nu P_L \gamma^\beta \nu_\beta \gamma^\mu\right] \tag{2.23}$$

since the trace of any odd number of gamma matrices vanish and

$$Tr[\gamma^\mu \gamma^\nu \gamma^5] = 0 \tag{2.24}$$

The two traces in the squared amplitude have the same structure.The Clifford algebra ensures

$$Tr[\gamma^\mu \gamma^\alpha \gamma^\nu \gamma^\beta (1 + \gamma^5)] = 4(\eta^{\mu\alpha}\eta^{\nu\beta} + \eta^{\mu\beta}\eta^{\nu\alpha} - \eta^{\mu\nu}\eta^{\alpha\beta} - i\epsilon^{\mu\alpha\nu\beta}) \tag{2.25}$$

where $\epsilon^{\mu\alpha\nu\beta}$ is the totally antisymmetric rank-4 tensor. The final step is only a matter of rather long algebra, which gives

$$|\bar{\mathcal{M}}|^2 = \frac{g^4}{4(q^2 - M_W^2)^2} e^\alpha \nu^\beta n_\rho p_\sigma (4\delta^\rho_\beta \delta^\alpha_\sigma) = \frac{g^4}{(q^2 - M_W^2)^2} (p \cdot n)(e \cdot \nu) \tag{2.26}$$

where the last two factors are the inner products of the particles four-momenta. In the center of mass frame

$$(p \cdot n) = (e \cdot \nu) = p(E + p) \tag{2.27}$$

and

$$q^2 = (n^\mu - p^\mu)(n_\mu - p_\mu) = -2p^2(1 - \cos(\theta)) \tag{2.28}$$

Finally the squared amplitude becomes

$$|\bar{\mathcal{M}}|^2 = \frac{e^4}{\sin^4(\theta_W)} \frac{p^2(E + p)^2}{(-2p^2(1 - \cos(\theta)) - M_W^2)^2} \tag{2.29}$$

The computation of the thermally average cross section require to integrate over the incoming and outcoming momenta. The integration

$$\int (dk_e)(dk_\nu)|\bar{\mathcal{M}}|^2 \tag{2.30}$$

over the electron and neutrino four-momenta can be heavily simplified remeberring that it is exactly the phase space of the 2-particles final state. The integration gives

$$\int (dk_e)(dk_\nu)|\bar{\mathcal{M}}|^2 = \int \left(\frac{d\sigma}{d\Omega}\right) d\Omega \tag{2.31}$$

where the standard differential cross section appears. In the center of mass frame, under our assumptions, it is [72]

$$\frac{d\sigma}{d\Omega} = \frac{|\bar{\mathcal{M}}|^2}{64\pi^2(E+p)^2} \tag{2.32}$$

Then we have to compute (we set the Boltzmann constant to 1 for simplicity)

$$\langle\sigma v\rangle = \int (dp)(dp')e^{-\frac{E+p'}{T}} \frac{e^4}{\sin^4(\theta_W)} \frac{2\pi\sin(\theta)p'^2}{(-2p'^2(1-\cos(\theta)) - M_W^2)^2} d\theta \tag{2.33}$$

The integral over the angle θ can be computed exactly:

$$\int_0^\pi \frac{\sin(\theta)d\theta}{[2p^2(1-\cos(\theta)) + M_W^2]^2} = -\frac{1}{2p^2}\left(\frac{1}{4p^2+M_W^2} - \frac{1}{M_W^2}\right) \tag{2.34}$$

Then we can expand the integration over the incoming momenta, rememberring that

$$\int (dp)(dp')\sigma(p,p') = \int_0^{+\infty} \frac{4\pi p^2 dp}{(2\pi)^3 2E} \int_0^{+\infty} \frac{4\pi p'^2 dp'}{(2\pi)^3 2p'} \sigma(p,p') \tag{2.35}$$

since the annihilation is isotropic in space. Then,

$$\int \frac{e^4 p^2 p' dp dp'}{(2\pi)^3 2E\sin^4(\theta_W)} e^{-\frac{E+p'}{T}} \left(\frac{1}{M_W^2} - \frac{1}{4p'^2+M_W^2}\right) \tag{2.36}$$

The integration over p' involves the exponential integral $Ei(x)$, giving

$$\int_0^{+\infty} p' e^{-\frac{E+p'}{T}} \left(\frac{1}{M_W^2} - \frac{1}{4p'^2 + M_W^2} \right) dp' = \frac{e^{-\frac{E}{T}} T^2}{M_W^2} + \frac{e^{-\frac{E}{T}}}{4} \cos\left(\frac{M_W}{2T} \right) Re\left[Ei\left(\frac{iM_W}{2T} \right) \right] \tag{2.37}$$

The exponential integral is defined in the complex plane as

$$Ei(z) = \int_0^z \frac{e^t - 1}{t} dt + \frac{1}{2} \left(\log(z) - \log\left(\frac{1}{z} \right) \right) + \gamma \tag{2.38}$$

where γ is the Euler-Mascheroni constant. The relation $Ei(\bar{z}) = \bar{Ei(z)}$ follows from the definition. The Taylor representation on the complex plane gives

$$Re\left[Ei\left(i\frac{M_W}{2T} \right) \right] = \frac{1}{2} \log\left(\frac{M_W^2}{4T^2} \right) + \gamma \tag{2.39}$$

The exponential integral has also an useful integral representation on the real axis

$$Ei(x) = pv \int_{-\infty}^{x} \frac{e^t}{t} dt \tag{2.40}$$

which tells that $\lim_{x \to -\infty} Ei(x) = 0$. in the neighbourhood of $-\infty$ the exponential integral can be Taylor-expanded, providing

$$Ei(x) \sim e^x \tag{2.41}$$

In the final step of the integration $e^{-\frac{E}{T}}$ factors out and then the integral can be simplified, since

$$\int \frac{p^2 dp}{E} e^{-\frac{E}{T}} = \int \sqrt{E^2 - m^2} e^{-\frac{E}{T}} \tag{2.42}$$

The last integral cannot be solved in terms of analytical functions, but we can assume that the energy of the photon-baryon fluid is larger than the rest mass of the proton ($m/E << 1$), since the termal bath is hot enough to allow a significant fraction of highly energetic protons. Under this approximation we Taylor-expand the root in the integral, giving

$$\int_m^{+\infty} E e^{-\frac{E}{T}} \left(1 - \frac{m^2}{2E^2}\right) dE = \left(T(T+m) - \frac{m}{2}\right) e^{-\frac{m}{T}} - \frac{m^2}{2T} Ei\left(-\frac{m}{T}\right) \tag{2.43}$$

The thermally averaged cross section follows:

$$\begin{aligned} \langle \sigma v \rangle = \frac{e^4}{2(2\pi)^3 \sin^4(\theta_W)} \left[T(T+m)e^{-\frac{m}{T}} - \frac{m^2}{2} Ei\left(-\frac{m}{T}\right)\right] \cdot \\ \left[\frac{T^2}{M_W^2} + \frac{1}{8}\cos\left(\frac{M_W}{2T}\right)\left(\log\left(\frac{M_W^2}{4T^2}\right) + \gamma\right)\right] \end{aligned} \tag{2.44}$$

During the cosmic expansion the temperature of the photon-baryon fluid drops and we can see that the termally averaged cross sections drops too. For annihilations of massive particles it drops exponentially like

$$\langle \sigma v \rangle \sim T^n e^{-\frac{m}{T}} \tag{2.45}$$

since

$$Ei\left(-\frac{m}{T}\right) \sim e^{-\frac{m}{T}} \tag{2.46}$$

If we disregard the proton mass, assuming weak interactions of massless fermion, the cross section still drops like T^4, following a power law, since the term proportional to $Ei(m/2T)$ vanish identically. It is interesting the dependence of the cross section from M_W^{-2}. Massless gauge bosons give an infinite cross section, but this singular behavior is given by the integration over the θ angle. Indeed, if $M_W = 0$, then

$$\int \frac{\sin(\theta)}{(1-\cos(\theta))^2} d\theta = \frac{1}{\cos(\theta) - 1} \tag{2.47}$$

which is singular around $\theta = 0$. This interesting aspect remembers the Rutherford scattering cross section singularity and it is clearly due to the fact that the cross section of Rutherford scattering is infinite since electromagnetic force is an infinite range interaction. This simply shows that annihilations and scatterings mediated by massless gauge fields, like the photon, should remain efficient during cosmic expansion. They are suppressed only when the center of mass energy drops under the treshold for

activating the interaction or creating massive final states, dropping suddenly. The recombination process, which is substained by photoionization of hydrogen atoms end electronic capture behaves in this way. When the photon energy is no more high for photoionizing hydrogen levels, then photon-baryon fluid recombines quickly.

2.1.2 Recombination

We have shown that the difference between small-ranged and infinite-ranged interactions plays a fundamental role in breaking the equilibrium of the primordial Universe. While the temperature drops all weak processes are suppressed and the only remeaning efficient interaction is mediated by the electromagnetic field. Around 1 eV electrons, protons and photons are still tightly coupled. Photons and electrons are coupled by Compton scattering and protons and electrons by Rutherford scattering. A fraction of free electrons may recombine with a fraction of free protons forming neutral hydrogen, while neutral hydrogen may photoionize creating a free proton and a free electron. We can define the fraction of free electrons and the fraction of free protons in the photon-baryon fluid as

$$X_e = X_p = \frac{n_e}{n_e + n_H} \tag{2.48}$$

where we assumed neutrality ($n_e = n_p$) and n_H is the number density of the hydrogen atoms. The term $n_e + n_H$ is the total number density of the baryons in the primordial fluid. Saha equilibrium condition states that

$$\frac{n_e n_p}{n_H n_\gamma} = \frac{n_e^0 n_p^0}{n_H^0 n_\gamma^0} \tag{2.49}$$

because we assumed that recombination goes on involving photons, which can be absorbed or emitted in the creation and destruction of bound states of the hydrogen atom. The process is

$$e^- + p \longleftrightarrow H + \gamma \tag{2.50}$$

We assume that the number density of photons is overwhelming in the photon baryon fluid, which simply states that electromagnetic interaction

is still efficient when all other interactions drop. Under this criterium, $n_\gamma = n_\gamma^0$, and we can write

$$\frac{X_e^2}{1-X_e} = \frac{1}{n_e + n_H}\left(\frac{m_e T}{2\pi}\right)^{\frac{3}{2}} e^{-\frac{me+m_p-m_H}{T}} \tag{2.51}$$

where the term $n_e + n_H$ scales like $a^{-3} = T^3$. It is clear that when temperature is high the exponential dominates and the left hand side requires $X_e \sim 1$ in order to be high. This corresponds to a higly degree of ionization. When the tempereture drops under the treshold $m_e+m_p-m_H$, recombination may take place.

The recombination process is in principle not easy, since it involves the recombination rate $\langle \sigma v \rangle$ of a free electron of being captured in *any* state of the hydrogen atom. Clearly electronic capture in excited states is followed by the emission of photons with lower energy than those emitted by electronic capture on the ground state 1s. Electrons captured in exicited states may spontaneously drop to a lower energetic level and emit a photon, enhacing the recombination process. Here we are not interested in this technical aspects and simply quote that the details of recombination have been deeply studied by Sunyaev and Zel'dovich, who showed that ground state recombination is less efficient than recombination on the 2s level.

2.1.3 Compton scattering

Compton scattering tights photons and electrons. Here we will look the high energy behavior of Compton scattering, since it will be involved in the Sunyaev-Zel'dovich effect. The cross section can be computed by basic QED rules. We fix the center of mass frame and consider an incoming photon interacting with an incoming electron. The kinematics in the center of mass frame requires

$$e^\mu = (E, 0, 0, p) \qquad k^\mu = (p, 0, 0, -p) \tag{2.52}$$

as constraints on the incoming momenta. The electron energy is $E^2 = p^2 + m^2$. The outgoing momenta are then

$$e'^{\mu} = (E, 0, p\sin(\theta), p\cos(\theta)) \qquad k'^{\mu} = (p, 0, -p\sin(\theta), -p\cos(theta)) \tag{2.53}$$

The S-matrix element $\mathcal{M}$ of the Compton scattering at tree level involves the contribution of the t-channel and the u-channel, which give

$$\begin{aligned} i\mathcal{M} = \bar{u}_e ie\gamma^{\mu}\epsilon^*_{\mu}(k')\frac{i\gamma^{\alpha}(e_{\alpha}+k_{\alpha})+im}{(e+k)^2-m^2}ie\gamma^{\nu}\epsilon_{\nu}(k)u_{e'}+ \\ \bar{u}_{e'}ie\gamma^{\mu}\epsilon_{\mu}(k)\frac{i\gamma^{\alpha}(e_{\alpha}-k'_{\alpha})+im}{(e-k')^2-m^2}ie\gamma^{\nu}\epsilon^*_{\nu}(k')u_e \end{aligned} \tag{2.54}$$

The term

$$S(k) = i\frac{\gamma^{\mu}k_{\mu}-m}{k^2-m^2+i\epsilon} \tag{2.55}$$

is the propagator of the exchanged electron. The vectors $\epsilon_{\mu}(k)$ and $\epsilon_{\nu}(k')$ are the polarizations of the incoming and outcoming photons respectively.

Since $k^2 = k'^2 = 0$, we can simplify the propagators, finding

$$i\mathcal{M} = -ie^2\epsilon^*_{\mu}(k)\epsilon_{\nu}(k')\bar{u}_e\left[\frac{\gamma^{\mu}\gamma^{\alpha}k_{\alpha}\gamma^{\nu}+2\gamma^{\mu}e^{\nu}}{2(e\cdot k)}+\frac{\gamma^{\nu}\gamma^{\alpha}k'_{\alpha}\gamma^{\mu}-2\gamma^{\nu}e^{\mu}}{2(e\cdot k')}\right]u_{e'} \tag{2.56}$$

To compute the unpolarized cross section we have to average over the incoming helicity states and summing over the outgoing ones. The helicity states of the photon correspond to the transverse polarizations. The transversality condition and the Ward identities ensure that in any tensorial amplitude $T^{\mu\nu}$

$$\sum_{hel}\epsilon^*_{\mu}(k)\epsilon_{\nu}(k)T^{\mu\nu} = -\eta_{\mu\nu}T^{\mu\nu} \tag{2.57}$$

Taking the squared modulus of the transition amplitude, we find

$$|\bar{\mathcal{M}}|^2 = \frac{e^4}{4}\left[\frac{A}{4(e\cdot k)^2}+\frac{B}{2(e\cdot k)(e\cdot k')}+\frac{C}{4(e\cdot k')}\right] \tag{2.58}$$

where A, B, and C are traces of products of Dirac matrices:

$$A = Tr[(\gamma^\alpha e'_\alpha + m)(\gamma^\mu\gamma^\beta k_\beta\gamma^\nu + 2\gamma^\mu e^\nu)\cdot (\gamma^\rho e_\rho + m)(\gamma_\nu\gamma^\sigma k_\sigma\gamma_\mu + 2\gamma_\mu e_\nu)] \tag{2.59}$$

and

$$B = Tr[(\gamma^\alpha e'_\alpha + m)(\gamma^\mu\gamma^\beta k'_\beta\gamma^\nu - 2\gamma^\mu e^\nu)\cdot (\gamma^\rho e_\rho + m)(\gamma_\nu\gamma^\sigma k_\sigma\gamma_\mu + 2\gamma_\mu e_\nu)] \tag{2.60}$$

The trace C is the same as A, provided that the substitution $k \to -k'$ is taken everywhere. The direct computation of the traces gives

$$\tfrac{A}{16} = [4m^4 - 2m^2 e\cdot e' + 4m^2 e\cdot k - 2m^2 e'\cdot k + 2(e\cdot k)(e'\cdot k)] \tag{2.61}$$

$$\tfrac{B}{16} = [16m^2(e'\cdot k) - 16m^2(e\cdot k') - 32m^4] \tag{2.62}$$

$$\tfrac{C}{16} = [4m^4 - 2m^2 e\cdot e' - 4m^2 e\cdot k' + 2m^2 e'\cdot k' + 2(e\cdot k')(e'\cdot k')] \tag{2.63}$$

Finally:

$$|\bar{\mathcal{M}}|^2 = 2e^4\left[\frac{e\cdot k'}{e\cdot k} + \frac{e\cdot k}{e\cdot k'} + \frac{2m^2}{e\cdot k} - \frac{2m^2}{e\cdot k'} + m^4\left(\frac{1}{e\cdot k} - \frac{1}{e\cdot k'}\right)\right] \tag{2.64}$$

The differential cross section in the center of mass frame is straightforward

$$\frac{d\sigma}{d\cos(\theta)} = \frac{1}{32\pi Ep}\frac{p}{(E+p)}|\bar{\mathcal{M}}|^2 \tag{2.65}$$

and inserting the four-momenta we find

$$\frac{d\sigma}{d\cos(\theta)} = \frac{e^4}{16\pi E(E+p)}\left[\frac{E+p\cos(\theta)}{E+p} + \frac{E+p}{E+p\cos(\theta)} + 2m^2\frac{\cos(\theta)-1}{(E+p)(E+p\cos(\theta))} + m^4\left(\frac{\cos(\theta)-1}{(E+p)(E+p\cos(\theta))}\right)^2\right] \tag{2.66}$$

In the low energy limit $p \to 0$ and $E \to m$. We immediately find that

$$\left.\frac{d\sigma}{d\cos(\theta)}\right|_{p\sim 0} = \frac{e^4}{16\pi m^2}(1+\cos^2(\theta)) = \frac{\pi\alpha_{em}^2}{m^2}(1+\cos^2(\theta)) \tag{2.67}$$

where in the last equality we recovered the fine structure constant α_{em} throught the relation $e^2 = 4\pi\alpha_{em}$.

The integral over the angle θ provides the full cross section

$$\sigma = \frac{8\pi\alpha_{em}^2}{3m^2} \tag{2.68}$$

which matches exactly the Thomson cross section for the diffusion of electromagnetic waves by a point source.

In the high energy limit we can disregard all mass terms into the differential cross section and find that

$$\left.\frac{d\sigma}{d\cos(\theta)}\right|_{m\sim 0} = \frac{e^4}{32\pi p^2}\left[\frac{1+\cos(\theta)}{2} + \frac{2}{1+\cos(\theta)}\right] \tag{2.69}$$

The differential cross section is singular around $\theta \sim \pi$, which shows that backward scattering his highly enhaced if high energy particles are involved. Integrating over the angle θ gives an infinite cross section, but we can regularize the integral changing the integration range from $[-1, 1]$ to $[-1+\epsilon, 1]$, for a suitably chosen cutoff ϵ.

Integrating we find

$$\sigma = \frac{2\pi\alpha_{em}^2}{s}\left(1 + 2\log 2 - 2\log(\epsilon)\right) \tag{2.70}$$

where we have made explicit the fine structure constant and the Mandelstam invariant s, defined as the center of mass squared energy. Finally we are able to remove the cutoff rememberring that the Mandelstam invariant u, defined as (the last equality holds in the center of mass frame and under our high energy limit)

$$u = (e - k')^2 = -2p^2(1+\cos(\theta)) \tag{2.71}$$

allows for expanding $1+\cos(\theta)$ around $\theta \sim \pi$. Rememberring that the Mandelstam invariants satisfy $u + s + t = 2m^2$, we find

$$\sigma = \frac{2\pi\alpha_{em}^2}{s}\left[1 + \log\left(\frac{2m^2}{s}\right)\right] \tag{2.72}$$

where the divergence is removed.

The high energy singular behaviour of the differential cross section around $\theta \sim \pi$ shows that there are huge contributions to the cross section coming from backward scattering processes. The same phenomenon do not appear in the low energy limit, which tells that backward scattering is preferred only in highly energetic interactions. In standard Compton processes the electron at rest is kicked by the incoming photons, which loses energy. In the high energy limit the rest mass of the electron is very small compared to the center of mass energy and the inverse process contribute more than in the low energy case. This *Inverse Compton Scattering* is characterized by an incoming photon which acquires energy due to the scattering on a relativistic electron. Such processes are primarly backward scatterings, that tells how the enhacement of the cross section around $\theta \sim \pi$ is due to taking into account their contributions.

The Inverse Compton scattering is quite common in cosmological contexts because it may occur whenever CMB photons scatter on high temperature electrons. We will discuss the role of Inverse Compton scattering in galaxy clusters further in the section on the Sunyaev-Zel'dovich effect.

2.2 Anisotropies

Up to now we assumed that the Universe is homogeneous and isotropic. The CMB is one of the most important observational proofs of the opposite. The temperature of the CMB is quite uniform, but not perfectly uniform. Such inhomogeneities (of order 10^{-5}) of the temperature appear as an anisotropic map of the CMB, which suggest how our Universe cannot be treated so easily.

The photon-baryon fluid is stressed by gravity and electromagnetic interactions, while Dark Matter evolves separately. If a small inhomogeneity arises into the primordial fluid, the tight coupling will propagate it to the photons, which will break their equilibrium distribution. Dark Matter inhomogeneities behaves in the same way, since their gravitational effects

will break the baryon equilibrium. We may conclude that any density inhomogeneity of the primordial fluid left its fingerprints on the distribution of the CMB photons and now they appear as small fluctuations around the mean temperature of the CMB.

2.2.1 Temperature fluctuations

We may statistically treat the CMB assuming that photons follow a distribution function f on the phase space which encodes informations on how photons satisfy the complex microscopic dynamics. The coarse-graining procedure leads to *Liouville equation*

$$L[f] = C[f] \tag{2.73}$$

for the distribution function. The Liouville operator L encodes the dynamics, which is summed up in the phase space by the Poisson brackets

$$\frac{df}{dt} = \{f, H\} \equiv \frac{\partial f}{\partial x}\frac{\partial H}{\partial p} - \frac{\partial f}{\partial p}\frac{\partial H}{\partial x} \tag{2.74}$$

since Hamilton equations

$$\dot{x} = \frac{\partial H}{\partial p} \tag{2.75}$$

$$\dot{p} = -\frac{\partial H}{\partial x} \tag{2.76}$$

hold for the full hamiltonian H of the whole ensemble.

The Liouville operator is the generalization of the Poisson brackets and it is simply defined as the total derivative of the distribution function due to the microscopic dynamics of all the involved particles.

In our case we have to deal with a phase space encoding the dynamics of particles moving into a curved geometry, then

$$L[f] = \dot{p}^\mu \frac{\partial f}{\partial p^\mu} + \dot{x}^\mu \frac{\partial f}{\partial x^\mu} \tag{2.77}$$

Since particles move along geodesics, we have to remember that

$$\dot{p}^\mu = -\Gamma^\mu_{\alpha\beta} p^\alpha p^\beta \tag{2.78}$$

which gives the generalization of the Boltzmann equation

$$p^\mu \partial_\mu f - \Gamma^\mu_{\alpha\beta} p^\alpha p^\beta \frac{\partial f}{\partial p^\mu} = C[f] \tag{2.79}$$

The term $C[f]$ is the collisional integral, which encodes the interactions that drive the dynamics. It is defined as the coarse graining of the interaction over all the other particles involved. Formally

$$C[f] = \sum_n \int d\phi^{(n-1)} |\mathcal{M}|^2_{(n)} (2\pi)^4 \delta^{(4)} \left(\sum p_{in} - \sum p_{out} \right) \tag{2.80}$$

where $|\mathcal{M}|^2_{(n)}$ is the transition amplitude of the processes involving exactly n particles and the delta function ensures the four-momentum conservation during the interaction. The phase space element $d\phi^{(n)}$ is defined as

$$\int d\phi^{(n)} = \int \prod_i^n (dk_i) \left[\prod_j^{N_{out}} f_j(k_j^{(out)}) - \prod_j^{N_{in}} f_j(k_j^{(in)}) \right] \tag{2.81}$$

where N_{in} is the number of incoming particles and N_{out} is the number of outgoing ones. Clearly $N_{in} + N_{out} = n$.

We see that the collisional integral involves interactions with an increasing number of particles, which may belong to the same family.

If $C[f] = 0$ no interactions are considered and we assume that the distribution function corresponds to the well-know equilibrium statistics. Fermions follows Fermi-Dirac distribution, while bosons distribute accordingly to Bose-Einstein. So, we assume that

$$f(E) = (e^{\frac{E}{T(t)}} \pm 1)^{-1} \tag{2.82}$$

where a time dependence of the temperature is allowed, because otherwise the time component of the collisionless Boltzmann equation

$$p^0 \partial_t f - \Gamma^0_{\alpha\beta} p^\alpha p^\beta \frac{\partial f}{\partial p^0} = 0 \tag{2.83}$$

would have only the trivial solution $f = const.$ Writing the Christoffel symbols of the FRW metric and rememberring that $p^\mu = (E, \vec{p})$, we find

$$E\partial_t f - H g_{ij} p^i p^j \partial_E f = 0 \tag{2.84}$$

Since $g_{ij}p^i p^j = p^\mu p_\mu - m^2$, we finally have to solve

$$E\partial_t f - H(E^2 - m^2)\partial_E f = 0 \tag{2.85}$$

Inserting the distribution functions provides a differential equation for the temperature

$$\frac{\dot{T}}{T} = -\frac{\dot{a}}{a}\left(\frac{E^2 - m^2}{E^2}\right) \tag{2.86}$$

For photons the solution is straightforward

$$T = T_0 \frac{a_0}{a} \tag{2.87}$$

while the solution for massive particles require some care. The energy of a massive particle moving along a geodesic in the FRW spacetime satisfies Eq. 1.85 and the Boltzmann equation acquires an extra factor, which depends only on the initial data:

$$\frac{\dot{T}}{T} = -\frac{\dot{a}}{a}\left(\frac{a_0^2(E_0^2 - m^2)}{a_0^2(E_0^2 - m^2) + m^2}\right) \tag{2.88}$$

The relation between the temperature and the scale factor for massive particles is like

$$T \sim \frac{1}{a^k} \tag{2.89}$$

for a given constant k. If we arbitrarly choose today as reference, $a_0 = 1$, then

$$k = 1 - \frac{m^2}{E_0^2} \tag{2.90}$$

Treating temperature fluctuations requires to slightly change the distribution functions. We define the function Θ as

$$f(E) = \left[\exp\left(\frac{E}{T(t)(1 + \Theta(\hat{n}, x, t))}\right) \pm 1\right]^{-1} \tag{2.91}$$

The function Θ depends on the direction $\hat{n}$ in the sky we are considering. The theory of CMB fluctuations involve long but simple calculations we do not quote here (see for instance [71]). We simply remember that we can develop the function Θ on a suitable basis of orthogonal functions on the sphere, defining the l-th multipole Θ_l by

$$\Theta(\hat{n}, x, t) = \sum_l (-i)^l \Theta_l(x, t) P_l(\hat{n}) \tag{2.92}$$

where $P_l(\hat{n})$ is the l-th Legendre polynomial. The same relation may be written in Fourier space and in terms of conformal time η, defined by the differential rule

$$\frac{d\eta}{dt} = \frac{1}{a} \tag{2.93}$$

The transformation from standard cosmic time and conformal time is a conformal map from the FRW spacetime to a static spacetime. If the FRW is flat, then the static spacetime is exactly Minkowski. Indeed the line element becomes

$$ds^2 = a(\tau)^2[-d\tau^2 + d\sigma^2] \tag{2.94}$$

being $d\sigma^2$ the space line element.

In order to deal with temperature fluctuations, we need to relate the multipoles Θ_l with the density inhomogeneities. There are many different approaches to perturbations of the standard homogeneous and isotropic FRW model based on different perturbative schemes. Here we follow a relativistically coherent criterium, based on metric perturbations. The underlying theory is simple: matter inhomogeneities should destroy spacetime symmetries, since matter is a source for the geometry of spacetime. The general relativistic approach is far different from the classical one based on perturbation theory of the density field. Indeed perturbing the metric requires in principle to define ten new functions which encode deviation from the maximally symmetric spacetime. Here we assume that only two scalar functions drive the metric fluctuations. The former function acts on g_{00}, the latter one works as a common factor for the six components of the metric of the space slices. In other words we assume that two potentials Ψ and Φ exist such that

$$\delta g_{00} = -2\Psi \tag{2.95}$$
$$\delta g_{ij} = 2a^2\Phi g_{ij} \tag{2.96}$$
$$\delta g_{0i} = 0 \tag{2.97}$$

The potentials play a role in the time dilation effect, which has an immediate consequence in the redshift of spectral lines.

In terms of conformal time and in Fourier space we can expand the collisional term of the Boltzmann equation and recover the BBGKY hierarchy for the multipoles. The derivation is quite long and we simply quote the final step.

$$\dot{\Theta}_0 = -k\Theta_1 - \dot{\Phi} \tag{2.98}$$
$$\dot{\Theta}_1 = \frac{k}{3}\left[\Theta_0 + \Psi\right] + \dot{\tau}\left(\Theta_1 - \frac{iv_b}{3}\right) \tag{2.99}$$
$$\dot{\Theta}_l = k\left[\frac{l}{2l-1}\Theta_{l-1} - \frac{l+1}{2l+1}\Theta_{l+1}\right] - \dot{\tau}\Theta_l \tag{2.100}$$

where v_b is the baryon velocity and $\dot{\tau} = -n_e\sigma a$ is the optical depth to Compton scattering and k is a given wavevector. The cross section σ can be approximated by the standard Thomson cross section, since the center of mass energy has sufficently dropped for disregarding high energy contributions to the Compton scattering.Nevertheless Compton scattering is still highly efficient and the mean free path of the photons is much shorter than the horizon. The photon-baryon fluid is cooling but electromagnetic interactions still dominate mantaining equilibrium between photons and free electrons. Under this approximation the multipoles are linked by the useful relation

$$\Theta_l \sim \frac{k\eta}{2\tau}\Theta_{l-1} << \Theta_{l-1} \tag{2.101}$$

which tells that they are perturbatively describing the temperature fluctuations.

Since temperature fluctuations are coupled to density fluctuations in the photon-baryon fluid, we need to add two extra equations for closing the hierarchy. We need continuity and Euler equations for the baryons

$$\dot{\delta}_b + ikv_b + 3\dot{\Phi} = 0 \quad (2.102)$$

$$\dot{v}_b + Hv_b + ik\Psi - \dot{\tau}\frac{3i\Theta_1 + v_b}{R} = 0 \quad (2.103)$$

The scalar R is the standard ratio between the density of baryons and the density of photons

$$R = \frac{4}{3}\frac{\rho_b}{\rho_\gamma} \quad (2.104)$$

which defines the speed of acoustic waves propagating in the photon-baryon fluid c_s (in units of c):

$$c_s = \frac{1}{\sqrt{3(1+R)}} \quad (2.105)$$

The density constrast δ_b defines the relative deviation of the baryon density from the mean density

$$\delta = \frac{\rho(x,\eta) - \bar{\rho}}{\bar{\rho}} \quad (2.106)$$

and it is coupled to the divergence of the peculiar velocity field at first oreder in standard eulerian theory of cosmological perturbations.

Solving the hierarchy at different orders explains the physics of the photon-baryon fluid. We simply remember that at first order the baryons drag the photons and the effect appears in the differential equation for the monopole

$$\frac{d}{d\eta}\left((1+R)\dot{\Theta}_0\right) + \frac{k^2}{3}\left(\Theta_0 + (1+R)\Psi\right) + \frac{d}{d\eta}\left((1+R)\dot{\Phi}\right) = 0 \quad (2.107)$$

giving a time-dependent effective mass $m_{eff} = 1+R$ to the oscillator. The gravitational potentials as source the effective gravitational acceleration acting on the oscillator and the general integral is well known

$$\begin{aligned}\Theta_0(k,\eta) + \Phi(k,\eta) = [\Theta_0(k,0) + \Phi(k,0)]S_1(k,\eta) + \\ \frac{k}{\sqrt{3}}\int_0^\eta dx[\Phi(k,x) - \Psi(k,x)]S_2(k,\eta - x)\end{aligned} \quad (2.108)$$

where

$$S_1(k,\eta) = \cos\left(k\int_0^\eta dx c_s(x)\right) \tag{2.109}$$

$$S_2(k,\eta) = \sin\left(k\int_0^\eta dx c_s(x)\right) \tag{2.110}$$

are the two independent solutions of the corresponding homogeneous equation. The sinusoidal functions set a time-varying reference scale given by

$$r_s = \int_0^\eta dx c_s(x) \tag{2.111}$$

which is the comoving sound horizon. Acoustic waves propagating with phase speed c_s travel r_s in a conformal interval η, while their amplitude and wavelength are not constant. The wavelength of the fundamental solutions varies in time since the cosmological expansion plays a non trivial role: during cosmic expansion the set of normal modes is characterized by time-dependent eigenfrequences, sice the space interval we are resolving with normal modes is scaling in time.

The first term has maxima and minima corresponding to the time-dependent wavenumbers

$$k_n = \frac{n\pi}{r_s} \tag{2.112}$$

which appear as a layout of peaks and dips in the TT-power spectrum of CMB anisotripes.

2.2.2 Power spectrum

In analogy with standard theory of cosmological perturbations, we are interested in defining the power spectrum $P(k)$ of CMB anisotropies. The power spectrum of the density contrast is defined in Fourier space as

$$\left\langle \delta(k), \delta(k') \right\rangle = (2\pi)^3 \delta_D(k-k') P(k) \tag{2.113}$$

where $\delta_D(x)$ is the Dirac delta function. It plays the role of a variance and it can be computed from the correlation function of a sample taking its Fourier transform.

Boltzmann equation provides the full hierarchy for the multipoles Θ_l and we want to extend the solution up to current conformal time η_0, since we are observing the CMB here and now. In the tight coupling approximation we find

$$\begin{aligned}\Theta_l(k,\eta_0) = -\int_0^{\eta_0} dx\dot{\tau}(x)e^{-\tau(x)}[\Theta_0(k,x)+\Psi(k,x)]j_l[k(\eta_0-x)] \\ +\int_0^{\eta_0} dx\dot{\tau}(x)e^{-\tau(x)}\frac{iv_b}{k}\frac{d}{dx}j_l[k(\eta_0-x)] \\ +\int_0^{\eta_0} dxe^{-\tau}\left(\dot{\Psi}(k,x)-\dot{\Phi}(k,x)\right)j_l[k(\eta-x)]\end{aligned} \tag{2.114}$$

provided that $j_l(x)$ are Bessel spherical functions. This interesting formula shows that the first two integrals contribute only near the recombination epoch η^*, since the *visibility function* $-\dot{\tau}e^{-\tau}$ is significantly non-vanishing only in the neigbourhood of recombination. Before η^* it is exponentially dumped since τ is big, after recombination the rate $\dot{\tau}$ drops to zero, since Compton effect is no more efficient and the mean free path of photons increases significantly. The last term represents the *Integrated Sachs-Wolfe Effect* and clearly depends on the evolution over all times of the metric perturbations. It creates a useful bridge between CMB observations and theoretical models of the growth of structures, since the variation of the metric potentials are mainly related to the accretion of structures like galaxies or clusters, at different epochs.

In order to define the power spectrum for CMB anisotropies, we remember that we can develop functions defined on a sphere upon spherical armonics Y_{lm}, providing

$$\Theta(\hat{n},\lambda) = \sum_{l=1}^{+\infty}\sum_{m=-l}^{+l} a_{lm}(\lambda)Y_{lm}(\hat{n}) \tag{2.115}$$

where the dependence on any other variable (here represented by λ) is supported by the coefficients a_{lm}.

From the orthonormality of the basis it follows that

$$a_{lm}(\lambda) = \int d\Omega_2 \bar{Y}_{lm}(\hat{n})\Theta(\hat{n},\lambda) \tag{2.116}$$

We are not able to make predictions on any given a_{lm}, but we may treat them statistically. The distribution of the temperature fluctuations is strictly linked to the early density fluctuations, which clearly resemble the early imprint of quantum fields interacting at higher energies in the primordial fluid. We have to make approximations on the early distribution of the density fluctuations, if we are not able to compute the distribution from prime principles. Here we simply assume that gaussian conditions hold, which ensures that a_{lm} have vanishing mean and nonvaniscing variance. The variance C_l is defined as

$$\langle a_{lm} a_{pq} \rangle = \delta_{lp} \delta_{mq} C_l \tag{2.117}$$

It is interesting to note that the C_ls do not depend on the number m. Rememberring that spherical harmonics are eigenfunctions of the angular momentum satisfying

$$L^2 Y_{lm} = l(l+1) Y_{lm} \tag{2.118}$$
$$L_z Y_{lm} = m Y_{lm} \tag{2.119}$$

we see that averaging over the two-dimesional sphere removes the dipendence on the z direction defined by the reference component of the angular momentum. In other word, z is a preferred direction in space which is removed by the average, since averaging over the sphere should provide an isotropic function. The dipendence on l cannot be removed by any symmetry argument and defines the power spectrum of CMB anisotropies in analogy with the power spectrum of density fluctuations.

Assuming that the temperature fluctuations are linked to the primordial density inhomogeneities by a k-dependent factor

$$\Theta(k) \sim f(k) \delta(k) \tag{2.120}$$

we can write the CMB power spectrum in terms of the power spectrum of matter. Simply we need to express a_{lm} in terms of the multipoles and we find

$$\left\langle \Theta(k) \Theta(k') \right\rangle = (2\pi)^3 \delta_D(k - k') P(k) f(k) f^*(k') \tag{2.121}$$

Then the C_l becomes

$$C_l = \int \frac{d^3k}{(2\pi)^3} P(k) \int d\Omega d\Omega' Y^*_{lm}(\hat{n}) Y_{lm}(\hat{n}') f^+(k,\hat{n}) f(k,\hat{n}') \qquad (2.122)$$

which can be computed directly developing Θ in multipoles and applying orthogonality relations among legendre polynomials. The calculation gives

$$C_l = \frac{2}{\pi} \int_0^{+\infty} dk k^2 P(k) f_l(k) \qquad (2.123)$$

where f_l is the enhacement of the l-th multipole

$$f_l(k) \sim f_l(k) \Theta_l(k) \qquad (2.124)$$

2.3 Sunyaev-Zel'dovich effect

The Sunyaev-Zel'dovich effect was described by Sunyaev and Zel'dovich in their papers [15, 16, 17].

The effect has longstanding observational consequences, since it allows to test cosmology. The CMB photons travelling from the last scattering surface follow geodesics into a non-completely homogeneous spacetime. Local inhomogeneities of the matter density grow during the history of the Universe and may form structures, like galaxies or clusters. A photon enterring a cluster may interact electromagnetically with the Intra-Cluster Medium (ICM), primarly composed by ionized gas. If the ICM is sufficently hot, the photon may experience inverse comptonization and gain energy. The fluctuation in energy of the CMB photons due to Sunyaev-Zel'dovich (SZ) effect are bigger than the standard fluctuations of the CMB temperature and can be detected, revealing the presence of the cluster.

Here we review the main physics of the effect, following [19, 15, 16, 17].

2.3.1 Diffusion processes

Let us focus on a photon coming from the last scattering surface which enters the ICM. The electrons of the hot gas of the cluster scatter the incoming photon, which changes its wavelength, providing a distortion in the CMB temperature spectrum. The photons are usually scattered by

the ICM thermal electrons (*thermal* SZ effect), but a coherent motion of the whole cluster can contribute. This *kinetic* SZ effect is much smaller than the thermal effect and generally can be neglected. The thermal SZ fluctuations are typically 10^{-4} K, and they can be clearly detected in the CMB. On the other hand the kinetic contributions to the SZ effect are one order of magnitude smaller, becoming comparable with the primary CMB fluctuations. Hence, we will always refer to the thermal SZ only in the following discussion.

In their works [15, 16, 17] Sunyaev and Zel'dovich describe the effect in terms of the solution to the Kompaneets equation, i.e. the non-relativistic limit of the Boltzmann kinetic equation for the Compton scattering. It is well known that the distribution function of collisionless CMB photons is conserved. The CMB spectrum is blackbody at a very high level of accuracy, as it was shown by the COBE-FIRAS experiment in [73], since homogeneity and isotropy play an important role. We showed that, under the geometric optics approximation, the intensity of radiation scales as $(1+z)^{-3}$, since

$$I_\omega(O) = \frac{I_{(1+z)\omega}(S)}{(1+z)^3} \tag{2.125}$$

If the observed intesity is Planckian

$$I_\omega(O) = \frac{2\hbar\omega^3}{(2\pi)^2 c^2}\left[\exp\left(\frac{\hbar\omega}{k_B T}\right) - 1\right]^{-1} \tag{2.126}$$

the scaling rule is satisfied only if T scales as $(1+z)$. This simple relation is satisfied for the FRW metric as a consequence of the geodesic equation, since we know that the CMB temperature, neglecting fluctuations, scales as a^{-1}. The conservation of the Planck distribution during cosmic expansion involve all our symmetry assumptions on cosmology and is strictly linked to the FRW metric. So, any small deviation from the perfect blackbody can be use for detecting deviations from the homogeneous FRW spacetime and testing perturbation theory or violations of the reciprocity theorem (see for instance [74]).

If radiant energy is produced during cosmic expansion due to local physical processes, we can write

$$\dot{\rho}_r = -4\rho_r + \epsilon(t) \tag{2.127}$$

where ϵ is the radiant energy density added at the time t. The same equation can be written for the radiant energy in a given frequency band $u(t, \nu)$

$$\frac{\partial u_\nu}{\partial t} = H\left(\nu\frac{\partial u_\nu}{\partial \nu} - 3u_\nu\right) + \epsilon_\nu \tag{2.128}$$

for a suitable contribution ϵ_ν. If we express the energy density as a function of the occupation number n

$$u_\nu = \frac{8\pi h\nu^3}{c^3} n(x) \tag{2.129}$$

where $x = \frac{h\nu}{k_B T}$ we can write a balancing equation for n. In the case of elementary processes affecting CMB photons, we can express the energy rate ϵ_ν due to Compton scattering in terms of x and find the Kompaneets equation

$$\frac{\partial n}{\partial t} = \frac{\sigma c n_e k_B T_e}{m_e c^2}\frac{1}{x^2}\frac{\partial}{\partial x}x^4\left[\frac{\partial n}{\partial x} + n^2 + n\right] \tag{2.130}$$

where σ is the Compton cross section, T_e the electrons temperature and n_e their number density. The equation states how the occupation number changes during any diffusion process involving electron-photon scattering.

If the electron density is not constant, we can rewrite the Kompaneets equation as

$$\frac{\partial n}{\partial y} = \frac{1}{x^2}\frac{\partial}{\partial x}\left[\frac{\partial n}{\partial x} + n^2 + n\right] \tag{2.131}$$

where we introduced the comptonization parameter y defined by the differential rule

$$\frac{dy}{cdt} = n_e \sigma \frac{k_B T_e}{m_e c^2} \tag{2.132}$$

2.3.2 Thermal SZ effect

Kompaneets equation allows a direct estimate of the variation of the CMB radiation intensity due to the thermal scattering of the CMB photons passing through hot ICM. Since electrons of the ICM are about $k_B T_e \sim 10^8$ eV, we can disregard n and n^2 in the Kompaneets equation, because x must be very small and the derivative must dominate. For an incident Planckian spectrum we can integrate the Kompaneets equation finding

$$\Delta n = xy \frac{e^x}{(e^x - 1)^2}(x \coth(x/2) - 4) \tag{2.133}$$

This solution should be modified for relativistic contributions, which we disregard here (see [75] and references therein for details on relativistic corrections). The corresponding variation of the CMB intensity is

$$\Delta I = i_0 y g_0(x) \tag{2.134}$$

where

$$i_0 = 2\frac{k_B^3 T_{CMB}^3}{h^2 c^2} \tag{2.135}$$

and the comptonization parameter y can be rewritten accordingly to the geometry of the cluster as

$$y = \int_{l.o.s} \frac{k_B T_e}{m_e c^2} n_e(l) \sigma_T dl \tag{2.136}$$

The integral is taken over the line of sight and the cross section σ_T can be evaluated at the tree level without any significat loss of precision (Thomson scattering). The distribution T_e gives the temperature profile of the ICM and it clearly depends on the physical assumptions made on the geometry of the cluster and on the local microphysics of the hot gas. The function g_0 is

$$g_0(x) = \frac{x^4 e^x}{(e^x - 1)^2}\left(x\frac{e^x + 1}{e^x - 1} - 4\right) \tag{2.137}$$

This function is positive for frequencies $\nu > 217$ GHz and negative otherwise, implying that the SZ effect appears as a right shift of the CMB intensity spectrum having a fixed point for $\nu = 217$ GHz.

We can easily compute the intensity variation in the Rayleigh-Jeans approximation of blackbody spectrum, taking the limit $x \to 0$.

Under this approximation we estimate the relative fluctuation of the CMB temperature produced by the thermal SZ effect:

$$\frac{\Delta T_{SZ}}{T} = -2y \tag{2.138}$$

which can be simplified further by assuming that the temperature profile and the electron density are constant along the line of sight:

$$\frac{\Delta T_{SZ}}{T} = -2\frac{k_B T_e}{m_e c^2} n_e \sigma_T l \tag{2.139}$$

This equation shows that the SZ effect is completely independent of the redshift, suggesting that it could be a very useful tool in testing cosmology.

The geometrical properties of the ICM enter the SZ effect through the size l of the cluster itself. Regarding specific models of the ICM temperature and density profiles, the geometry of the cluster is generally accounted for by the integration over the line of sight. This clearly shows how assumptions must be made about the real shape of the ICM. We are not interested in discussing models of the cluster geometry, so from now on we will simply assume that the depth of the cluster is comparable with its transverse size, which is generally accepted as a first-step approximation appropriate for treating cosmology from SZ surveys.

Chapter 3

Backreaction

The observed Universe is **not** homogeneous. This observational statement is in sharp contrast with the basic assumptions underlying the Cosmological Principle and the theoretical model of the Universe given by the FRW spacetime.

On large scales the homogeneity assumption can be restored and isotropy is enforced by the observation of the CMB. But a complete relativistically coherent model of the Universe should break these approximation and a full solution of the Einstein field equations is needed, involving the stress-energy tensor $T^{\mu\nu}$ of the whole inhomogeneous Universe. This approach is huge and overwhelming, since a complete knowledge of the inhomogeneities affecting matter, radiation and other sources for the gravitational field is required for finding the *full* metric of the Universe. We have also to deal with the longstanding problem represented by the cosmological constant, which may be considered as a deviation from the first formulation of the equation of gravity. We would like to use cosmological probes as test for cosmology, measuring the cosmological parameter and the relative distribution of energy in the Universe, but this require to assume that the laws of gravity are known. On the other hand we would like to test gravity itself, since local inhomogeneities are strictly related to gravity and laws of gravity should have played a role in the evolution of local structures, leaving their fingerprints in the observed inhomogeneous Universe. But this approach requires to know cosmology.

In other words the problems of testing the laws of gravity and the

problem of testing cosmology are strictly related to one another and their solutions need approximations. There are many ways of addressing these fascinating aspects of present cosmology. Here we will focus on the *averaging scheme* and the corresponding *averaging problem*, which led to the formulation of the backreaction hypothesis.

3.1 The averaging problem

Since the Universe can be treated as homogeneous and isotropic on large scales, we may approach observational cosmology assuming that cosmological informations are indeed only average informations. Since on small scales standard laws that hold for the FRW model may break down, any measure or derivation that involves physical laws described in the FRW context should hold after smoothing out inhomogeneities on a sufficently large scale.

This logic naturally leads to inquire if the time evolution of the Universe on average is the same as the time evolution of a homogeneous one. This question carries many consequences, as asking whether Einstein field equations are the same on average and whether an homogeneous solution (like FRW) corresponds to the average of an inhomogeneous one.

There were many different approaches to the averaging problem, which can be roughly summed up into three distinct classes (see [76]):

1. Perturbative expansion of the metric
2. Covariant and non-covariant volume averaging schemes
3. Macroscopic gravity

The difficulties that arise in the averaging procedure have different origins. Mathematically a coherent averaging scheme on a curved manifold and for high order tensors is needed, physically averaging Einstein equations faces an immediate bad behavor due to the intrinsic non linearity of General Relativity. Let us, for instance, take the brakets $\langle\cdot\rangle$ as a sort of consistent average procedure, the Einstein equations become

$$\langle g^{\mu\alpha} R_{\alpha\nu}\rangle - \frac{1}{2}\delta^{\mu}_{\nu}\left\langle g^{\alpha\beta} R_{\alpha\beta}\right\rangle = 8\pi G \langle T^{\mu}_{\nu}\rangle \tag{3.1}$$

and the metric is intrisically coupled to the Ricci tensor. In principle the metric and the curvature are not independent and so

$$\langle g^{\mu\alpha} R_{\alpha\nu} \rangle = \langle g^{\mu\alpha} \rangle \langle R_{\alpha\nu} \rangle + C^{\mu}_{\nu} \tag{3.2}$$

where C^{μ}_{ν} is a correlation tensor. If the correlation tensor enters the theory we need a way for finding it without using Einstein equations.

The approach of macroscopic gravity is based on the analogy among gravity and electromagnetic force. The electromagnetic force has strict microscopic laws, given by Maxwell equations, which cannot be easily solved when we are dealing with a huge number of interacting objects. On the other hand we can find a satisfactory treatment of the electromagnetic force on average, introducing the polarization tensor and the averaged sources.

Unfortunately Einstein equations cannot be treated as Maxwell ones, due to their non-linearity. In [76] the author shows that the averaged dynamics of the Universe in the context of Macroscopic Gravity is far away the FRW dynamics. On the other hand, using a simple toy model they show that adding a suitable correlation tensor to Einstein equations in the case of a macroscopic conformally flat spacetime leads to a macroscopic gravitational field exerting a negative effective pressure, which can be seen as a binding energy for the whole Universe. The corresponding Friedmann equations are modified by extra terms which allows for treating the macroscopic gravitational field as a cosmological fluid with equation of state

$$p = -\frac{1}{3}\rho \tag{3.3}$$

which behaves like a Dark Energy component. This suggest that solving the avergaing problem can be a useful step towards the solution of the Dark Energy debate and the problem of cosmic acceleration.

3.2 Cosmological backreaction

We refer to *cosmological backreaction* as a precise averaging scheme. The name is due to the extra terms that arise in the main equations as a consequence of the averaging procedure which are strictly related to the

density inhomogeneities in the newtonian approximation. In a relativistic approach the backreaction is generalized and related to the smoothing of the curvature of the bare metric. In this case it acquires a deeper meaning we will explain later. We will follow the theory of backreaction as it was developed primarly by Buchert along his works. Other schemes are possible and the current debate is widely open, primarly facing the problem of averages on light-cones and their theoretical consequences. Buchert's approach based on spatial averages faced a lot of theoretical difficulties we will not discuss here, sice we are only interested in upgrading tests against data of models based on Buchert's scheme. For other models and the theoretical aspects we refer the reader to the literature suggested in paper references.

3.2.1 Euler-Newton equations

The avergaing problem in General Relativity is very involved. In the Newtonian approximation it looks easier and the backreaction can be well defined. We follow [26] in dealing with the backreaction in the Newtonian context.

Since matter filling the Universe can be treated as a fluid, we choose to deal with the fluid dynamics both in the Eulerian and in the Lagrangian approach suitably. The Eulerian prescription states that the fluid is described in terms of well defined fields giving the mass density and the stream velocity at any given point $\vec{x}$ in space. In other words we employ the Eulerian picture of fluid dynamics if we are able to write a consistent set of differential equations for the density $\rho(\vec{x}, t)$ and the velocity $\vec{v}(\vec{x}, t)$ which encode the standard Newtonian dynamics. If the fluid is freely streaming, no other functions are needed, since the acceleration must be pointwise null, otherwise an extra field $\vec{a}(\vec{x}, t)$ is required in other to satisfy Newton second equation. The acceleration field is not an unknown and must be explicitly written in order to deal with the forces involved in the fluid dynamics.

We are interested in the Eulerian dynamics of a self-gravitating pressurless fluid, which describe the non-relativistic matter in the Universe. The set of equations is

$$\begin{aligned} \partial_t \rho + \vec{\nabla} \cdot (\rho \vec{v}) &= 0 && (3.4) \\ \partial_t \vec{v} + (\vec{v} \cdot \vec{\nabla}) \vec{v} &= \vec{g} && (3.5) \\ \vec{\nabla} \times \vec{g} &= 0 && (3.6) \\ \vec{\nabla} \cdot \vec{g} &= \Lambda - 4\pi G \rho && (3.7) \end{aligned}$$

The first equation is simply the continuity equation and corresponds to mass conservation. The fluid stream is continuous and mass is conserved pointwise, because of the balancing rule among streams enterring and exiting any elementary volume of the fluid. The second equation is Euler equations and it corresponds to the second law of dynamics

$$\frac{d\vec{v}}{dt} = \vec{g} \tag{3.8}$$

where $\vec{g}$ is the acceleration field. Here we used $\vec{g}$ since the acceleration is purely gravitational. The expansion of the full derivative gives the convective term. The remaining equations are the well known equations of Newtonian gravity, stating that the gravitational field is irrotational and sourced by the mass. It is purely attractive if no cosmological constant Λ is added.

For solving the Euler-Newton system we divide the tensor $\partial_i v_j$, corresponding to the gradient of the velocity field, into irreducible representations of the rotation group:

$$\partial_i v_j = \sigma_{ij} + \frac{1}{3}\delta_{ij}\theta + \omega_{ij} \tag{3.9}$$

where θ is the diagonal part, σ_{ij} is the symmetric traceless part and ω_{ij} is the antysimmetric one. By definition it follows that

$$\theta = \vec{\nabla} \cdot \vec{v} \qquad \omega_{ij} = -\epsilon_{ijk}\omega_k \tag{3.10}$$

where ω_k is proportional to the curl of the velocity field

$$\vec{\omega} = \frac{1}{2}\vec{\nabla} \times \vec{v} \tag{3.11}$$

The Euler-Newton equations become

$$\frac{d\rho}{dt} = -\rho\theta \tag{3.12}$$
$$\frac{d\vec{\omega}}{dt} = -\frac{2}{3}\vec{\omega}\theta + \sigma_{ij}\omega_{ij} \tag{3.13}$$
$$\frac{d\theta}{dt} = \Lambda - 4\pi G - \frac{1}{3}\theta^2 + 2(\omega^2 - \sigma^2) \tag{3.14}$$

where

$$\sigma^2 = \frac{1}{2}\sigma_{ij}\sigma_{ij} \qquad \omega^2 = \frac{1}{2}\omega_{ij}\omega_{ij} \tag{3.15}$$

The last equation is dynamically crucial, since the expansion scalar θ plays a central role in the averaging scheme.

In order to average the Euler-Newton equations, let us pass to the Lagrangian picture of fluid dynamics. In the Lagrangian approach the fluid is described as a collection of particles moving along their streamline. Since the fluid satisfies continuity equation, no intersections among different streamlines is allowed, since otherwise the Eulerian velocity field would not be well defined at intersections. This enables a parameterizzation of each streamline with a Lagrangian coordinate $\vec{X}$, which correspond to the standard Eulerian one at a given fixed reference time t_i, so

$$\vec{X} = \vec{x}(t_i) \tag{3.16}$$

Correspondingly, fixing the Lagrangian coordinate selects a well-defined streamilne and the evolution of the fluid particle can be studied using Lagrangian dymanics, provided that the time coordinate is chosen as a good parameter along the streamline itself. In other words we are able to find a map between the Eulerian coordinate $\vec{x}$ and the Lagrangian coordinate $\vec{X}$ which relates the two pictures. We can write

$$\vec{x} \equiv \vec{f}(\vec{X}, t) \tag{3.17}$$

where $\vec{X}$ does not depend on time. The differences between the two pictures rely on this map: in the Eulerian picture we need to find solutions to a given system of differential equations involving vectors and scalar fields, in the Lagrangian approach the basic unknown is the map $\vec{f}$. In

principle no differences seem to arise, but the Lagrangian approach is more flexible than the Eulerian one in dealing with singularities in the density field, since the density itself is no more an unknown, but can be computed directly from the function $\vec{f}$. When the density diverges, as it may happen when studying the growth of structures in the history of the Universe, the Lagrangian theory help to describe better than the Eulerian approach the physics up to shell-crossing and the formation of pancakes. Indeed the mass inside a given volume element is invariant under changes of coordinate frames, so we have to write

$$\rho(\vec{x},t)d^3x = \rho(\vec{x}(\vec{X},t),t)Jd^3X \tag{3.18}$$

where

$$J = \det\left(\frac{\partial\vec{x}}{\partial\vec{X}}\right) \tag{3.19}$$

is the Jacobian of the diffeomorphism defined by the map $\vec{f}$. This provides the formula linking the Eulerian density with $\vec{f}$

$$\rho(\vec{x},t) = \rho(\vec{X},t_i)J^{-1}(\vec{X},t) \tag{3.20}$$

and the continuity equation changes accordingly

$$\frac{dJ}{dt} = -J\theta \tag{3.21}$$

This simply shows that the singularities in the Eulerian density field correspond to null eigenvalues of the Jacobian determinant. Expanding the determinant in terms of its eigenvalues allows for studying the dynamics of pancakes in the directions orthogonal to the null eigenspace, describing how plane or linear collapse goes on.

For the averaging procedure we have to select a domain D at a given time t_i on which we take the average. The volume of D is easily computed in Eulerian coordinates

$$V = \int_{D(t_i)} d^3x \tag{3.22}$$

which can be written as

$$V = \int_{D(t)} d^3x = \int_{D(t_i)} J d^3X \tag{3.23}$$

in the lagrangian approach.

If we define an effective scale factor a_D such that

$$a_D^3(t) = V(t) \tag{3.24}$$

it follows

$$\frac{dV}{dt} = \frac{d}{dt}\int_{D(t_i)} J d^3X = \int_{D(t_i)} \frac{dJ}{dt} d^3X \tag{3.25}$$

and using the continuity equation

$$\frac{dV}{dt} = \int_{D(t)} \theta d^3x \tag{3.26}$$

which explains why θ is known as the expansion scalar.

Now we need to define the average. We skip the difficulties assuming the average of a *scalar* over a domain D in terms of Eulerian coordinates as

$$\langle A \rangle_D = \frac{1}{V}\int_D A d^3x \tag{3.27}$$

which immediately implies that

$$\langle \theta \rangle_D = 3\frac{\dot{a}_D}{a_D} \equiv 3H_D \tag{3.28}$$

This consequently defines an effective Hubble parameter for the domain D.

3.2.2 Commutation rule

The definition of the average has a direct consequence: the time derivative of an average is different from the average of a time derivative. Indeed

$$\frac{d}{dt}\langle A\rangle = \frac{d}{dt}\frac{1}{V}\int A d^3x = -\frac{\dot{V}}{V}\langle A\rangle + \frac{1}{V}\int d^3X(\dot{A}J + A\dot{J}) = \\ -\langle\theta\rangle\langle A\rangle + \frac{1}{V}\int d^3X(\dot{A}J + A\theta J) \tag{3.29}$$

which leads to

$$\frac{d}{dt}\langle A\rangle - \left\langle \dot{A}\right\rangle = \langle A\theta\rangle - \langle A\rangle\langle\theta\rangle \tag{3.30}$$

This equation defines a non-trivial commutator between the time derivative and the averaging integral which depends on the expansion scalar θ.

The commutation rule has a crucial meaning: the dynamics of average scalars differs slightly from the standard dynamics and taking averages after having evolved a physical system in time is far different from evolving in time the system composed by the averages. Since the expansion scalar is related to the fluid velocity, we see that the non-trivial commutator is related to the divergence of the flow, which is a local function. This suggests that the origin of the commutation rule is somewhat related to the sources of the fluid flow, since the velocity is divergenceless only if no sources exist. Indeed the commutator becomes trivial if the expansion scalar is trivially null, but the equation

$$\langle\theta A\rangle = \langle\theta\rangle\langle A\rangle \tag{3.31}$$

has a more general solution, which is given by a θ constant in space. Then the continuity equation provides

$$\partial_t\rho + (\vec{v}\cdot\vec{\nabla})\rho + \rho K(t) = 0 \tag{3.32}$$

where K is the value of $\vec{\nabla}\cdot\vec{v}$. The solution is very general and solving it may be hard, since the velocity is not specified. But a significant simplification exists for velocity fields linear in $\vec{x}$, which we can generally write $\vec{v} = H(t)\vec{x}$. We rewrite the operator $\vec{v}\cdot\vec{\nabla}$ in spherical coordinates and it does not depend on the spherical angles, since the dot product is invariant under rotations, then

$$\dot{\rho} + \frac{|v|}{r}\frac{\partial\rho}{\partial r} + K(t)\rho = 0 \tag{3.33}$$

reduces to

$$\dot{\rho} + H\partial_r \rho + K\rho = 0 \tag{3.34}$$

under the approximation $\vec{v} = H(t)\vec{x}$. The template solution

$$f(r, \theta, \phi, t) = S(\theta, \phi)e^{\lambda(t)r} \tag{3.35}$$

solves the equation for a suitable spherical function $S(\theta, \phi)$. Indeed the function λ should satisfy

$$\dot{\lambda} + \frac{H}{r}\lambda + 3\frac{H}{r} = 0 \tag{3.36}$$

because $\vec{\nabla} \cdot \vec{v} = 3H$. The solution follows from Lagrange criterium

$$\lambda(t) = -3e^{\int_{t_0}^{t} \frac{H(s)}{r} ds} \int_{t_i}^{t} \frac{H(\tau)}{r} e^{\int_{\tau_i}^{\tau} \frac{H(s)}{r} ds} d\tau + Ce^{-\int_{t_0}^{t} H(s) ds} \tag{3.37}$$

This solution shows that the standard mean density $\bar{\rho}$ of the homogeneous FRW Universe, which satisfies

$$\dot{\bar{\rho}} + 3H\bar{\rho} = 0 \tag{3.38}$$

is not the only density consistent with a vanishing commutator. Then, assuming the existence of a Hubble flow is more general than standard homogeneity.

3.2.3 Newtonian backreaction

Now we can apply the definition of averages at the Euler-Newton system. The computation is straightforward

$$\tfrac{d}{dt} \langle \rho \rangle + \langle \rho \rangle \langle \theta \rangle = 0 \tag{3.39}$$

$$\tfrac{d}{dt} \langle \vec{\omega} \rangle - \left\langle (\vec{\omega} \cdot \vec{\nabla}) v \right\rangle + \langle \vec{\omega} \rangle \langle \theta \rangle = 0 \tag{3.40}$$

$$\tfrac{d}{dt} \langle \theta \rangle - \Lambda + 4\pi G \langle \rho \rangle - \tfrac{2}{3} \left(\left\langle \theta^2 \right\rangle - \langle \theta \rangle^2 - 2 \left\langle \omega^2 \right\rangle - 2 \left\langle \sigma^2 \right\rangle \right) = 0 \tag{3.41}$$

The first equation states that the mass in the domain D is conserved and corresponds to $M = a^3 \langle\rho\rangle$.

Since

$$\frac{d}{dt}\langle\theta\rangle = 3\frac{d}{dt}\frac{\dot{a}_D}{a_D} = 3\frac{\ddot{a}_D}{a_D} - \frac{1}{3}\langle\theta\rangle^2 \tag{3.42}$$

the last equation (Raychaudhuri equation), coupling the fluid with gravity, can be written as

$$3\frac{\ddot{a}_D}{a_D} + 4\pi G\frac{M}{a_D^3} - \Lambda = \frac{2}{3}\left\langle(\theta - \langle\theta\rangle)^2\right\rangle + 2(\left\langle\sigma^2 - \omega^2\right\rangle) \tag{3.43}$$

This equation is similar to the second Friedmann equation, provided that the density of the Universe is substituded by an effective density

$$\rho_{eff} = \langle\rho\rangle - \frac{1}{6\pi G}\left\langle(\theta - \langle\theta\rangle)^2\right\rangle + \frac{1}{2\pi G}(\left\langle\sigma^2 - \omega^2\right\rangle) \tag{3.44}$$

Raychaudhuri equation shows that shear and vorticity play a role in changing the dynamics of averages. In order to find the main consequences for cosmological acceleration, we assume that the cosmological fluid follows the Hubble flow and the local inhomogeneities are represented by a peculiar velocity field $\vec{u}$ which measures deviations from the Hubble flow.

Then

$$\partial_i v_j = H(t)\delta_{ij} + \partial_i u_j \tag{3.45}$$

and

$$\theta = 3H + \vec{\nabla}\cdot\vec{u} \tag{3.46}$$

Now we assume that $H(t) = \dot{a}_D/a_D$, which corresponds to an average null divergence of the peculiar velocity field. We should be careful in handling this equation: the function $H(t)$ which defines the Hubble flow cannot, in principle, be computed by the log-derivative of the scale factor. This important relation holds for the homogeneous FRW spacetime, but it drops with the homogeneity hypothesis. In the averaged context taking the log-derivative of the effective scale factor should provide an effective Hubble parameter H_D, which in principle may not be related to $H(t)$.

Stating that $H(t) = H_D$ means that every domain D expands following the underlying Hubble flow. Looking at the dynamics of a given volume D we should be able only to compute H_D, not $H(t)$, which now should be treated as an unphysical function. Here the assumption we followed simply skips the problem.

The second invariant of $\partial_i v_j$ is

$$2\mathbf{II} = \frac{2}{3}\theta^2 + 2(\omega^2 - \sigma^2) = 6H^2 + 4H\vec{\nabla}\cdot\vec{u} + \vec{\nabla}\cdot(\vec{u}(\vec{\nabla}\cdot\vec{u}) - (\vec{u}\cdot\vec{\nabla})\vec{u}) \quad (3.47)$$

Inserting this expression into the Raychaudhuri equation we find the *averaged Raychaudhuri equation*

$$3\frac{\ddot{a}_D}{a_D} + 4\pi G\frac{M}{a_D^3} - \Lambda = \frac{1}{a_D^3}\int_{\partial D}(\vec{u}(\vec{\nabla}\cdot\vec{u}) - (\vec{u}\cdot\vec{\nabla})\vec{u})d\vec{S} \quad (3.48)$$

where the equality follows applying Gauss theorem to the boundary of the domain D.

We note that the r.h.s. of the averaged Raychaudhuri equation is a full divergence and in principle it does not vanish. We define this new source *Newtonian backreaction*, which is given in general by the formula

$$Q_D = \frac{2}{3}\left\langle(\theta - \langle\theta\rangle)^2\right\rangle + 2\left\langle\omega^2\right\rangle - 2\left\langle\sigma^2\right\rangle \quad (3.49)$$

The interpretation of the backreaction term is quite easy. We assumed that the Hubble flow represent the mean motion of a given domain D and that peculiar velocities describe the local inhomogeneities as deviations from the Hubble flow. In this picture the backreaction term states that the peculiar velocity acts on the average dynamics as the source which drives the deviation from the standard dynamics of a homogeneous model. This shows that the dynamics of an average model is far different from the standard dynamics of a homogeneous model and that we should take care in using FRW when dealing with averaged objects in observational cosmology.

Unfortunately the Newtonian backreaction is a full divergence term, then it vanishes under particular geometrical conditions on the topology of the domain D which are not related to the inhomogeneous structure of

the Universe at all. For example if the domain has a topologically trivial boundary the backreaction must vanish since ∂D can be contracted to a point. This aspect play a negative role in N-body simulations, since usually periodic boundary conditions are assumed. Toroidal friedmannian models admit a Hubble flow, which corresponds to a self-similar evolution of the torus without rotations, and are often employed in N-body simulations. In this cases we may choose the domain D to coincide with the whole toroidal space, which is compact, and may try to compute the backreaction term, but it would be useless, because the boundary is trivial. Consequently toroidal models used in N-body Newtonian simulations failed in looking for newtonian backreaction (see the appendix of [26] for further details).

3.3 Relativistic approach

The averaging problem should be correctly approached in the context of General Relativity. We will show Buchert's derivation of backreaction in the relativistic framework as it is developed primarly in [28, 30].

A general working prescription is assumed, since Buchert's approach is based on spatial averages. It is well known that this approach faces troubles because a spatial domain is not causally connected. If we are interested in cosmological observations on average, we should imagine that the smoothing domain D is somewhat related to the future lightcone divergin from us. In principle we may assume that the smoothing scale is as big as the lightcone itself: we *see* cosmological informations as light rays, so the averaging problem is traslated to smooth the lightcone of an inhomogeneous Universe and understand how the coarse-graining affects cosmological observables. Here we do not discuss this fascinating theoretical aspect and simply describe Buchert's approach leaving the reader to the wide literature.

Buchert's averaging scheme is based on spatial averages. This assumptions require a prescription for defining what *spatial domains* are in a relativistic context. As a generalization of the newtonian approach, the average of a spatial domain requires to assume that we are always able to foliate spacetime as the direct product of a time direction and a 3D internal space slice. This 3+1 foliation of the spacetime is known as Arnowit-Deser-Misner prescription (see [14] for details) and implicitly

works in deriving the FRW metric.

The intrinsic covariant structure of Einstein equations does not allow to well-define any Cauchy problem for the metric tensor, considered as the basic unknown of a differential equation. Clearly the initial values must be substituted by general boundary conditions, which, in principle, cannot coincide with the standard initial conditions set for a general differential equation involving time as the basic parametrization of its solution. The ADM formalism allows for separating a time coordinate, which gives a simple framework for well-posed Cauchy problems.

The foliation of spacetime into 3D space slices labelled by a continuous parameter is ensured by the general requirement of global hyperbolicity. Any globally hyperbolic spacetime admits such a foliation. The labelling parameter (usually assessed as t) is known as *universal time*, but it may not coincide with the time coordinate of any observer.

Taking two different slices Σ_t and Σ_{t+dt} corresponding to an infinitesimal shift of the parameter t, we have to remember that distances among adiacent hypersurfaces may be measured along the path normal to Σ_t or along the coordinate lines, which are not required to be orthogonal to the time line. The distance between two adjacent surfaces along the normal can be written as

$$d = \alpha(x^i, t)dt \tag{3.50}$$

where α is known as the *lapse function*. The space shift on Σ_{t+dt} between two points starting at X^i on Σ_t and moving respectively along the normal and along the coordinate line is written as

$$\Delta x^i = -\beta^i(x^j, t)dt \tag{3.51}$$

where β^i is called *shift vector*. In principle the lapse function and the shift vector are free functions, since the foliation of spacetime remembers the intrinsic symmetry under reparametrization of a manifold. In order to deal with any problem we have to *gauge fix* the lapse function and the shift vector.

In other words the line element can be written generally as

$$ds^2 = (-\alpha^2 + \beta^2)dt^2 + 2\beta_i dx^i dt + \gamma_{ij}(x^i, t)dx^i dx^j \tag{3.52}$$

where $\gamma_{ij}(t)$ is the metric of Σ_t. The lapse function plays a role in volume measures, since the invariant volume element (for vanishing β)

$$dV = \sqrt{-\det(g)}d^4x = \alpha\sqrt{\det(\gamma)}dtd^3x \tag{3.53}$$

scales with α.

Assumg our foliation of spacetime the normal vector n^μ has coordinates

$$n^\mu = \left(\frac{1}{\alpha}, -\frac{\beta^i}{\alpha}\right) \tag{3.54}$$

If we ask that the comoving observers has four velocity u^μ orthogonal to the hypersurfaces Σ, we immediately see that a vanishing shift vector and a constant lapse function are required. So, we can in principle write

$$x^\mu = (t, X^i) \tag{3.55}$$

where X^i are spanning the space slice. Since the fluid-flow is orthogonal to the hyphersurface parameterized by X^i, these coordinates are Lagrangian coordinates for the fluid flow, since they behave exactly as standard Lagrangian coordinates in the non-relativistic case. Correspondingly the four velocity of comoving observers becomes

$$u^\mu = (1, 0, 0, 0) \tag{3.56}$$

as we have already showed.

3.3.1 Fluid dynamics

In the Newtonian case we coupled the basic equations of hydrodynamics with Newtonian gravity by adding the Poisson equation. In a relativistic context gravity is contained into the geometry of the spacetime, so we need to take care of fluid motion on a curved manifold. The metric will satisfy the Einstein field equations

$$R_{\mu\nu} - \frac{1}{2}g_{\mu\nu}R + \Lambda g_{\mu\nu} = \frac{8\pi G}{c^4}T_{\mu\nu} \tag{3.57}$$

as usual. We add a cosmological constant Λ and we do not specify the explicit form of the stress-energy tensor $T_{\mu\nu}$. The stress-energy tensor must be divergenceless

$$\nabla_\mu T^{\mu\nu} = 0 \tag{3.58}$$

as a consequence of Bianchi identities.

The ADM prescription forces to write the line element as

$$g_{\mu\nu}dx^\mu dx^\nu = ds^2 = -dt^2 + g_{ij}(t, \vec{X})dX^i dX^j \tag{3.59}$$

where t is the universal time. The hypersurfaces are described in terms of their first fundamental form, the metric g_{ij} and the extrinsic curvature

$$K_{ij} = -h_i^\mu h_j^\nu \nabla_\mu u_\nu \tag{3.60}$$

u_ν being the four-velocity of the comoving observers and $h_{\alpha\beta}$ the projector onto the hypersurfaces orthogonal to u_ν as usual.

Under the ADM foliation, the Einstein field equations break giving constraints and dynamical equations. The constraints are

$$\frac{1}{2}\left(R + (K_i^i)^2 - K_j^i K_i^j\right) = 8\pi G + \Lambda \tag{3.61}$$

$$D_i K_j^i - \partial_j K = 0 \tag{3.62}$$

We defined the reduced covariant derivative D_i as the covariant derivative with respect to the metric of the space slices g_{ij}

$$D_i K_l^j = \partial_i K_l^j + \Gamma_{ia}^j K_l^a - \Gamma_{il}^a K_a^j \tag{3.63}$$

where the connection Γ_{bc}^a refers to g_{ij} too.

The dynamical parts of the Einstein equations are

$$\dot{\rho} = K_i^i \rho \tag{3.64}$$

$$\tfrac{d}{dt} g_{ij} + 2 g_{ik} K_j^k = 0 \tag{3.65}$$

$$\tfrac{d}{dt} K_j^i = (K_a^a) K_j^i + R_j^i - (4\pi G\rho + \Lambda) g_j^i \tag{3.66}$$

where we introduced the density $\rho(t)$ of the irrotational fluid into the stress-energy tensor

$$T_{\mu\nu} = (\rho + p) u_\mu u_\nu - p g_{\mu\nu} \tag{3.67}$$

and set the pressure p to zero.

We divide the extrinsic curvature tensor K_i^j in a symmetric traceless part and a trace part as

$$-K_i^j = \sigma_{ij} + \frac{1}{3}\theta g_{ij} \tag{3.68}$$

where $\theta = -K_i^i$. No antisymetric part is allowed since the extrinsic curvature is a symmetiyc tensor by definition. The trace θ plays the role of the expansion scalar in newtonian theory and $-K_i^j$ can be treated as an *expansion tensor*, suggesting that in a relativistic framework the averaging procedure should match the geometry in a more complicated way.

Correspondingly the Einstein equations and the conservation law for the stress-energy tensor become

$$\tfrac{1}{2}R + \tfrac{1}{3}\theta^2 - \sigma^2 = 8\pi G\rho + \Lambda \tag{3.69}$$

$$D_i\sigma_j^i = \tfrac{2}{3}\partial_j\theta \tag{3.70}$$

$$\tfrac{d}{dt}\rho = -\theta\rho \tag{3.71}$$

$$\tfrac{d}{dt}g_{ij} = 2g_{ik}\sigma_j^k + \tfrac{2}{3}\theta g_{ij} \tag{3.72}$$

$$\tfrac{d}{dt}\sigma_j^i = -\theta\sigma_j^i - R_j^i + \tfrac{2}{3}\left(\sigma^2 - \tfrac{1}{3}\theta^2 + 8\pi G\rho + \Lambda\right)\delta_j^i \tag{3.73}$$

We have implicitly used Raychaudhuri equation (here $2\sigma^2 = \sigma_j^i\sigma_i^j$)

$$\dot{\theta} + \frac{1}{3}\theta^2 + 2\sigma^2 + 4\pi G\rho - \Lambda = 0 \tag{3.74}$$

which follows combining the trace of the last equation in 3.69 and the first one. For more details look at [28].

Now we can handle the problem of taking spatial averages. The trace of

$$\frac{d}{dt}g_{ij} + 2g_{ik}K_j^k \tag{3.75}$$

provides the general result

$$K_j^i = -\frac{1}{2}g^{ik}\dot{g}_{kj} \tag{3.76}$$

and defining

$$J(t, X^i) \equiv \sqrt{\det(g_{ij})} \tag{3.77}$$

we can compute the time derivate of the volume element, which should play a crucial role in taking averages. The operatorial identity

$$\exp(Tr(A)) = \det(\exp(A)) \tag{3.78}$$

provides

$$\frac{d}{dt}\log(J) = \frac{1}{2}g^{ik}\dot{g}_{ij} = -K^i_j \tag{3.79}$$

and the fundamental relation

$$\dot{J} = \theta J \tag{3.80}$$

still holds in the relativistic approach.

Following [28] we define an effective scale factor for any given domain D embedded into a space hypersurface as the measure of its edge at any given time:

$$a_D(t)^3 = \frac{V_D(t)}{V_{D_i}} = \frac{1}{V_i}\int_{D(t)} J d^3X \tag{3.81}$$

where V_{D_i} is the volume of the domain at a given initial time.

We are now able to define the 3D average of a scalar function over the domain D by simply integrating over the normal coordinates that parameterize D inside the constant-time slice of the spacetime:

$$\langle A\rangle = \frac{1}{V_D}\int A(X)\sqrt{\det(g_{ij})}d^3X \tag{3.82}$$

The average of the expansion rate

$$\langle\theta\rangle_D = \frac{\dot{V}_D}{V_D} = 3\frac{\dot{a}_D}{a_D} \equiv 3H_D \tag{3.83}$$

gives the definition of the effective Hubble rate H_D.

Using the definition of θ we may integrate

$$\dot{\rho} = -\theta\rho \equiv \frac{\dot{J}}{J} \tag{3.84}$$

finding

$$\rho(t) = \rho(t_i)\frac{J(t_i)}{J(t)} \tag{3.85}$$

which ensures that the mass inside the domain D

$$M = \int_D \rho(X,t)J(X,t)d^3X \tag{3.86}$$

is constant.

3.3.2 Modified Friedmann equations

Averaging Raychaudhuri equation provides a modified Friedmann equation for the effective scale factor of the domain D

$$3\frac{\ddot{a}_D}{a_D} + 4\pi G\langle\rho\rangle_D - \Lambda = Q_D \tag{3.87}$$

which accounts for the dynamics of D given the completely new source Q_D. Since the mass inside D is constant, we may substitute

$$\langle\rho\rangle = \frac{M}{V_{D_i}a_D^3} \tag{3.88}$$

The new term Q_D is the analogue of the newtonian backreaction. It naturally arises from the averaging procedure and can be written as a function of the principal invariants of the extrinsic curvature of the space slices as

$$Q_D = 2\langle\mathbf{II}\rangle_D - \frac{2}{3}\langle\mathbf{I}\rangle_D^2 \tag{3.89}$$

or in terms of the expansion scalar and the shear like

$$Q_D = \frac{2}{3}\left\langle(\theta - \langle\theta\rangle_D)^2\right\rangle_D - \left\langle\sigma_i^j\sigma_j^i\right\rangle_D \tag{3.90}$$

Averaging Eq. 3.69 provides

$$3\left(\frac{\dot{a}_D}{a_D}\right)^2 - 8\pi G\langle\rho\rangle_D - \Lambda = -\frac{\langle R\rangle_D + Q_D}{2} \tag{3.91}$$

This equation requires some care. It shows the fashion of the first Friedmann equation, since it involves H_D^2. The main difference between the standard equation and the averaged one is the extra source term represented by the backreaction and the averaged Ricci scalar, which are functions of time and are intrinsically domain-dependent. Here we can see that the relativistic approach involves the mean Ricci curvature in the equation driving the average dynamics, suggesting a complicated coupling between the backreaction itself and the geometry.

In the FRW spacetime the Friedmann equations can be linked by an integration, since $\ddot{a}/a = \dot{H} + H^2$. For example in a flat Universe filled by irrotational dust only we may write

$$\dot{H} = -\frac{4}{3}\pi G\rho - H^2 \tag{3.92}$$

and inserting the first Friedmann equation

$$H^2 = \frac{8\pi G\rho}{3} \tag{3.93}$$

gives trivially the continuity equation $\dot{\rho}+3H\rho = 0$, which is a fundamental identity of the theory.

The integrability condition is a consequence of the the conservation of $T^{\mu\nu}$ combined with Einstein equations. We may require that the same integrability condition still works in the averaged context, linking Eq. 3.87 and Eq. 3.91. This assumption leads to an independent relation between the averaged Ricci curvature and the backreaction:

$$\frac{1}{a_D^6}\partial_t(Q_D a_D^6) + \frac{1}{a_D^2}\partial_t(\langle R\rangle_D\, a_D^2) = 0 \tag{3.94}$$

The link between the backreaction and the geometry of the 3D hypersurfaces we used for the foliation of spacetime is now clear, giving a fully relativistic interpretation of the backreaction problem.

3.3.3 Effective cosmological parameters

As in [28, 34], we can define new effective parameters by following the same procedure we have used for the definition of a_D. We have already introduced the effective Hubble parameter

$$H_D = \frac{\dot{a}_D}{a_D} \tag{3.95}$$

which represents the expansion rate of a given domain.

The effective density parameters for matter, curvature, cosmological constant and backreaction are

$$\Omega_m^D = \frac{8\pi G}{3H_D^2} \langle \rho \rangle_D \tag{3.96}$$

$$\Omega_R^D = -\frac{\langle R \rangle_D}{6H_D^2} \tag{3.97}$$

$$\Omega_\Lambda^D = \frac{\Lambda}{3H_D^2} \tag{3.98}$$

$$\Omega_Q^D = -\frac{Q_D}{6H_D^2} \tag{3.99}$$

The previous definitions can be substituted into the modified Friedmann equation in order to obtain the so called *cosmic quartet* relation

$$\Omega_m^D + \Omega_k^D + \Omega_\Lambda^D + \Omega_Q^D = 1 \tag{3.100}$$

which is an extension of the usual relation between the density parameters in the usual FRW context. This extended relation accounts for a non-vanishing curvature Ω_k^D and for the backreaction term Ω_Q^D, which can be thought as a further energy component explaining the missing energy of the Universe. The parameter related to the cosmological constant is present in the model in order to account for the contribution of the cosmological constant to the total energy content of the Universe. It seems quite simple to look at the backreaction as a component which can substitute the cosmological constant in explaining the missing energy, but the previous calculation shows how their behaviour is dynamically different and how the cosmological constant can still play its role.

Following Buchert [34] we set $\Omega_\Lambda^D = 0$ in the following calculations and we may also define an X-component which encodes all the energy contributions coming from the geometry:

$$\Omega_X^D = \Omega_k^D + \Omega_Q^D \tag{3.101}$$

suggesting that energy is required to curve spacetime and also to coarse-grain it.

3.4 Testing backreaction

The idea of explaining Dark Energy as an effect of local inhomogeneities has been studied since [77, 78]. Most approaches assumed that the FRW spacetime is the underlying zero-order of a perturbative expansion which represent the local inhomogeneities as small deviation from the homogeneous and isotropic solution. In [34] the same idea is developed in a different way. The authors face the problem disregarding the assumption that the FRW solution describes perturbatively the effective evolution of an inhomogeneous Universe. The underlying hypothesis is weaker: the kinematics of a homogeneous and isotropic state does not necessarily agree with the kinematics of a homogeneous and isotropic solution. They do not care of the nature of the local inhomogeneities, which explicitly should not be seen as perturbative deviations from a FRW underlying model. At the same time the averaged properties of Einstein equations still work, suggesting that an interpretation of Dark Energy in terms of backreaction may require to break perturbative schemes and study the effective models in more general contexts.

3.4.1 Template metric

Following Buchert's approach (see [34]) requires to face the problem of finding an *effective* form of the metric. The true metric of the inhomogeneous spacetime is completely unknown and the approximation of small deviations around an FRW *zero-order* must be disregarded.

We can look at the problem under general principles, following the argument proposed in [79]. The definition of the average may be assumed as the working prescription for coarse-graining the matter distribution.

Coarse-graining the matter field means that we know how to coarse-grain the stress energy tensor in the Einstein equations, but no prescription is given for averaging the metric itself. Moreover the averaging scheme we developed still contains the determinant of the bare metric, which should be consistently substituted by the averaged one, and then is not completely well-defined if we do not specify how to deal with the geometry.

We have already shown that many different point of view exist in approaching the averaging problem under general principles. Here we simply follow the qualitative argument in [79], which leads to the template metric used in [34]. The authors of [79] note that some scheme must be assumed for coarse-graining the metric, but we can try to skip the intrinsic difficulties of such a definition following physical imputs on the final form of the coarse-grained metric. Since at large scales the matter distribution seems homogeneous and the CMB is highly isotropic, the coarse-graining procedure of the metric tensor should provide an averaged spacetime similar to the FRW. The crucial assumption on the averaging schemes proposed in [79] is the coincindence of the scale factor $a(t)$ of the FRW metric with the effective domain-dependent $a_D(t)$ as it is defined by Buchert. This aspect requires some care: in the context of averaged models the scale factor $a(t)$ is, in principle, meaningless, since the cosmic expansion may be measured only computing the effective a_D on a given scale, so it must be replaced, but the substitution $a(t) \to a_D(t)$ seems arbitrary. Behind this strong prescription two principles are working. First, at any given time the coarse graining procedure acts on a given volume smoothing the density. In the procedure all the information on the detailed structure of the density field is lost and so many different cosmologies may be averaged giving the same value of the smoothed density. The value of the smoothed density is time-dependent, since the coarse-graining is taken at a given fixed time, so we have only to assume that the Universe is sufficently big that all possible configurations of matter which can be realized on a given scale can be smoothed to some homogeneous state with the right value of the mean density. In this sense the coarse-graining is statistically consistent. Then, fixed the coarse-graining volume D, the FRW which we find as the output of the averaging scheme must be dominated by a mean density whose dynamics is driven by the *mean* expansion scalar of the domain D, which ensures that the correct Hubble parameter must be given by

$$\langle\theta\rangle_D = 3H_D \tag{3.102}$$

This equation implies that the corresponding scale factor in the coarse-grained FRW is a_D as defined by Buchert. This shows why the substitution $a(t) \to a_D(t)$ may work.

An important consequence of this scheme is related to the curvature of the coarse-grained FRW. When the smoothing procedure acts on the metric it must give an FRW, but no prescriptions are given, in principle, on the curvature k, since many values of k may be degenerate with the same value of the averaged density.We have to account for this extra freedom, which have interesting consequences.

The idea that the averaging scheme on the metric tensor should provide an highly symmetric space can be tackled with other arguments and can be treated better in the framework of the Ricci flow renormalization procedure. The renormalization on an inhomogeneous geometry decreases the intrinsic inhomogeneities and smoothes them down, which leads naturally to a constant curvature space (see [29, 31, 35] and references therein for a complete discussion).This suggests again that the best candidate for the output of the coarse-graining procedure should be FRW-like.

The main difference between the coarse-grained spacetime and the usual FRW lies in the following: the FRW is made of 3-slices which have the same constant curvature, while Buchert's template metric has constant curvature slices each with a different value of the curvature itself.

Then we can write the metric as

$$g_{\mu\nu}dx^\mu dx^\nu = -dt^2 + \frac{1}{H_{D_0}^2}\frac{a_D^2}{a_{D_0}^2}\left(\frac{dr^2}{1-k_D(t)r^2} + d\Omega^2\right) \tag{3.103}$$

The non standard form of this *quasi-FRW* metric, containing the extra factor

$$\frac{a_D^2}{H_{D_0}a_{D_0}^2} \tag{3.104}$$

has been proposed in [34] in order to deal with dimensionless ccordinate distances and scale factors.

The parameter $k_D(t)$, which describes the time variation of the 3-space curvature, must be related to the full spacetime Ricci scalar, in analogy with the FLRW model. So, we also assume that

$$\langle R\rangle_D = \frac{k_D(t)|\,\langle R\rangle_{D_0}\,|a_{D_0}^2}{a_D^2} \tag{3.105}$$

We can recover the usual FLRW metric when D becomes very large by setting $k_D(t_0)|\,\langle R\rangle_{D_0}\,| = k_{D_0}/6$ with a constant k_{D_0}.

It is very important to notice that the template metric is not a simple dust solution of the Einstein equations. Indeed the true metric describing the inhomogeneous Universe is not known and this metric should only be an effective solution of the field equations, provided that the smoothing procedure can be correctly defined for the tensors involved in Einstein equations.

Now we can use the template metric to compute the main observables in the coarse-grained cosmology. The first step requires to compute the paths of light rays, which are changed from the standard ones since the curvature is time-dependent. This important step tells us that the template metric sums up the effects of the coarse-grained inhomogeneities changing the path of light. In other words the final effect of the averaging scheme is changing only the way light propagates in space. This clearly **shows the effect of the coarse-graining**, since all the details of the inhomogeneous structure, which are contained in the completely unknown bare metric, are lost and only their mean effect on light can be seen and used to discover the difference between a true homogeneous cosmology and an averaged one.

Following Buchert [34] we compute the distance between two points on two slices at different cosmic time. First we remember that the distance between two points in the same slice is given by

$$l(t) = a_D(t)\int_0^r \frac{dx}{\sqrt{1-k_D(t)x^2}} \tag{3.106}$$

and so we can compute the derivative of this distance with respect to cosmic time in order to evaluate the infinitesimal distance between points belonging to different slices which are separated by an infinitesimal time dt:

$$\frac{dl}{dt} = H_D(t)l(t) + a_D(t)\frac{dk_D(t)}{dt}\int_0^r \frac{x^2 dx}{1 - k_D(t)x^2} \tag{3.107}$$

We can identify the standard Hubble flow (first term on the r.h.s) and an extra term which arises as a consequence of the time dependence of the curvature parameter. If we focus on the path of a photon, the l.h.s of the last equation is simply the speed of light, so the equation reduces to

$$\frac{dr}{dt} = \frac{c}{a_D(t)}\sqrt{1 - k_D(t)r^2} \tag{3.108}$$

which is a differential equation for the coordinate distance travelled by a photon.

If we need to compute an observable, we have to solve the non-trivial problem of the light paths in an inhomogenous background. Here we face this problem by solving directly the photon path equations. We introduce formally an effective redshift

$$1 + z_D = \frac{(g_{ab}k^a u^b)_S}{(g_{cd}k^c u^d)_O} \tag{3.109}$$

where k^a is the light wave-vector, u^b is the comoving observer 4-velocity, S labels the source and O the observer as usual. Since the wave-vector is normalized such that at the observer $k^a u_a = -1$, we simply have

$$1 + z_D = (a_D k^0)_S \tag{3.110}$$

The wave-vector satisfies the geodesic equation $k^\nu \nabla_\nu k^\mu = 0$, which can be written in the context of our template as

$$\frac{1}{\hat{k}^0}\frac{d\hat{k}^0}{a_D} = -\frac{r^2(a_D)}{2(1 - k_D(a_D)r^2(a_D))}\frac{dk_D(a_D)}{da_D} \tag{3.111}$$

In this equation the function $r(a_D)$ is the coordinate distance, which can be derived as a function of the effective scale factor by solving equation (3.108) written in a different way

$$\frac{dr(a_D)}{da_D} = -\frac{H_{D_0}}{a_D^2 H_D(a_D)}\sqrt{1 - k_D(a_D)r^2} \tag{3.112}$$

with the boundary condition $r(a_{D_0}) = 0$.

The previous model allows the computation of important observables in cosmology, like the luminosity distance and the angular diameter distance:

$$d_A(z_D) = \frac{c}{H_{D_0}} a_D(z_D) r(z_D) \tag{3.113}$$

$$d_L(z_D) = (1 + z_D)^2 d_A(z_D) \tag{3.114}$$

The main point is encoded in the relation between the effective scale factor and the effective redshift. This relation is given by the solution of the geodesic equation and differs from the usual one

$$1 + z = \frac{1}{a} \tag{3.115}$$

which can be recovered by imposing that the parameter k_D is constant.

In the backreaction context the previous relation is substituted by a wider relation

$$1 + z_D = f(a_D) \tag{3.116}$$

where the function $f(a_D)$ is computed numerically because the geodesic equation 3.111 cannot be easily solved analitically.

3.4.2 Morphon field

In [33] the relativistic backreaction model is linked to standard cosmologies based on scalar fields showing that an useful correspondence may be built if a mean field approach is used in treating matter inhomogeneities. The authors disregard the standard approach of adding a scalar field source in the stress-energy tensor of the inhomogeneous spacetime, but describe with a homogeneous scalar field the spatially averaged degrees of freedom. The morphon field encodes the kinematical backreaction and models the Universe capturing the total effect of deviation from the standard FRW dynamics. Since it is strictly related to the geometry of the spatial slices of the bare spacetime, the authors suggest that the morphon should be interpreted as modelling the vaccum. Correspondingly, the morphon field

can be seen as a way of dealing with the problem of computing the effect of coarse-graining the vacuum field equations.

In [33] it is also demonstrated that the morphon is able to reproduce any standard cosmology with Dark Energy modelled as a quintessence field like any other scalar field depending on the possibility of modelling the shape of the morphon potential. This result enhaces the idea of interpreting Dark Energy as a backreaction effect.

Following [33] we assume irrotational dust only filling the Universe and no curvature nor cosmological constant on the FRW side of the correspondence. This choice is justified since the Λ term can be seen as a particular case of quintessence and the constant curvature of non-flat slices can be interpreted as a particular case of backreaction.

The effective Friedmann equations 3.87 and 3.91 can be rewritten in standard form if we substitute standard density and pressure with their effective counterparts

$$\rho_D^{eff} = \langle\rho\rangle_D - \frac{Q_D + \langle R\rangle_D}{16\pi G} \tag{3.117}$$

$$p_D^{eff} = \frac{\langle R\rangle_D - 3Q_D}{48\pi G} \tag{3.118}$$

After these substitutions the effective Friedmann equations behave like the standard ones and can be solved if an *effective equation of state*

$$p_D^{eff} = F(\rho_D^{eff}, a_D) \tag{3.119}$$

is assumed. The effective equation of state **cannot** be treated exactly as the standard one. The equation of state must be scale-dependent, since the effective parameters are intrinsically scale-dependendent, while the standard one is scale-invariant. The scale-dependence arises from the evolution history of the inhomogeneities on any given scale and the equation of state define the *cosmic state* on a given spatial scale.

We may introduce here a scalar field ϕ_D, the morphon, which evolves accordingly to an effective potential U_D. We assume that the morphon is responsible for the effective pressure and densities exerted by the backreaction, then

$$\rho^D_{eff} = \langle\rho\rangle + \rho^D_\phi \tag{3.120}$$
$$p^D_{eff} = p^D_\phi \tag{3.121}$$

The pressure and the density of a scalar field are known

$$\rho^D_\phi = \frac{\epsilon}{2}\dot{\phi}^2_D + U_D \tag{3.122}$$
$$p^D_\phi = \frac{\epsilon}{2}\dot{\phi}^2_D - U_D \tag{3.123}$$

where $\epsilon \in \{-1, 1\}$ generalizes the scalar field (with $\epsilon = 1$) to the phantom field, with negative kinetic energy, corresponding to $\epsilon = -1$.

Expressing the effective density and pressure in terms of $Q_D$and $\langle R\rangle_D$ provides

$$Q_D = 8\pi G(U_D - \epsilon\dot{\phi}^2_D) \tag{3.124}$$
$$\langle R\rangle_D = -24\pi G U_D \tag{3.125}$$

These relations show that the morphon potential is proportional to the average spatial curvature of the hypersurfaces, while the backreaction can be interpreted as a kinetical contribution to the energy of the morphon. If we identify the term

$$E^D_k = \frac{1}{2}\dot{\phi}^2_D \tag{3.126}$$

as the kinetic energy of the morphon, we immediately see that for vanishing backreaction a sort of virial condition

$$2\epsilon E^D_k - U_D = 0 \tag{3.127}$$

is satisfied, which suggest that the coarse graining of the local inhomogeneities can be read as a statistical breaking of an equilibrium condition, which correspond to the standard FRW solution. Since the condition is scale-dependent, we may say that scales with vanishing backreaction are *in equilibrium* and evolves like the standard homogeneous and isotropic solution, while the others are not.

The integrability condition reduces to the Klein-Gordon equation for a scalar field minimally coupled with the FRW metric:

$$\ddot{\phi}_D + 3H_D + \epsilon U'[\phi_D] = 0 \tag{3.128}$$

These relations require to define an effective equation of state for the morphon

$$p_\phi^D = w_\phi^D \rho_\phi^D \tag{3.129}$$

which has nothing to do with the general effective equation of state which accounts also for the matter content. We have already shown that quintessence model violate the strong energy condition

$$\rho + 3p > 0 \tag{3.130}$$

in order to explain cosmic acceleration. In the morphon model the strong energy condition is violated by the effective sources and the cosmic expansion may be explained, but in principle it is not violated by the *true* sources, which are ordinary matter and radiation. This interesting result clearly explain why the backreaction may be considered as a solution to the Dark Energy problem which do not require any new exotic cosmic fluid nor modification of gravity laws.

The morphon is able to reproduce the cosmological constant if we set $\dot{\phi}_D = 0$ and the potential U_D to a constant value U_{D_i}. The corresponding backreaction is constant too: $Q_D = 8\pi G U_{D_i}$.

3.4.3 Scaling solutions

In [33, 34] the correspondence substained by the morphon field is studied in term of scaling solutions of the backreaction problem. We postulate that solutions with the exact scaling

$$Q_D = Q_{D_i} a_D^p \qquad \langle R \rangle_D = \langle R \rangle_{D_i} a_D^n \tag{3.131}$$

exist, for some real exponents. The existence of such solutions is suggested by the integrability condition, which is trivially satisfied if $p = -6$ and $n = -2$. This quite trivial solution (it is the only solution with $n \neq p$)

corresponds to a quasi-Friedmannian Universe with a negligible backreaction decoupled from the scalar curvature. The backreaction and the mean scalar curvature evolve separately. This suggest that the average dynamics behave like an FRW solution and soon all scales have the same constant curvature, providing a morphon model which becomes rapidly indistinguishable from the standard FRW. On the contrary the solution $n = p$ corresponds to a direct coupling between backreaction and scalar curvature and it is more interesting, since the coupling is a true relativistic effect, which should be considered as an intrinsic property.

In this case we assume that a backreaction parameter r^D exists satisfying

$$Q_D = r^D \langle R \rangle_{D_i} a_D^n \tag{3.132}$$

and the integrability condition forces

$$r^D = -2\frac{1+3r^D}{1+r^D} \tag{3.133}$$

The value $r^D = -1$ is singular and corresponds to the trivial case of a cosmological model with vanishing backreaction and curvature, i.e. the Einstein-de Sitter model.

Inserting the scaling solution into the definitions of the morphon density and pressure gives

$$\dot{\phi}_D^2 = -\epsilon\frac{R_{D_i}}{8\pi G}\left(r^D + \frac{1}{3}\right)a_D^n \tag{3.134}$$

$$U_D = -\frac{R_{D_i}}{24\pi G}a_D^n \tag{3.135}$$

which allows for distinguish between a scalar field and a phantom field:

Table 3.1: Morphon field

	$R_{D_i} < 0$	$R_{D_i} > 0$
$r^D < -\frac{1}{3}$	PHANTOM FIELD	SCALAR FIELD
$r^D > -\frac{1}{3}$	SCALAR FIELD	PHANTOM FIELD

Now we are able to write an analytical formula for the morphon field

$$\phi_D = \frac{\sqrt{-2\epsilon n}}{(n+3)\sqrt{\pi G}} \sinh^{-1}\left(\sqrt{(1+r^D)\frac{\Omega_R^{D_i}}{\Omega_m^{D_i}} a_D^{n+3}}\right) \tag{3.136}$$

and for the potential U_D:

$$\begin{aligned} U_D = \frac{2(1+r^D)}{3}\left[(1+r^D)\frac{\Omega_R^{D_i}}{\Omega_m^{D_i}}\right]^{\frac{3}{n+3}} \times \\ \langle\rho\rangle_{D_i} \sinh^{\frac{2n}{n+3}}\left[\frac{n+3}{\sqrt{-\epsilon n}}\sqrt{2\pi G}\phi_D\right] \end{aligned} \tag{3.137}$$

The above solution adds a new singularity for $r = 1/3$ which corresponds to an Einstein-de Sitter scenario with a renormalized initial dust density. (see [33] for details) In the limit case of a vanishing matter source, corresponding to a vacuum Universe, the solution still holds, provided that we take the limit $\phi_D \to +\infty$. This interesting feature clearly shows that the morphon field plays the role of the coarse-graining procedure of the metric. If the introduction of the morphon would have simply be a different way of dealing with the average of matter inhomogeneities, no solution should exist in the vacuum limit.

Putting the scaling solution into the definition of the Ricci scalar and backreaction we derive the equations we will handle in testing backreaction:

$$
\begin{aligned}
Q_D &= r\,\langle R\rangle_D && (3.138)\\
\langle R\rangle_D &= \langle R\rangle_{D_i}\, a_D^n && (3.139)\\
Q_D &= -\frac{n+2}{n+6}\,\langle R\rangle_{D_i}\, a_D^n && (3.140)\\
\Omega_X^D &= -\frac{2\,\langle R\rangle_{D_i}\, a_D^n}{3(n+6)H_D^2} && (3.141)\\
H_D^2(a_D) &= H_{D_0}(\Omega_m^{D_0} a_D^{-3} + \Omega_r^{D_0} a_D^{-4} + \Omega_X^{D_0} a_D^n) && (3.142)\\
k_D(a_D) &= -\frac{(n+6)\Omega_X^{D_0} a_D^{n+2}}{|(n+6)\Omega_X^{D_0}|} && (3.143)\\
\frac{dr}{da_D} &= \sqrt{\frac{1-k_D(a_D)r^2}{\Omega_m^{D_0} a_D^{-3} + \Omega_r^{D_0} a_D^{-4} + \Omega_X^{D_0} a_D^n}} && (3.144)
\end{aligned}
$$

where $\Omega_X^{D_0}$ is the X-component parameter at a given initial time. We have generalized Larena's equations adding the radiation component $\Omega_r^{D_0}$ at the given initial time to the effective Hubble parameter. We assumed that

$$\Omega_r^{D_0} a_D^{-4} \tag{3.145}$$

provides the correct scaling of the radiation energy density with the effective scale factor. This assumption is based on the analogy with the usual homogeneous case.

Finally we may rewrite the relation between the effective density and pressure in the well known form of a conservation law:

$$\dot{\rho}_{eff}^D + 3H_D(\rho_{eff}^D + p_{eff}^D) = 0 \tag{3.146}$$

where

$$p_{eff}^D = w^D \rho_{eff}^D \tag{3.147}$$

defines explicitly the domain-dependent effective parameter w^D. We remember that it is not defined as an average over the domain D although it should be constant all over D, assuming the standard values $w = 0$ or $w = 1/3$ for ordinary matter and radiation.

Chapter 4

Probing backreaction

In [34] the template metric (Eq. 3.103) is used for testing backreaction. Since inhomogeneities are not treated as perturbations around a FRW background, the authors check how the main differences between the averaged dynamics and the standard FRW solution leave their fingerprints in the observable Universe.

The morphon field plays a crucial role, since it provides an interesting relation between the backreacted scenario and Standard Cosmology. The authors focus on the correspondence between a flat FRW model with Dark Energy modelled as a quintessence field of constant equation of state and a backreacted Universe filled with dust whose effective metric is given by Eq.3.103. They perform a likelihood analysis based on two sets of cosmological measurements in order to jointly constrain the effective cosmological parameter $\Omega_m^{D_0}$ and the backreaction scaling index n. They combine constraints obtained analyzing the SuperNova Legacy Survey (SNLS) and $WMAP$ 3-yr data [41] on the TT-power spectrum of the CMB.

The SN Ia studied in [9] provide a set of angular diameter distances which can be directly checked against the predictions coming from the two theoretical models on both sides of the correspondence substained by the morphon field. The analysis involving the anisotropy spectrum of the CMB is a little more involved, since cosmological information is stored in CMB data as a slight modification of the shape of the power spectrum.

We followed the same path proposed in [34] in order to upgrade the likelihood analysis to the present status of cosmological observations. In

[34] the authors found that data give different joint constraints on $\Omega_m^{D_0}$ and n for the two models: the backreaction model should predict a denser Universe. We perform the same likelihood analysis involving joint constraints on the matter density $\Omega_m^{D_0}$ and the Dark Energy equation of state parameter w^D, which is related to n by

$$w^D = -\frac{n+3}{3} \tag{4.1}$$

We improve the data sets adding Supernovae angular diameter distances derived from the *Union2.1* catalog and CMB data on the TT-power spectrum of CMB anisotropies as recently measured by $WMAP$-9 yr and the *Planck* mission.

We add extra constraints coming from the analysis of the angular diameter distances of a set of galaxy clusters published in [24]. Here we review the basic theoretical aspects driving our likelihood analysis and show what current data suggest and show our own results.

4.1 Luminosity distances of Supernovae Ia

Distant SN Ia recently showed (see [1, 2, 3, 4] and references therein) that the Universe is living a phase of accelerated expansion. The FRW model is not able to explain cosmological observations based on surveys of SN Ia without introducing Dark Energy, regardless of whether it behaves like a cosmological constant or a quintessence field.

Supernovae of type Ia take place at the end of the stellar life. The hydrodynamic equilibrium is achieved by the opposite contribution of the gravitational field of the star and the radiation pressure, which prevent the gravitational collapse. When the radiation pressure drops at the end of the main sequence, the gravitational collapse starts and, if a new equilibrium state is possible, the star turns into a white dwarf, where the gravitational collapse is arrested by the intrinsic quantum pressure of degenerate electrons exerting exchange forces. The corresponding pressure has an upper limit, which selects the maximum mass that can collapse into a white dwarf, well known as the Chandrassekar limit and corresponding to about 1.44 $M_\odot$. Otherwise the gravitational collapse cannot stop and other objects form.

If the mass of a white dwarf increases, for example as a consequence of accretion from a nearby star, near the Chandrassekar limit the white dwarf becomes highly unstable and may turn into a Supernova of type Ia. The physical processes involved in the formation of SN Ia are currently debated, but clearly the critical point is reached near the Chandrassekar limit, suggesting that the treshold energy should be the same for all SN Ia, corresponding to a common intrinsic luminosity. This very useful property makes SN Ia standard candles and cosmological rulers, since it is possible to derive the luminosity distance of a source knowing both the intrinsic and the apparent luminosity (see [8]). If m is the apparent magnitude and M is the absolute one, the relation

$$m - M = 5 \log_{10} \left(\frac{d_L}{10\text{pc}} \right) + K \tag{4.2}$$

gives the reduced luminosity distance $d_L = (H_0/c)D_L$ up to a correction K due to cosmic expansion that we can handle easily. The magnitude m can be measured from the light curves of SN, while the asolute magnitude M is not known in principle, leaving the formula completely useless. The problem can be skipped if the SNe are standard candles, like those of type Ia, since the terms drop and the luminosity distances can be computed.

4.1.1 The catalogs

We first perform our analysis on the SNLS catalog [9]. This dataset is used in order to directly compare our constraints with those obtained in [34]. It is composed by two subsamples of SNe Ia characterized by different redshift ranges. The former is composed of 44 nearby Supernovae already known from the literature, the latter records 73 measured distant events. The nearby Supernovae are chosen such that $z > 0.015$ in order to reduce the influence of peculiar velocities on the measurement procedure.The maximum redshift for these Supernovae is $z = 0.125$. The sample of distant Supernoave contains secure events (SN Ia) and probable Supernovae Ia (SN Ia*), for which the spectrum fits the theoretical SN Ia prediction better than any other type, but other possibilities are not completely ruled out. The redshifts range from $z = 0.249$ to $z = 1.01$.

Then we upgrade our analysis adding data from a more recent catalog, the *Union2.1*. The sample [7] is an update of the *Union2* (see [6]). The

Union2 sample is one of the largest SN Ia samples and it is composed of 557 SN Ia with redshifts ranging from $z = 0.015$ to $z = 1.4$. The sample has improved the previous *Union* sample [5] with new measurements of high redshift events, combining different data sets. The *Union2.1* updates the previous *Union2* sample by adding 23 secure or probable SN Ia from the *Hubble Space Telescope Cluster Survey* and from the low redshift sample of Contreras et al. [10]. The light curves have been obtained using the single light fitter SALT2 and the candidates had to fulfill strict quality requirements.

4.1.2 Distance modulus statistical analysis

We statistically analyze type Ia supernovae data. The main observable is the distance modulus, related to $d_L(z, \theta)$ through

$$\mu(z) = 5 \log_{10}(d_L) + \mu_0. \tag{4.3}$$

The luminosity distance depends also on a set of parameters, which here are simply denoted with θ. The shift μ_0 is a nuisance parameter which encodes the dependence on the SN absolute magnitude M.

In the context of a FRW Universe the reduced luminosity distance can be written in terms of the Hubble function $H(z)$ as

$$d_L(z, \theta) = (1 + z) \int_0^z \frac{H_0}{H(z', \theta)} dz' \tag{4.4}$$

where all parameters but the redshift are encoded in θ. For a likelihood analysis the dimensional factor c/H_0 is not important at all, because it provides an overall factor in the final expression of the likelihood, which is completely removed by normalizing the likelihood. In other words, it is possible to interchange the reduced luminosity distance with its full counterpart in the definition of the χ^2 associated to the distance modulus without loss of generality.

It is easy to see that the logarithm extracts the overall factor c/H_0, which simply adds up to the nuisance parameter μ_0. On the other hand, any redefinition of the nuisance parameter

$$\mu_0' = \mu_0 + \log(f(c, H_0)) \tag{4.5}$$

leaves the likelihood invariant. This clearly shows that the values of c and H_0 are dummy parameters in our likelihood analysis, because any variation of their value corresponds to a redefinition of the nuisance parameter.

The minimization of the χ^2, defined as

$$\chi^2 = \sum_{\{SN\}} \frac{(\mu_{theory} - \mu_{data})^2}{\sigma^2_{data}} \tag{4.6}$$

clearly depends on the nuisance parameter μ_0 that we remove by marginalizing over (see [36] for details about the marginalization and [39, 40] and references therein for similar applications). The marginalization can be carried out analitically in a tricky way, as we will show in the next paragraph.

Let us now look at the variance σ^2_{data} of the data sample. In each catalog the errors are composed by many contributions coming from different aspects of the measurement procedure.

In [9] the error on the distance modulus is modelled with two distinct contributions:

$$\sigma^2_{data} = \sigma^2(\mu_B) + \sigma^2_{int}, \tag{4.7}$$

where σ_{int} is an intrinsic dispersion of SN absolute magnitudes and the B-band distance modulus. μ_B is computed in terms of the Supernova rest-frame B-band magnitude m^*_B, the absolute magnitude M and it is parameterized by four parameters α, β, s and c as

$$\mu_B = m^*_B - M + \alpha(s-1) - \beta c. \tag{4.8}$$

Here m^*_B, s and c are estimated from the SN light-curve fits, while M, α and β are fitted by minimizing the residuals from the Hubble diagram. The definition of the distance modulus error therefore must account for many contributions coming from the covariance matrix of m^*_B, s and c. At the same time the minimization with respect to α and β introduces a bias towards increasing errors, because the χ^2 has to decrease. In [9] the authors fix α and β during the uncertainty calculation and then update them iteratively in the minimization procedure.The error $\sigma(\mu_B)$ accounts also for a peculiar SN Ia velocity dispersion of 300 Km/s. The intrinsic

uncertainty σ_{int} is set to an initial arbitrary value of 0.15 and then it is iteratively computed by imposing a reduced $\chi^2 = 1$

The uncertainties in each updated version of the Union catalog (see [5, 6, 7]) are computed in a similar way. In [6] the authors parameterize the distance modulus error as

$$\sigma^2_{data} = \sigma^2_{ext} + \sigma^2_{sys} + \sigma^2_{lc} \tag{4.9}$$

They iteratively minimize the χ^2 in order to fit the best cosmology and the statistical errors: σ^2_{lc} is the propagated error from the covariance matrix V of the light-curve fits

$$\sigma^2_{lc} = V_{m_B} + \alpha 2 V_{x_1} + \beta^2 V c + 2\alpha V_{m_B,x_1} - 2\beta V_{m_B,c} - 2\alpha\beta V_{x_1,c} \tag{4.10}$$

where α and β are the x_1 and color corrections coefficient in the definition of the distance modulus

$$\mu_B = m_B + \alpha x_1 - \beta c - M \tag{4.11}$$

as discussed in [6].

The error σ_{ext} encodes the peculiar velocity dispersion of 300 km/s and other uncertainties coming from Galactic extinction corrections and gravitational lensing. Potential sample-dependent systematic errors which have not been accounted for are inserted into σ_{sys}, together with the intrinsic SN Ia dispersion. The value of σ_{sys} is computed by setting it to an initial arbitrary value and then requiring a reduced $\chi^2 = 1$ for each sample. The data are then refitted with the derived value of σ_{sys}.

The full cosmological analysis considers also a number of further systematic effects. These enter the calculation through a full covariance matrix between SN Ia at different redshifts. The diagonal elements of the covariance matrix are simply given by σ^2_{data}, while off-diagonal terms account for the correlation between different SNe.

In our statistical analysis we neglect this covariance contribution, following [39, 40]. This poorly degradates the constraints and it could be considered as an acceptable approximation.

4.1.3 Marginalization

The marginalization over the nuisance parameter μ_0 can be carried out in a simple way. Following [39, 40], we minimize χ^2 with respect to μ_0. This procedure is quite general and it is formally equivalent to the brute-force marginalization, (see the appendix for a proof) as discussed under general assumptions in [36, 37].

It is quite easy to rewrite the χ^2 as

$$\chi^2 = c_1 - 2c_2\mu_0 + c_3\mu_0^2 \tag{4.12}$$

where the coefficients c_i are

$$c_1 = \sum_j \frac{(\mu(z_j)^{data} - 5\log(d_l(z_j,\theta)))^2}{\sigma^2_{data}(z_j)} \tag{4.13}$$

$$c_2 = \sum_j \frac{\mu(z_j)^{data} - 5\log(d_l(z_j,\theta))}{\sigma^2_{data}(z_j)} \tag{4.14}$$

$$c_3 = \sum_j \frac{1}{\sigma^2_{data}(z_j)} \tag{4.15}$$

The minimum of the χ^2 with respect to μ_0 is obtained for

$$\mu_0^{min} = \frac{c_2}{c_3} \tag{4.16}$$

and the minimum χ^2, which corresponds to the marginalized χ^2_M is simply

$$\chi^2_M = c_1 - \frac{c_2^2}{c_3} \tag{4.17}$$

hence, the marginalized likelihood we use is given by

$$L_M = e^{-\frac{\chi^2_M}{2}} \tag{4.18}$$

In the marginalization procedure a prior probability density function for the nuisance parameter should be selected. The minimization procedure described here hides the problem, since no assumptions are made

on μ_0. It is interesting, however, to note that the equivalence between the marginalization procedure and the minimization with respect to the nuisance parameter works assuming gaussian priors for μ_0 and it does not break down in the limit of a very wide gaussian ($\sigma \to +\infty$), which reproduce a constant flat prior. This limit, which clearly corresponds to unconstrained values for μ_0 with equal probability, reproduces the procedure we used, regardless of any assumption on μ_0 and justifies the working prescription. See the appendix for more details.

4.2 Angular diameter distances from SZ effect

We have already shown how the Sunyaev-Zel'dovich (SZ) effect works in the hot ICM of galaxy clusters.The detection of galaxy clusters is enhaced by the thermal SZ effect since the fluctuation of the CMB temperature induced by the inverse Comptonization is remarkably comparable with the intrinsic CMB temperatufre inhomogeneities (see [15, 16, 17] for details). Then, the frequency shift caused by the inverse Compton scattering of a photon going through the ICM can be detected and the the presence of a galaxy cluster can be discovered.

4.2.1 Surface brightness and angular size

The SZ effect allows a computation of the angular diameter distance based on simple assumptions. This calculation mainly depends on the physics of the ICM and the cluster geometry, while it is mainly independent of the background cosmology. This quite striking aspect must be handled with care. The independece from cosmology is clearly based on the microphysics of the SZ effect, which does not involve any cosmological assumption. But the final computation of the angular size cannot be freed by the intrinsic dependency on geodesic motion of light rays, which ensures that somewhere the metricity of spacetime must be assumed. Deriving distances from the path of light rays implicitly involves the reciprocity theorem, which works in a metric theory under the approximation of geometric optics. Then we have to mind that Etherington's rule works behind the determination of angular diameter distances from the SZ effect.

We estimate the theoretical angular diameter distance of a cluster by

comparing the radiation emitted by the ICM in the X-ray band and the CMB radiation which is absorbed in the inverse Compton scattering. Indeed the emitted energy is proportional to the square of the electron density, while the absorbed one is linearly dependent. Both depend on the cluster depth along the line of sight, so it follows that the ratio between the square of the absorbed energy and the emitted one is a rough estimate of the cluster size along the line of sight. The estimate of the transverse size of the cluster given its depth is possible when making assumptions on the geometry of the ICM.

Let us remind that the bolometric surface brightness of the cluster in the X-ray band is

$$b_X = \frac{1}{4\pi(1+z)^4} \int n_e^2(l)\Lambda_e(l)dl \tag{4.19}$$

where the electron cooling function $\Lambda_e(l)$ measures the loss of energy of the ICM due to X-ray emission.

In the previous formula a FRW cosmology is implicitly assumed and the factor $(1+z)^{-4}$ is directly linked to the definition of the proper distance in the FRW model. It follows directly from the ray-tracing equation in the usual FRW:

$$1 + z = \frac{a(t)}{a(t_0)} \tag{4.20}$$

The absorbed background radiation can be computed with the equations of the SZ effect. We can write the SZ intensity fluctuations following Birkinshaw's work [19]

$$\Delta I = i_0 \int n_e \sigma_T \psi \left(\frac{h\nu}{k_B T_{CMB}}, T_e \right) dl \tag{4.21}$$

The new function $\psi(x, T_e)$ accounts for relativistic non-trivial corrections to the inverse Compton scattering. The functions T_e and n_e describe the temperature and density profiles of the ICM in the case of a general cluster geometry.

We follow Birkinshaw and model the ICM using reference values and form factors depending on three angles θ,ϕ and ξ:

$$
\begin{aligned}
n_e(\vec{r}) &= n_e^{(0)} f_n(\theta,\phi,\xi) && (4.22)\\
T_e(\vec{r}) &= T_e^{(0)} f_T(\theta,\phi,\xi) && (4.23)\\
\Lambda_{ee}(E,T_e) &= \Lambda_{ee}^{(0)} f_\Lambda(\theta,\phi,\xi) && (4.24)\\
\psi(x,T_e) &= \psi^{(0)} f_\psi(\theta,\phi,\xi) && (4.25)
\end{aligned}
$$

The reference values $n_e^{(0)}$, $T_e^{(0)}$, $\Lambda_{ee}^{(0)}$ and $\psi^{(0)}$ are measured in the cluster centre and the angle ξ is chosen such that $\xi = D_A/l$. The angle θ parameterizes the angular distance between the cluster centre and the line of sight, while ϕ is the usual azimuthal coordinate around the line of sight. The surface brightness and the SZ intensity become

$$
\begin{aligned}
b_X(\theta,\phi) &= \frac{\Lambda_e^{(0)}(n_e^{(0)})^2 D_A}{4\pi(1+z)^4}\int f_n^2 f_\Lambda d\xi = N_X\Theta^{(1)} && (4.26)\\
\Delta I(\theta,\phi) &= \psi^{(0)} I_0 n_e^{(0)}\sigma_T D_A \int f_n f_\psi d\xi = N_{SZ}\Theta^{(2)} && (4.27)
\end{aligned}
$$

These equations allow the computation of the angular diameter distance:

$$
D_A = \frac{N_{SZ}^2}{N_X}\left(\frac{\Lambda_e^{(0)}}{4\pi(1+z)^4 i_0^2\psi_0^2\sigma_T^2}\right) \qquad (4.28)
$$

It is interesting to note that the factors $(1+z)^n$ in the previous formulae may be easily misunderstood. In the FRW cosmology we can always make the substitution 4.20,but it does not work in the averaged scenario, since the ray-tracing equation for the template metric is slightly different. In other words the standard homogeneous and isotropic cosmology allows a simple exchange between volume factors and redshift factors in the basic formulae. The same substitution drops for the template metric, so volume factors and redshif factors should be treated with care, avoiding simplifications in every formula among them.

We are convinced that in deriving the relation among the surface brightness and the angular diameter distance only coherent redshif factors are involved, then the same formula apply when the FRW is substituted

with the template metric, provided that the redshift z is changed with the effective one z_D.

The motivation of our claim is based on the reciprocity rule and the optical theorem. Nowhere in deriving the reciprocity relation volume factors a^n are required, but only the definition of redshift works. Consequently the optical theorem, which is a direct consequence of reciprocity, is not affected by any volume factor. In other words we are stating that the basic laws of physics involved in the reciprocity theorem and in any law of geometric optics on a curved manifold depend only on the metricity of the manifold and on the definition of redshift as a ratio of frequences, regardless of what the relation between z and the scale factor a may be. The authors in [34] implicitly assume the same point of view, since they save the reciprocity relation for the template metric.

4.2.2 Temperature profiles

The angular diameter distance depends also on the form factors of the cluster through the ratio N_{SZ}^2/N_X. These functions encode the physical properties of the ICM giving their distribution inside the cluster. Many models for the ICM were proposed in the past years. The spherical β-model [18] is an isothermal ($f_T = 1$, $f_\Lambda = 1$) model based on the spherical simmetry of the electron density

$$f_n = \left(1 + \frac{\theta^2 + \xi^2}{\theta_c^2}\right)^{-\frac{3}{2}\beta}, \tag{4.29}$$

where the β exponent drives the decrease of the ICM density moving away from the cluster centre. The parameter $\theta_c = r_c/D_A$ is the angular size of the core radius r_c, which defines the surface whose brightness is half the brightness of the centre. This model provides simple expressions for $\Theta^{(i)}$:

$$\Theta^{(1)} = \sqrt{\pi}\frac{\Gamma(3\beta - \frac{1}{2})}{\Gamma(3\beta)}\theta_c \left(1 + \frac{\theta^2}{\theta_c^2}\right)^{\frac{1}{2}-3\beta}, \tag{4.30}$$

$$\Theta^{(2)} = \sqrt{\pi}\frac{\Gamma(\frac{3}{2}\beta - \frac{1}{2})}{\Gamma(\frac{3}{2}\beta)}\theta_c \left(1 + \frac{\theta^2}{\theta_c^2}\right)^{\frac{1}{2}-\frac{3}{2}\beta}. \tag{4.31}$$

In [24] two sets of angular diamter distances are computed assuming alternatively the isothermal spherical β-model and the improved *double* β-model, which break the assumption of isothermality. Indeed, the central density of a cluster may be high enough that the radiative cooling time is less than the age of the cluster, leading to lower temperatures and higher densities. The density profiles of these cool core clusters show two distinct components: a central density peak and a broad shallower distribution, which requires a different modelling of the density profile. Mohr [20] and La Roque [21] proposed a model based on a weightened superposition of two copies of the isothermal β-model

$$n_e(r) = n_e^{(0)} \left[f \left(1 + \frac{r^2}{r_{c1}^2} \right)^{-\frac{3\beta}{2}} + (1-f) \left(1 + \frac{r^2}{r_{c2}^2} \right)^{-\frac{3\beta}{2}} \right], \qquad (4.32)$$

which depends on two distinct core radii r_{c1} and r_{c2} to fit the cool core cluster density profile better. The central density $n_e^{(0)}$ gives the maximum of the density and the weigth f accounts for the fractional contributions $(0 \leq f \leq 1)$ of the central peak and the outer regions to the total density. (see [23, 24] for a comparison between the models)

The measurement of angular diameter distances based on combined X-ray and SZ data requires a sample of galaxy clusters which is independent of selection effects. For example, the selection based on X-ray surface brigthness preferentially include clusters which are elongated along the line of sight. This effect induces systematic errors in estimating the angular diameter distance, because our assumption of spherical symmetry underestimates the line of sight size of the cluster.

The catalog, compiled by Bonamente et al. [24], is composed of 38 clusters in the redshift range $0.14 < z < 0.89$. The authors chose a sample of known X-ray clusters from the Chandra X-ray satellite data and measured the SZ effect separately with the *Owens Valley Radio Observatory* (OVRO) and the *Berkeley-Illinois-Maryland Association* (BIMA) interferometers. The angular diameter distances were computed through a maximum likelihood joint analysis of BIMA/OVRO and Chandra measurements. The ICM was modelled using both the spherical β-model and the double β-model.

The angular diameter distances are affected by statistical plus systematic uncertainties. The total error associated to each measurement is not symmetric due to the systematic effects. In the following analysis we quite oversestimated the error associated to each distance assuming the larger uncertainty proposed by the catalogs.

4.2.3 Likelihood analysis

The likelihood analysis for the angular diameter distances is similar to the SN Ia case.

We numerically compute

$$\chi^2 = \sum \frac{(D_A^{data} - D_A(p)^{theory})^2}{\sigma_{data}^2} \tag{4.33}$$

and the associated likelihood

$$\mathcal{L} = \frac{1}{N} e^{-\frac{\chi^2}{2}}, \tag{4.34}$$

where N is the normalization constant.

We treated the errors following recent works on Dark Energy constraints from clusters distances, like in [80]. The authors use angular size versus redshift data for galaxy clusters from [24] too. There are three different sources for the error σ_{data}. We can write

$$\sigma_{data}^2 = \sigma_{stat}^2 + \sigma_{sys}^2 + \sigma_{mod}^2 \tag{4.35}$$

where the first and the second contributions are the statistical and systematic uncertainties respectively. The last contribution σ_{mod} accounts for the error in modelling the cluster. The modelling error are given in percentage in Table I of [24] and the other uncertainties are listed in Table III. We assumed no error for the measured redshifts. This assumption is reasonable because the uncertainties in the redshifts are negligible with respect to the errors on the X-ray and SZ measurements.

The angular diameter distances depend parametrically on H_0, which we treat as a nuisance parameter. In this case no simplifying formula helps us and the analytical marginalization requires to compute gaussian integrals and to assume priors on H_0.

For a flat prior on H_0 the marginalization integral is not easily computable, since it is

$$L_M = \frac{1}{N}\int_0^{H_{max}} e^{-\sum_i \frac{(D_A^i - \frac{c}{H_0} d_A^i)^2}{2\sigma_i^2}} \frac{dH_0}{H_{max}} \tag{4.36}$$

where H_0 runs from 0 to the maximum value H_{max} and d_A is the reduced angular diameter distance defined in analogy with the reduced luminosity distance. We see that the integral cannot be evaluated easily due to the $1/H_0$ dependence in the exponent.

If we consider a gaussian prior on H_0

$$p(H_0) = \frac{1}{\sqrt{2\pi}\sigma_{H_0}} e^{-\frac{(H_0 - \bar{H}_0)^2}{2\sigma_{H_0}^2}} \tag{4.37}$$

the marginalization integral is

$$L_M = \int p(D_A|H_0^{-1}) P(H_0^{-1}) d(H_0^{-1}) \tag{4.38}$$

Since the absolute probability for the nuisance parameter is conserved under any change of variable, we may write

$$dP = P(H_0^{-1}) d(H_0^{-1}) = G(H_0) dH_0 \tag{4.39}$$

where the pdf $G(H_0)$ is simply

$$G(H_0) = P(H_0^{-1}) \frac{d(H_0^{-1})}{dH_0} = \frac{P(H_0)}{H_0^2} \tag{4.40}$$

So, the marginalized likelihood reads

$$L_M = \int p(D_A|H_0) G(H_0) H_0^2 dH_0 \tag{4.41}$$

If $G(H_0)$ is gaussian, the marginalization integral cannot be computed analitically.

4.3 Distances from the CMB

It is well known that the Cosmic Microwave Background encodes much information about the early Universe. Current observational data shows that the TT-power spectrum of the temperature fluctuations of the CMB is dominated by a sequence of peaks and dips, which carry the imprints of the early inhomogeneities of the photon-baryon fluid filling the Universe up to the time of recombination. In recent years measurements of the quantity $l(l+1)C_l/(2\pi)$ improved drastically. We make use on two different sets of parameters in order to constrain the backreaction model. On the one hand we perform a likelihood analysis for the CMB shift parameters, on the other hand we use the cosmic distance information which is encoded into the location of the peaks in the CMB power spectrum.

4.3.1 Acoustic peaks

We have shown that the computation of the TT-power spectrum of the CMB requires to solve the Boltzmann equation for the photon-baryon fluid which fills the early Universe and the Einstein field equations describing the geometry of the spacetime. It is well known that a full solution has been derived in the context of a linearly perturbed FRW spacetime. Since the backreaction effect is sourced by the local inhomogeneities of the matter field, this approach still works in the backreacted scenario, but some care is needed. We assume the working prescription that is suggested in [34]. The density inhomogeneities associated with the growth of structures are negligible at the recombination epoch, so the effective metric can be well represented by a linearly perturbed FRW. This tells that no significant difference arises between the averaged dynamics and small perturbations around the homogeneous solution. Moreover, if the early Universe can be considered as a wekly perturbed FRW (for the forementioned reasons) up to the recombination epoch, the location of the CMB multipoles can be computed from the measured anisotropy power spectrum without any assumption on the late-time cosmology, which allows us to treat the physics of the CMB regardless of any contribution from backreaction.

We have already computed the power spectrum C_l of the CMB temperature fluctuations 2.123, showing that it involves the superposition of multipoles. The shape of the function is dominated by peaks and dips

corresponding to

$$l_m = l_a(m - \phi_m) \tag{4.42}$$

where m takes positive integer values for the peaks and half-integer positive values for the dips. The correction ϕ_m accounts for the shift of the $m-th$ peak from the simple linear rule $l_m = ml_a$. It depends on the matter content of the early Universe, on the baryon density, on the redshift of the last scattering surface and on the spectral index n_s of the primordial fluctuations. Those corrections parameterize the effect of gravitational dragging effects occuring up to recombination which displace the position of the peaks with respect to the characteristic angular scale subtended by the sound horizon r_s.

We know that the CMB multipoles show a layout of maxima and minima corresponding to the wavenumbers

$$k_n = \frac{n\pi}{r_s} \tag{4.43}$$

selecting the crucial role played by the comoving sound horizon. The first extremum happens at

$$k_s = \frac{\pi}{r_s} \tag{4.44}$$

corresponding to a fixed angular scale $\theta_s = \frac{\pi}{l_a}$, where l_a defines the fundamental multipole.

Ratios between scales at the recombination epoch can be translated into ratios between angular scales, since the distance of the last scattering surface from the observer is known and common. Consequently, if the l-th multipole subtends an angle

$$\theta_l = \frac{\pi}{l} \tag{4.45}$$

then it is easy to note that for a given scale k_n the relation

$$n = \frac{k_n}{k_s} = \frac{\theta_s}{\theta_n} = \frac{l_n}{l_a} \tag{4.46}$$

must hold in general.

The fundamental multipole l_a has a deep physical meaning and is clearly defined as

$$l_a = \pi \frac{r(a^*)}{r_s(a^*)} \tag{4.47}$$

where a^* is the scale factor corresponding to the epoch of recombination, r is the comoving distance and r_s is the comoving sound horizon at decoupling.

This simply proves that the n-th peak or dip of the CMB power spectrum should be linearly displaced in the tight coupling approximation of the photon-baryon fluid, provided that any extra effect is disregarded.Unfortunaltely extra effects are not negligible and they has been modelled by fitting formulae for the shifts ϕ_n. For each position we use the fitting formulae given by Doran and Lilley in [45]. Following [34], we neglect Early Dark Energy, because the energy density is negligible at the redshift of recombination for standard Dark Energy models such as a cosmological constant or a standard scalar field. We set the spectral index to the value provided by the *Planck* Mission $n_s = 0.96$ as the best (see [54]), instead of setting $n_s = 1$ as Larena et al. do in [34]. After these assumptions the only quantity we leave free to vary in our likelihood analysis is the baryon density $\Omega_b h^2$, which we include as the other parameters Ω_m, w and H_0.

The ratio R in the speed of sound

$$R = \frac{4}{3}\frac{\rho_b}{\rho_\gamma} = \frac{\Omega_b}{\Omega_\gamma} \tag{4.48}$$

depends on the cosmological parameters Ω_b and Ω_γ, which represent respectively the baryon and the photon density today. We should be care that other relativistic species (like neutrinos) do not enter this ratio, but they are involved in the computation of the comoving distance, so the whole radiation density ρ_r is defined as

$$\rho_r = \rho_\gamma + \rho_\nu + \rho_e \tag{4.49}$$

where ρ_ν accounts for the contribution of neutrinos and ρ_e encodes extra-relativistic species. Since we are able to derive the neutrino density in

terms of their absolute temperature by integrating the Fermi-Dirac distribution, we can write

$$\rho_\gamma = \frac{\pi^2}{15} T_\gamma^4 \qquad \rho_\nu = \frac{7}{8}\frac{\pi^2}{15} N_\nu T_\nu^4 \tag{4.50}$$

where N_ν is the number of different neutrino species at the epoch of photon decoupling. In the standard model of particle physics $N_\nu = 3.04$ (see for instance [55],[56]). The numerical factors come from the integration of the Fermi-Dirac distribution. In the thermal history of the Universe it is possible to relate the temperature of neutrino with the temperature of photons (see [63]) through the equation

$$T_\nu = \left(\frac{4}{11}\right)^{\frac{1}{3}} T_\gamma \tag{4.51}$$

For the extra relativistic species, there are some troubles. We do not exactly know their nature and we cannot know if they should be comprised as fermions or bosons, so their quantum statistics is unknown. Nevertheless they are usually parameterized like they were neutrinos. This trick simply accounts for the extra species substituting the number N of massless neutrino species fixed by the Standard Model to an effective one (N_{eff}) given by the formula

$$\rho_\nu + \rho_e = \frac{7}{120}\pi^2 N_{eff} T_\nu^4 \tag{4.52}$$

So, the radiation density can be predicted as (see [43])

$$\rho_r = \rho_\gamma \left[1 + \frac{7}{8}\left(\frac{4}{11}\right)^{4/3} N_{eff}\right] \approx \rho_\gamma (1 + 0.2271 N_{eff}) \tag{4.53}$$

It is well known that neutrinos can be treated as free-streaming particles, since their interactions become important only for $z \sim 10^{10}$. In [43] other extra-relativistic species are also treated as free-streaming particles, because under these assumptions the measured TT-spectrum of the CMB anisotropies allows for constraining N_{eff}. Indeed the extra species affect the Friedmann equation

$$H^2 = \frac{8\pi G}{3}(\rho_m + \rho_r) \tag{4.54}$$

changing the radiation density. It follows that an increase in N_{eff} reduces the comoving sound horizon r_s at the decoupling epoch and the angular diameter distance at the redshift of recombination. Since the expansion rate after the equality epoch is less affected and the radiation energy component becomes less important, the sound horizon is more affected by a variation of N_{eff} than the angular size. These effects combine and affect the fundamental multipole l_a, leaving fingerprints into the angular scale and, consequently, modifying the positions of the peaks of the CMB power spectrum. A detailed discussion of other effects related to N_{eff} can be found in [43].

Here we simply assume $N_{eff} = 3.04$, because all predictions given by $WMAP$-9 about N_{eff} are consistent with the standard model value $N = 3.04$. This allows us disregard the effect of extra-relativistic particles in the early Universe and take $N = 3.04$ as a prior for our likelihood analysis.

In order to compute the photon density, we can use the measurement of the CMB mean temperature T_{CMB} provided by $WMAP$-9. Using the Stefan-Boltzmann law the photon density is

$$\rho_\gamma = \frac{4\sigma}{c^3} T_{CMB}^4 \tag{4.55}$$

where σ is the Stefan-Boltzmann constant. The corresponding parameter Ω_γ is simply

$$\Omega_\gamma = \frac{\rho_\gamma}{\rho_{crit}} \tag{4.56}$$

where the critical density is $\rho_{crit} = \frac{3H_0^2}{8\pi G}$. The corresponding cosmological parameter is

$$\Omega_r = \frac{\rho_r}{\rho_{crit}} \tag{4.57}$$

In the following we assume for the CMB mean temperature the value given by $WMAP$-9 ([43]) $T_{CMB} = 2.72548$. We neglect any uncertainty on this value.

The sound horizon is given by the integral

$$r_s(a^*) = \frac{c}{H_0}\int_0^{a^*} \frac{da}{a^2\sqrt{\Omega_m^0 a^{-3} + \Omega_r^0 a^{-4} + (1-\Omega_m^0-\Omega_r^0)a^{-3(1+w)}}\sqrt{3(1+R(a))}} \tag{4.58}$$

The scale factor a^* corresponding to the time of recombination is computed in terms of the redshift z^* of the last scattering surface through the standard relation

$$a^* = \frac{1}{1+z^*} \tag{4.59}$$

where useful fitting formulae for z^* are given in [46, 47] and references therein:

$$z^* = 1048(1 + 0.00124(\Omega_b h^2)^{-0.738})(1 + g_1(\Omega_m h^2)^{g_2}) \tag{4.60}$$

where

$$g_1 = \frac{0.0783(\Omega_b h^2)^{-0.238}}{1 + 39.5(\Omega_b h^2)^{0.763}} \tag{4.61}$$

$$g_2 = \frac{0.56}{1 + 21.1(\Omega_b h^2)^{1.81}} \tag{4.62}$$

The recombination redshift depends only on the matter content of the primordial photon-baryon fluid separately through the matter and the baryon density parameters. Finally the positions of the CMB peaks are given by the fitting formulae found by Doran and Lilley in [45] and depend on the ratio

$$r^* = \frac{\Omega_r(z^*)}{\Omega_m(z^*)} \tag{4.63}$$

which can be computed easily in terms of the mean CMB temperature.

4.3.2 CMB shift parameters

The shift of the acoustic peaks of the CMB can be quantified by using a different set of observables. Following [48] and [49] we perform a likelihood analysis involving the set of observables (l_a, R, z^*) provided by $WMAP$-9 in [43]. Here l_a is the fundamental multipole of the CMB defined in Eq. 4.47, z^* is the redshift of recombination and R is defined by [50]

$$R = \frac{\sqrt{\Omega_m^0}}{\sqrt{\Omega_k^0}} S_k\left(\sqrt{\Omega_k^0}\int_0^{z^*}\frac{H_0}{H(z)}dz\right) \tag{4.64}$$

for a curved FRW Universe,provided that $S_k(x)$ is defined by 1.58.

The definition of R can be rewritten in the useful form

$$R = \sqrt{\Omega_m^0}\frac{H_0}{c}y \tag{4.65}$$

where y is the solution to the differential equation governing the path of radial photons in the FRW metric. In other words, y solves

$$\frac{dr(a)}{da} = \frac{c\sqrt{1-kr^2}}{H(a)a^2} \tag{4.66}$$

assuming that $r = r(a)$. In general the Hubble function is defined as

$$H(a) = H_0\sqrt{\Omega_m^0 a^{-3} + \Omega_r^0 a^{-4} + \Omega_k^0 a^{-2} + (1-\Omega_m^0-\Omega_r^0-\Omega_k^0)a^{-3(1+w)}} \tag{4.67}$$

but we set $\Omega_k^0 = 0$, since we are dealing with a flat FRW Universe. The parameter R has been used for analyzing CMB data many times in the context of FRW models (see for instance [42, 38, 48, 51]) and in local voids ones ([52]). The parameter R is quite model-dependent and in [46] the authors suggest a way for extracting model-independent constraints from the R parameter. The model dependency of R is discussed in [51], where a likelihood analysis is carried out involving extra parameters, like positive neutrino masses and tensor modes. The authors infer constraints for R and l_a using $WMAP$-3 data. They sum up their results in Table 1 of [51], which clearly show that the R parameter is quite model dependent. Fortunately changes of cosmic curvature or minimal modifications of the

Dark Energy parameters does not significantly affect the value of R. On the other hand, the dependency on more exotic parameters, like positive neutrino masses, tensorial modes or a running spectral index, is much stronger. Under our assumptions the R parameter should be stable, since no tensorial modes nor massive neutrinos are considered.

We note that the method based on the position of the peaks requires care, but it has a wide field of application, as both [51] and [45] state, showing that it still works well both for models with early Dark Energy and models with late time geometry or photon dynamics departing from a standard FRW. The later case is relevant for our study, since in the backreaction context it may play a role.

4.3.3 Shift parameters and backreaction

In order to perform our likelihood analysis involving R, z^* and l_a, we need to write them in the framework of backreaction. The recobination redshift z^* can be estimated directly using Doran and Lilley's fitting formulae ([45]), since **we assume they still work**. This assumption is simply required since otherwise the full theory of CMB should be reformulated assuming the template metric as the underlying geometry of spacetime. We will see that this approach will play a crucial role.

A formula for (4.47) is given for the template model in [34]:

$$l_a = \pi \frac{\bar{r}(a_D^*)}{r_s(a_D^*)} \tag{4.68}$$

where $\bar{r}$ is the solution of Eq. 3.108 corresponding to the effective scale parameter a_D^*. The authors define a_D^* as the effective scale factor of recombination. The correspondence between a_D^* and the redshift z^*, computed from Doran and Lilley's formulae, should be given, in principle, from the solution of Eq. 3.111, since the standard equality

$$a = \frac{1}{1+z} \tag{4.69}$$

does not hold in the backreacted scenario. This theoretical aspect is treated in [53], where the authors found that their model of backreaction is not consistent with CMB data due to a wrong prediction of the

size of the sound horizon. We found the same inconsistency between the model and the CMB data provided by $WMAP$-9 and *Planck*.

So, we followed a different approach in order to recover the consistency that is showed in [34]. We assumed that, since the Universe is almost FRW up to the time of recombination,

$$l_a = \pi \frac{\bar{r}(\frac{1}{1+z^*})}{r_s(\frac{1}{1+z^*})} \tag{4.70}$$

The underlying idea is simple: the multipole l_a should be affected only by how the early time physics, imprinted in the CMB, is projected to an observer today. The projection is affected by the backreaction since the path of photons from the last scattering surface is perturbed by the growing inhomogeneities, so the comoving distance must be computed correctly from the template metric. On the contrary the sound horizon should be not affected by the backreaction and the standard formula should hold. This aspect face a non-trivial question, which regards the value of a^*. The obvious generalization given by the substitution

$$a(t) \to a_D(t) \tag{4.71}$$

may be misleading. Indeed the evolution of the Universe from the initial singularity up to recombination follows the standard homogeneous and isotropic dynamics, which corresponds to a FRW metric. The recombination redshift, which is computed by Doran and Lilley's fitting formulae, set the volume of the Universe, since the standard relation $a^{-1} = 1 + z$ holds. This tells us that at the time of recombination the standard solution fixes a boundary condition on the size of the Universe that is intrisically related to the homogeneous and isotropic model and to the physics of the photon baryon fluid. On the other hand the dynamics of a domain D driven by the backreaction is clearly different from the standard one. It is easy to imagine that the domain D follows the standard homogeneous dynamics up to the time of recombination (since the backreaction effect is assumed undistinguishable from a linerly perturbed FRW), then it deviates from the standard dynamics. We should note here that the standard relation $a^{-1} = 1 + z$ breaks for a linearly perturbed FRW too, but only for this case we disregard the perturbative corrections and retain only the lowest order, which corresponds to the standard relation. In other words up to

the time of recombination we assume that $a(z) = (1+z)^{-1}$ as a good approximation. Nevertheless, after recombination, the standard relation between the scale factor and the redshift breaks down accordingly to the geodesics equation coming from the affine connection induced by the template metric. This trivial picture suggests immediately the misleading aspect we have to face: the standard scale factor $a(t)$ and the effective one $a_D(t)$ may not have the same value today.

Mathematically the problem is well defined. We are dealing with two functions (a and a_D) which are solutions of two distinct ordinary differential equations. The two solutions must coincide in a certain interval $z > z^*$. We forced as a boundary condition of the Cauchy problem that today the two functions must concide too, since we assumed that $a_0 = a_{D_0} = 1$. This further assumption may be critical. Let us follow [53], writing the solution of equation 3.111 in the form

$$z_D = \frac{1}{a_D} \exp\left[\frac{1}{2}\int_\eta^{\eta_0} \frac{r^2 \dot{k}_D}{1 - k_D r^2} d\eta'\right] - 1 \tag{4.72}$$

where η is the conformal time and η_0 is today. This solution satisfies the boundary condition $a_D(\eta_0) = 1$. Clearly if we set $z_D = z^*$, we immediately see that $a_D(z^*) \neq a^*$, since the exponential acts as a monotonic factor. This clearly shows that the effective scale factor does not agree with the standard solution in the interval $z > z^*$, since a and a_D assume different value at the boundary.

The consequence is easy: if we assume that a and a_D take the same value at z^*, then we have to relax the boundary condition $a_{D_0} = 1$; if we assume that $a_{D_0} = 1$, then the two solutions a and a_D may concide only when $z \to +\infty$, breaking the assumption that the backreaction effects are negligible up to the time of recombination. Indeed assuming that backreaction effects are negligible means that no significant deviation should arise between a and a_D.

In [53] the problem of a discontinuous effective parameter is assessed in a completely different way. The authors assume that the effective curvature k_D vanishes for $z > z^*$ and they claim an *ad hoc* parameterization for $z < z^*$.Then they show that the model is incosistent with $WMAP$ data. We note that the prize for solving the continuity problem seems high: the scaling solutions of the backreaction problem fix the form of k_D

imposing that $k_D \sim a^{n+2}$ and this aspect cannot be disregarded without breaking the scaling assumption. The main consequence is that k_D never vanishes completely and we may believe that in principle no solution to the backreaction problem exists which corresponds to the *ad hoc* parameterization suggested in [53]. Here we want to look at the problem taking into account the scaling solution, because we are convinced that any solution to the backreaction equations is the crucial point which gives meaning to the correspondence substained by the morphon field and to the whole analysis. Any toy model, altought it is useful, may in principle correspond to unphysical approaches to the backreaction problem. Clearly we are convinced that incosistencies eixst, but we are interested in discussing whether they are definitely related to the formulation of the backreaction problem or not. Moreover we may ask ourselves whether these incosistency may be disregarded because their effects on predictions made on recent data are negligible with respect to experimental uncertainties.

We have argued that an incosistency arises because of the choice of boundary conditions. In principle it may be solved by a suitable redefinition of the boudary conditions. For example we may relax the condition $a_{D_0} = 1$, assuming that $a_{D_0} = L$, where L is

$$L = \lim_{\eta \to \eta_0} a_D(\eta) \tag{4.73}$$

provided that the solution $a_D(\eta)$ satisfies the boundary condition $a_D(z_D = z^*) = a^*$. Such solution should exist because only ordinary differential equations are involved and, for standard forms of the function k_D, the Cauchy theorem on the existence and uniqueness of the solution works. Consequently the limit L should exist. Clearly the existence of L is not striking, since the size of the Universe today remains unknown and enter the theory as a new parameter.

Another possibility is relaxing the assumption that the two solutions coincide for $z > z^*$. Logically this does not seem completely correct, but we may argue that the difference between the two solution can be disregarded since it should be small. But this faces a trouble, because clearly the relation

$$a^{-1} = 1 + z \tag{4.74}$$

implicitly contains the boundary condition $a_0 = 1$. On the contrary the generalization

$$1 + z = \frac{a_0}{a} \tag{4.75}$$

still represent a FRW Universe and we may simply state that the solution a_D satisfying the boundary condition $a_{D_0} = 1$ follows a FRW expansion for $z > z^*$ provided that $a_0 \neq 1$, which corresponds to a solution of the geodesic equation for the FRW with a new boundary condition at $z = 0$. Again such solution must exists by virtue of the Cauchy theorem.

Following this point of view we are assuming a further boundary condition for the domain D, whose size is fixed to $a_D(z^*) = a_0/1 + z^*$ at the time of recombination and we are stating that the we are able to set the size of domain D today, but no information are available on the size of the corresponding volume which follows the homogeneous solution.

Finally we are convinced that the incosistency should be faced looking at the physics. The redshift of recombination is given by the fitting formula, which has been computed *assuming a perturbed FRW* as the metric of the early Universe. Usually when such assumptions are made the common boundary condition for the FRw solution is $a_0 = 1$, which simply tells us that both the physics of the CMB and the fitting formulae should be consistent with the first approach. Moreover such inconsistency should be small in some sense, since $WMAP$-3yr data were treated giving consistent constraints in [34], suggesting that statistical uncertainties were big enough to cover this unpleasant aspect.

For these reasons we studied if recent data from CMB are able to show a bad behavior in predicting the cosmological parameter Ω_m and the Dark Energy exponent w. We assumed that the effective solution and the homogeneous one should be joined at z^*, where z^* is computed by the fitting fomula. Correspondingly the cosmic size at recombination must be given by $a^* = 1/(1 + z^*)$ in both cases. We claim that a reason for this choice can be found in prime principles, provided that the incosistency cannot be removed and we try to avoid it making an approximation. The first law of thermodynamics says that in standard FRW

$$T \sim \frac{1}{a}, \tag{4.76}$$

consistently with the scaling $T \sim (1+z)$ found in the geometric optics approximation.

We may start from a more general point of view, based on the definition of entropy in statistical mechanics. The temperature of any statistical ensemble is defined as the derivative of the entropy at constant volume and number of particles. Clearly we have some troubles in applying the definition to a volume of the expanding Universe filled with photons, since the volume is not constant. We may avoid this problem in standard FRW applying the basic definitions of statistical mechanics to comoving volumes. We are convinced that this assumption is tricky, since it is a direct consequence of the conformality properties of the FRW metric. Passing to conformal time we may always write

$$ds^2 = a^2(\eta)(-d\eta^2 + dx^2) \tag{4.77}$$

where a^2 play the role of a conformal factor. Clearly standard theory of conformal invariance helps us in dealing with the scaling properties of the canonical partition function: if we require that the partition function

$$Z = \int d\mu e^{-\frac{H(q,p)}{kT}} \tag{4.78}$$

scales as a power law under a conformal transformation, then we must require that $H(q,p)/(kT)$ is invariant, otherwise a non-power scaling is added. Here $d\mu$ is the integration measure on the phase space and $H(q,p)$ is the Hamiltonian. This proves that the temperature T must scale as the hamiltonian.

We immediately note that in standard FRW the geodesic equation gives $E \sim a^{-1}$ for photons, but this relation should in principle be broken when the metric is substituted with the template. The reason is clear: the dependence of the energy on a comes from the geodesic equation, which is slightly different in the backreacted context.

Now we can easily see the incosistency arising around the values of a^* and z^*. If we apply the standard FRW metric (as we do up to decoupling) we should write the ratio between the mean temperature of the CMB T_d at the decoupling epoch and the present temperature T_m as

$$\frac{T_m}{T_d} = a_D^* \tag{4.79}$$

being a_D^* the effective scale factor at decoupling. The l.h.s. ratio is fixed by actual measurements (like $WMAP$-9) and by the pre-recombination physics, which is independent of backreaction. Indeed the temperature T_d of decoupling depends on the microphysics of the photon-baryon fluid and should not in principle be affected by the late time effects, like backreaction. So, we argue that the r.h.s. is well predicted by $1/(1+z^*)$.

On the contrary if we apply the general definitions we should rewrite the geodesic equation in terms of the Christoffel's symbols of the template metric and then recover the constraint

$$-m^2 = g_{\mu\nu} p^\mu p^\nu \tag{4.80}$$

in terms of the template. Here we face a trouble, since the constraint holds for the bare metric of the inhomogeneous spacetime and we should average it in order to correctly apply the template metric. Averaging this equation is unclear, since correlation terms arises when taking the average of the righ hand side. Moreover we may ask ourselves if the standard definitions of statistical mechanincs still work in the averaged context. Indeed the scaling properties of the canonical partition function help us since the standard FRW is conformally related to a static spacetime, but this crucial feature does not fit the template metric, since the time dependent curvature $k_D(t)$ does not allow to write the effective metric as conformally equivalent to a static one. We can, in principle, state that we are not even sure that standard definitions may be applied without suitable modifications.

If we postulate that standard statistical mechanincs holds for the backreacted model, we will find that the temperature still scales as the energy, but in the case of photons

$$T \sim (1 + z_D) \tag{4.81}$$

by definition. The new dependence on a_D is understood in the definition of the effective redshift, which encodes the new geodesic equation. The contraddiction on the value of a^* is now complete, since instead of equation 4.79 we should write

$$\frac{T_d}{T_m} = 1 + z^* \tag{4.82}$$

but they cannot be consistent since $(1+z^*)a_D^* \neq 1$. In order to recover the consistency we have to recompute a^* or z^* from prime principles, applying the template metric and beeing careful that each equivalence between a^* and $(1+z^*)^{-1}$ must be rewritten. Unfortunately they have been computed assuming a FRW spacetime, like the fitting formulae for z^* we have to use, because all the microphysics of the CMB has been computed on a slightly perturbed FRW.

We try to address the problem in a practical way. Since there are no simple way to avoid the fitting formula for z^* we arbitrarly decided that consistency requires to assume $a^* = (1 + z^*)^{-1}$ and correspondingly the size of the Universe at recombination must be fixed by standard pre-recombination physics. We know that the inconsistency now is traslated to a different size of the Universe in the backreaction context (or a different boundary condition today), but we are still interested in understanding if the discrepancy may be disregarded or it may be considered small with respect to statistical errors related to current cosmological measures.

Finally all these aspects drive us to look at the correspondence substained by the morphon field in a more careful way. The correspondence exists between a backreacted solution and a flat FRW Universe filled with Dark Energy, but the two models on the sides of the correspondence may in principle require suitably different boundary conditions. This aspect clearly does not destroy the theoretical value of the correspondence, but becomes important whenever we test it against CMB data, since only in this case an extra boundary condition enters the model implicitly trought the size of the Universe at decoupling and incosistencies may arise if the boundary conditions are not properly checked.

For the shift parameter R, no formula is given in the context of the template metric. We generalize formula (4.65) as

$$R = \sqrt{\Omega_m^{D_0}} y(1/(1 + z^*)) \tag{4.83}$$

because the factor H_0/c is removed by the definition of the comoving distance in the case of the template metric. The comoving distance y is a function of a_D as it immediately follows from the differential equation (3.108). Here we have used again the assumption that $a_D^* = 1/(1 + z^*)$.

4.3.4 Data sets: Shift parameters

For our analysis of CMB data we used different data sets. For the method based on the CMB shift parameters we rely on data published in [43], which we remember here:

$$l_a^{WMAP} = 302.40 \tag{4.84}$$
$$R^{WMAP} = 1.7246 \tag{4.85}$$
$$z_*^{WMAP} = 1090.88 \tag{4.86}$$

The corresponding errors are recorded in the full covariance matrix. In Table 11 of [43] the inverse covariance matrix is published:

$$C^{-1} = \begin{pmatrix} 3.182 & 18.253 & -1.429 \\ 18.253 & 11887.879 & -193.808 \\ -1.429 & -193.808 & 4.556 \end{pmatrix} \tag{4.87}$$

In this case the definition of the χ^2 is slightly changed, because we have to account for non diagonal terms in C^{-1} coupling data. The correct definition is

$$\chi^2 = -2\log L = (x-d)^T C^{-1}(x-d) \tag{4.88}$$

where the vector x is organized such that $x = (l_a, R, z^*)^T$ and the corresponding vector d storages data.

4.3.5 Data sets: peaks

No direct measurements of the position of the peaks of the TT power spectrum of the CMB are available from $WMAP$-9 or *Planck*. We followed a simple fitting procedure based on the local interpolation of the CMB spectrum with given parabolas. We used such an approach for time economy, because a full fitting procedure based on MCMC algorithm would require at least 14 fitting parameters in order to reconstruct the shape of the spectrum up to the third peak. Our fitting procedure is explained in detail in the appendix. Here we only record the position of the first three peaks and the first dip of the CMB spectrum we obtained with our fitting procedure and the corresponding error. We disregarded every correlation

between the data points provided by $WMAP$-9 and by *Planck* for the CMB spectrum. So, we assumed no covariance between our predictions of the peaks positions. Our data are recorded in Table 4.1.

Table 4.1: Positions of the CMB peaks and related errors

	WMAP-9	PLANCK
l_1	220.9 ± 0.9	219.9 ± 0.7
l_{dip}	415.4 ± 1.65	419.2 ± 1.05
l_2	537.8 ± 2.9	537.0 ± 1.7
l_3	813.5 ± 9.8	813.6 ± 1.6

We see that the positions of the CMB peaks obtained by fitting $WMAP$-9 data are in wonderful agreement with those provided by *Planck*. The position of the first dip, on the other hand, shows a not so good behaviour. The fitted positions are only marginally consistent and a ruff estimate of the deviation gives

$$|l_{dip}^{PLANCK} - l_{dip}^{WMAP}| \sim 2.8\bar{\sigma} \tag{4.89}$$

where we have defined $\bar{\sigma}$ as the mean error: $\bar{\sigma} = (\sigma_{WMAP} + \sigma_{PLANCK})/2$.

Our fitting procedure is affected by the number of points of the CMB spectrum we decide to use for modellizing the dip. The choice of the point which identifies the end of the first peak and the beginning of the dip is quite arbitrary, like the same choice for the point separating the dip and the second peak. This continuity condition is correctly handled only in a full MCMC treatment of the fitting procedure, because each point joining two parabolas is parameterized by a continuity parameter that is left free to vary along the Markov chain. This aspect is disregarded in our simple fitting procedure, so the continuity of the spectrum is ensured imposing that the fitting curve for the first peak ends exactly where the fitting curve of the dip begins. It is clear that this procedure does not ensure anything about the smoothness of the spectrum at the turning point between the two fitting curves and this could be, in princible, a source of mistakes. For more details see the Appendix.

4.3.6 Data analysis: procedure

We analyze the different data sets separately, then we show combined constraints in the plane $\Omega_m^{D_0} - w$ for the two models on both sides of the correspondence driven by the morphon. We have performed a likelihood analysis using a grid-based Mathematica code. The likelihoods depend on different sets of parameters:

$$L_{SN} \equiv L_{SN}(\Omega_m^{D_0}, w) \tag{4.90}$$

$$L_{Clusters} \equiv L_{Clusters}(\Omega_m^{D_0}, w, H_0) \tag{4.91}$$

$$L_{CMB} \equiv L_{CMB}(\Omega_m^{D_0}, w, H_0, \Omega_b h^2) \tag{4.92}$$

The likelihood for the SN Ia does not depend on H_0 because the marginalization is done analitically.

For the clusters data we need to marginalize numerically the likelihood, which depends on H_0. The marginalization is done by assuming an HST gaussian prior centered in $H_0 = 72$ Km/s/Mpc with $\sigma_{H_0} = 8$ Km/s/Mpc. The Gaussian prior is consistent with the exact marginalization we carried on for the SN Ia likelihood. This property is based on the exact computation, which holds both for a Gaussian prior and a flat one.

The CMB model depends also on the baryon density $\Omega_b h^2$ The dependence is introduced by the fitting formulae and carries information about the physics of the primordial photon-baryon fluid. We are not interested in predicting the baryon density, so we marginalize over $\Omega_b h^2$. The marginalization is done numerically, assuming a Gaussian BBN prior $\Omega_b h^2 = 0.0214 \pm 0.0015$. The integration is carried over $\Omega_b h^2$ and then it is carried over H_0. In principle no difference arises exchanging the integration order.

Finally, we compare the marginalized likelihoods in order to show different constraints imposed by our data. Combinations between data are made multiplying the marginalized likelhoods and they gives combined constraints on the parameters of the model.

We used the notation $\Omega_m^{D_0}$ everywhere (instead of using the more standard Ω_m for the FRW case) in order to remember easily the underlying equivalence between the backreacted model and the Friedmanniann counterpart.

4.4 Data analysis: FRW

Here we sum up the likelihood constraints for the flat FRW filled with Dark Energy represented by a quintessence field of constant parameter w. This model is the first side of the correspondence constructed by the morphon field.

Analyzing this model we assumed $a_0 = 1$ as the basic boundary condition for the scale factor and the figures we show here will be used to make comparison with the averaged model. We will care to understand whether recent data, reducing statistical uncertainties, are able to suggest the incosistency we argued from prime principles.

Preliminarly we give 1σ and 2σ likelihood constraints on the parameters $\Omega_m^{D_0}$.

Figure 4.1 sums up the most important aspects of our analysis. The common red ellipses are constraints coming from cluster data. Unfortunately the red fields are very wide due to the huge uncertainties in modelling the cluster geometry. Consequently current cluster data do not significantly improve constraints we can infer from SN Ia.

Constraints on Supernovae are slightly getting better in present years. The smaller blue fields refer to the Union2.1 catalog, the wider ones to the SNLS. We see that the improvements on measuring uncertainties and adding new elements to the data set have direct consequences on the constraints.

The green fields comes from the anlysis of CMB data. The upper panels of figure 4.1 shows constraints given by the position of the first three peaks and the first dip of the CMB TT-power spectrum. The bottom ones show constraints derived from the method based on the CMB shift parameters. The second set gives narrower ellipses since the full covariance matrix is used in the analysis. Moreover the position of the CMB peaks has been fitted by a simple fitting procedure, disregarding covariance among the points in the spectrum. This effect clearly enhaces the errors on the position of each peak and this justifies why the second method provides better constraints (see the appendix for more details). We do not show constraints from $WMAP$-9 derived from the position of the peaks because the uncertainties on the position of each peak is too big. We used the same fitting procedure we employed for the *Planck* data in order to extract the position of the peaks from the CMB power spectrum measured by

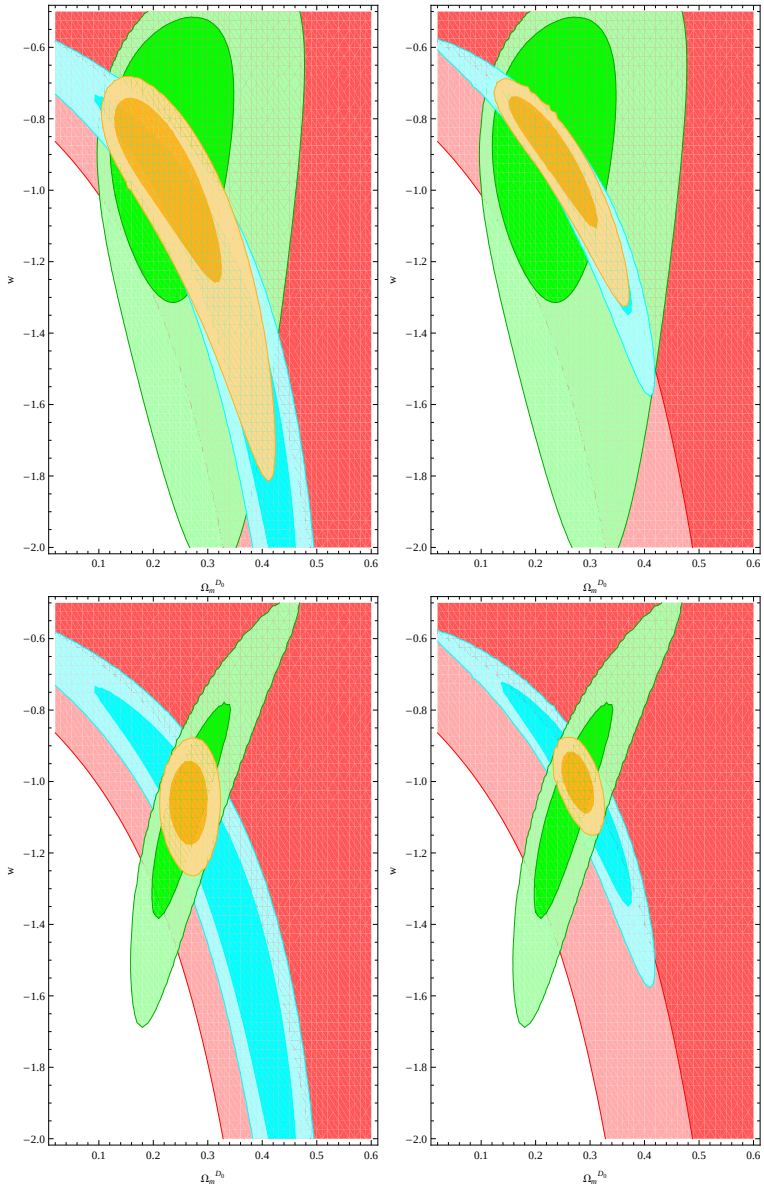

Figure 4.1: 1σ and 2σ likelihood contours for the effective parameters $\Omega_m^{D_0}$ and w for the FRW model. Red fields are given by clusters. Green fields comes from CMB data: *Planck* constraints from CMB peaks are given in the upper panles, $WMAP$-9 constraints from the CMB-shift on the lower ones. The blue fields are provided by SNIa: SNLS constraints are shown in the left panels, Union2.1 constraints are in the right panels. The yellow ellipses are joint constraints.

WMAP-9, but intrisic errors were bigger and the final output is worse than what *Planck* data give.

We note that current data are all consistent with the ΛCDM Universe, which is represented by the constant line $w = -1$, consistently with the most recent checks.

For completeness in figure 4.2 we treat two interesting aspects. The left panel shows the improvement induced by combinig cluster data on the constraints given by *Planck*. Even if cluster data do not really improve the combined constraints, they slightly move constraints from *Planck* towards a denser Universe, suggesting that more precise measurements of cluster distances based on the SZ-effect may be used as an independent probe of cosmology which can be fruitfully combined with CMB data.

The right panel of figure 4.2 shows a comparison between constraints coming from two different sets of *WMAP*-9 data. The wide purple fields correspond to constraints deduced by the position of the first three peaks and the first dip of the CMB power spectrum, the green contours are constraints derived from the CMB-shift parameters. The purple ellipses are very wide due to the combination of *WMAP*-9 intrinsic uncertainties and our fitting procedure, which may overestimate the error on the position of each peak. The covariance among the points of the measured power spectrum were disregarded, enhacing the uncertainties. Clearly the method based on the shift parameters is better and predictions from *Planck* data are more precise.

We note that the ellipses derived from the shift parameters in the right panel of figure 4.2 are completely contained into the others, suggesting that extracting cosmological information from the CMB-shift parameters is related to the procedure based on the position of the peaks. The two approaches are similar since they both require to predict the fundamental multipole l_a.

4.5 Data analysis: backreaction

We perform the same likelihood analysis testing the average model based on the template metric 3.103. We show separately how the constraints change for each data set. In Fig. 2 of [34] the authors show combined constraints from the SNLS and the positions of the CMB peaks from

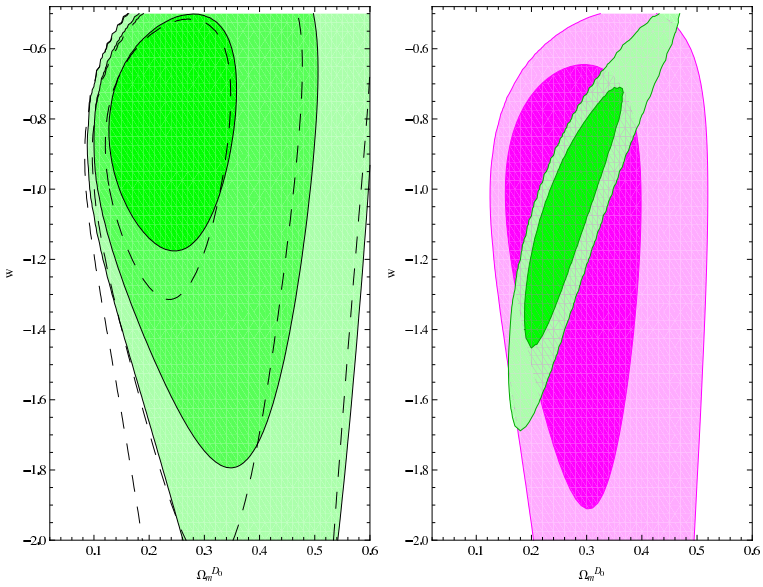

Figure 4.2: 1σ, 2σ and 3σ likelihood contours for the effective parameters $\Omega_m^{D_0}$ and w for the FRW model. Left panel: improvement of *Planck* constraints (empty contours) combining clusters data (filled contours). Right panel: comparison between constraints provided by the position of the CMB peaks and dips (purple fields) and those given by the CMB shift parameters (green fields); only $WMAP$-9 data were used.

WMAP-3. The main feature is clear: likelihood contours move slightly towards a denser Universe if the backreaction is assumed. This effect can be considered the signature of curvature. The bare metric is curved and any *on average* description of the Universe can be separated from the corresponding flat FRW cosmology since the coarse-graining procedure does not completely destroy the information about the curvature of the bare metric. Their analysis is carried on the parameter space defined by $\Omega_m^{D_0}$ and the scaling index n, our is still performed in $\Omega_m^{D_0}$ and w. No significant difference arises between this two procedures.

First we separately analyze each data set, showing results in figure 4.3. Contours in the upper left panel comes from the SNLS data and show the predicted behaviour. Filled ellipses, corresponding to the backreaction model, are slightly pushed towards higher values of $\Omega_m^{D_0}$, accordingly to Fig. 2 of [34]. The Union2.1 catalog (in the upper central panel) behaves likewise. Predictions from this data set are better than those given by the SNLS, since the total uncertainties on each data point has been reduced: the error bars associated to each distance modulus measurement are lower and the set is composed of much many data points.We note that contours corresponding to the backreacted scenario overlap those for the flat FRW model only at 3σ, which suggests that late-time observations may provide a way for distinguish between models based on Dark Energy and backreacted ones, provided that statistical and systematic uncertainties are relatively small.

The upper right panel of figure 4.3 shows constraints from clusters data. The big errors on modelling the clusters do not allow significant predictions, but we observe that contours behave well when backreaction is considered. This aspect is completely new, since the method based on angular diameter distances from distance clusters, altought related to, is independent from the method based on SN Ia distance modulus. The main difference is hidden in the marginalization over nuisance parameters, which are different. The marginalization procedure for the SN samples is carried out analitically and the nuisance parameter is left unconstrained. On the contrary the marginalization over H_0 for the clusters data is carried out numerically over a limited set assuming a gaussian prior. Assuming a flat prior on a wide interval like $H_0 \in (0, 200)$ does not really affect the probability contours, showing that contributions to the marginalized

likelihood coming from higher or lower values of H_0 are intrisically small, regardless of how they are weighted by the prior.

In the lower panels we show constraints we can derive from our set of CMB data. In general we note that our fitting procedure for extracting the position of the peaks of the CMB spectrum does not provide good contours with respect to predictions coming from SN data. We are not able to distinguish whether the statistical error on the mesurement of the CMB multipole l_a provided by $WMAP$-9 and *Planck* is actually too big or our fitting procedure is too weak, enhacing errors on the peak positions. The likelihood is not concentrated on a small area of the parameter space and the best contours can be derived using the method based on the CMB-shift parameters.

We can notice an evident feature: contours do not seem to have a definite behaviour similar to what we found for the SN Ia and SZ clusters. The 1σ region of the likelihood is not definitely pushed towards higher values of $\Omega_m^{D_0}$. Contours computed using the position of the CMB peaks do not allow to understand this feature well, since they are dominated by too big uncertainties. Data from *Planck* suggest that the ellipses move toward lower values of $\Omega_m^{D_0}$ since the right edges are squeezed upon the left ones, which correspond to a quite steep decrement in the 3D likelihood. The choice of the prior plays a role here.A flat prior on H_0 slightly pushes the left edges of the contours towards lower values of $\Omega_m^{D_0}$, but the blanck regions corresponding to the FRW model behave likewise and we may only conclude that CMB data may show a bad behaviour. Data from $WMAP$-9 are even worse: contours derived from the positions of the peaks on the CMB power spectrum are dominated by the huge uncertainties and the 1σ regions corresponding to the backreacted model and to the FRW generally overlap.

The method based on the CMB-shift parameters shows clearly that contours move towards a less dense Universe when backreaction is considered. This bad behaviour goes against preditions from SNe and clusters. Moreover we note that the filled contours in the lower left panel of figure 4.3 are surprisingly similar to those found analyzing *Planck* data. We are convinced that this aspect play an important role. Since the CMB-shift parameters are sligtly model-dependent we could have argued that the bad behaviour might have been caused by the model dependency of the ob-

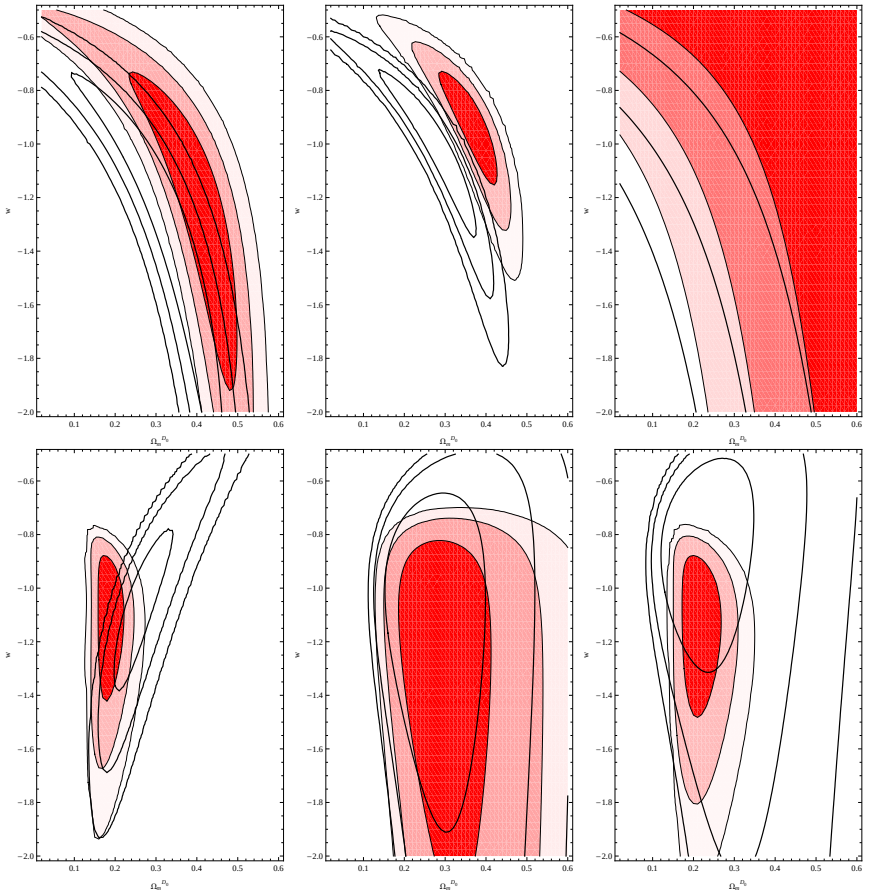

Figure 4.3: Comparison between the backreaction model (filled contours) and a flat FRW with quintessence of constant equation of state (blank contours). 1σ, 2σ and 3σ likelihood contorus are shown for different data sets. Upper left: SNLS data. Upper central: Union2.1 data. Upper right: Clusters. Lower left: $WMAP$-9 yr CMB-shift parameters. Lower central: $WMAP$-9 yr CMB peak. position. Lower right: *Planck* CMB peak positions.

servables involved, but the similarity with predictions from *Planck* ensures that such an hypothesis may be disregarded, since no model dependency affects the method based on the positions of the CMB peaks and dips.

We are then convinced that the reason underlying the *bad behaviour* of the contours predicted from CMB data for the backreaction model should be searched into the apparent inconsistency related to the boundary conditions. We have assumed both $a_{D_0} = a_0 = 1$ as boundary conditions for the differential equations, since they are widely used and assumed in [34]. We have shown that in this case the two solutions $a(t)$ and $a_D(t)$ should not assume the same value at the recombination redshift z^*. Clearly this aspect has a longstanding consequence in the computation of the sound horizon, since it is carried out integrating over the scale factor from $a = 0$ up to $a = a^* = (1 + z^*)^{-1}$. For the flat FRW model such computation is correct, but for the backreaction model the procedure breaks. Indeed we should integrate over a_D from $a_D = 0$ up to the decouplig epoch, **which is not** $(1 + z^*)^{-1}$. The reason is simply that assuming the same boundary condition today creates troubles in the definition of the decoupling epoch. In the FRW model it is defined by z^* and a^*, which are related consistently by the physics of the CMB and the relation $a^{-1} = 1 + z$. When this relation breaks, as it happens in the backreacted scenario, we are left with the ambiguity of defining the decouplig epoch using z or a_D. Logically we may assume that the decopling epoch is fixed by its redshift, but this clearly face the overwhelming problem that fitting formulae for z^* may fail in predicting z^* from the physics of the CMB if the standard relation $a^{-1} = 1+z$ breaks. Indeed we have argued that under the boundary condition $a_{D_0} = 1$ the effective scale factor a_D follows a friedmannian solution for $z > z^*$, but the condition $a_0 = 1$ must be relaxed, which immediately tells that any fitting formula given for a FRW Universe where implicitly $a_0 = 1$ is assumed will fail in predicting z^*. This reflects into a wrong prediction of the sound horizon and consequently in an error in predicting the fundamental multipole l_a. The fingerprints that a failure in predicting l_a may explain the bad behavior are found in the similarity of the ellipses computed from the CMB-shift parameters and those given by *Planck* since both methods rely explicitly on the multipole l_a. Moreover the CMB-shift parameters contains z^* as a one of the three main observables and this should enhace the bad behavior since the failure in

predicting the decoupling epoch when backreaction is added enters the likelihood analysis twice and separately.

On the other hand it is clear that the recombination epoch is given by the microphysics of the photon-baryon fluid, which cools down while Universe expands. This naively suggests that *the size of the Universe should play a central role* in the decoupling process and the decoupling redshift should be computed *after the size of the Universe at decoupling* is known from the elementary processes that dominates the primordial Universe. This point of view is thermodynamically supported, since the decopling epoch is characterized by a well-defined temperature, which corresponds to a well-defined size of the Universe in any FRW model. Consequently the recombination redshift should be computed by using the basic relation $a^{-1} = 1 + z$, but clearly if the effective solution a_D follows , for sufficently high z, a friedmaniann solution, then the prediction of the recombination redshift from the size of the Universe may fail up to a constant factor, since we are not able to specify the value of the boundary condition a_0.

Whatever point of view we choose, we are convinced that current data are showing that the incosistency of the boundary conditions cannot be disregarded as a small effect in making predictions using CMB data, since they have non-trivial consequences on the theoretical value of the fundamental multipole l_a.

The combined contours are shown in figure 4.4.

Upper panels show constraints from the SNLS and lower ones those from the Union2.1 catalog, corresponding in both cases to the blue fields. Constraints from CMB data are drawn with green fields. The two panels on the left shows the better ones, corresponding to the analysis based on the shift parameters. The central panels are dominated by the wide constraints we derived unsing $WMAP$-9 data on the position of the peaks and dips of the CMB spectrum. The uncertainties play a significant role. On the contrary in the right panels the green fields are derived from *Planck* data and suggest immediately that recent experiments on the CMB are able to provide more accurate constraints.

Yellow ellipses are joint constraints and show the consequences of the bad beahvior of constraints based on CMB data when backreaction is added. Since ellipses based on clusters and SN Ia data move slightly predicting a denser Universe and those based on CMB data move in the

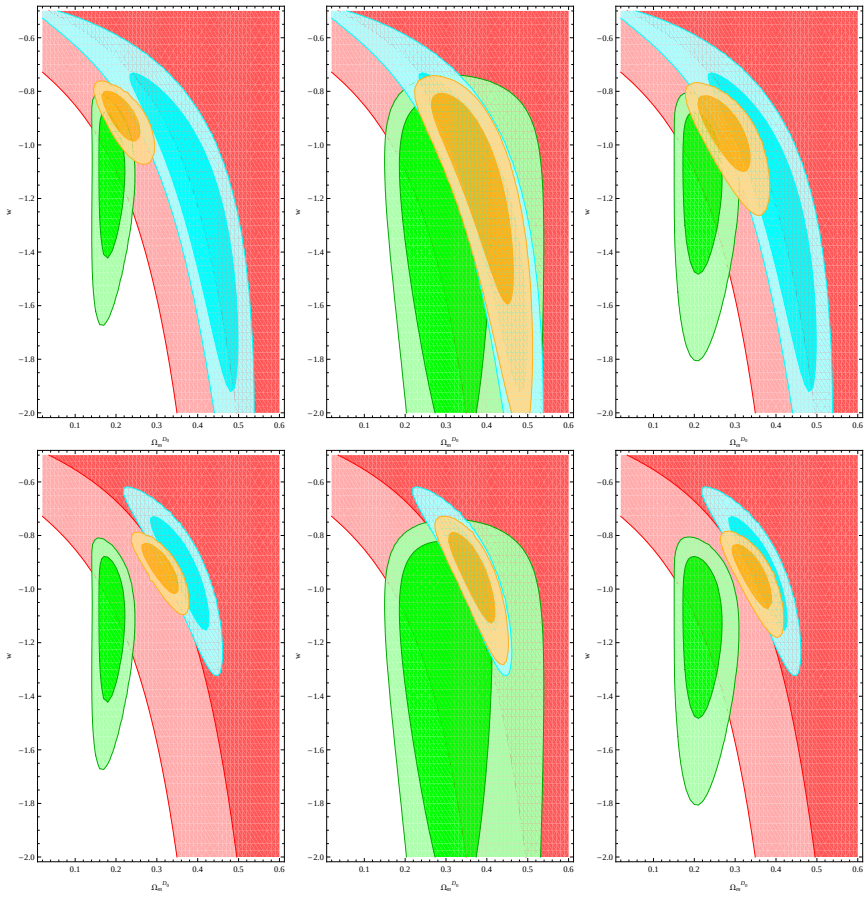

Figure 4.4: 1σ and 2σ likelihood contours for the effective parameters $\Omega_m^{D_0}$ and w for the averaged model. Red fields are given by clusters. Green fields comes from CMB data: $WMAP$-9 constraints from the CMB-shift parameters are given in the left panles, $WMAP$-9 constraints from the position of the peaks appear in the central ones, constraints from *Planck* are shown in the right panels. The blue fields are provided by SNIa: SNLS constraints are shown in the upper panels, Union2.1 constraints are in the lower ones. The yellow ellipses are joint constraints.

opposite direction, the region of the parameter space corresponding to non-trivial overlap probability must become narrower respect to the standard FRW case. The method based on the CMB-shift parameters and, separately, *Planck* data provide constraints that do not overlap those from the Union2.1 catalog neither at 2σ. They suggests that methods based on CMB data seem to provide constraints that are only marginally compatible with standard constraints coming from SN Ia. Clearly we need some accuracy in order to see this effect, because big uncertainties expand the ellipses and the overlapping region may increase.

We are not able to distinguish whether joint constraints are suggesting that the averagaing procedure based on Buchert's approach and Larena's template metric in Eq. 3.103 is being ruled out by recent improvements on data precision or the incosistency on the boundary conditions $a_{D_0} = a_0 = 1$ cannot be disregarded further. We are convinced that figure 4.4 is telling that current CMB data can be successfully used for constraining models based on backreaction, but much care is needed since predictions may be strongly affected by correctly defining observables in the backreacted scenario. CMB data are sufficently precise for shading light on many consistency problems that may arise in assuming standard approximations for describing the physics of the CMB when backreaction is considered and the effects of smoothing are described under the point of view assessed in [34]. We have pointed out that if $a_{D_0} = a_0 = 1$ is assumed, then the functions $a_D(z_D)$ and $a(z)$ cannot take the same value at z^* and that $a_D(z^*)$ should not predict the correct size of the Universe at decoupling, since it should be $(1+z^*)^{-1}$ if the evolution of the scale factor follows the standard FRW solution for $z > z^*$. This incosistency is solved relaxing the boudary condition $a_0 = 1$, but this hypothesis implicitly may destroy the validity of the fitting formula which predicts z^*. In other words the critical aspect of our likelihood analysis is hidden behind the value of z^*, which enters directly the multipole l_a and the method based on the shift parameters.

We are also interested in studying the combination of two sets of data for making predictions in the backreaction context. In figure 4.5 and 4.6 we show separately the improvement given by cluster data and SN Ia to constraints coming from the CMB when backreaction is considered.

In figure 4.5 we show how constraints derived from the method based

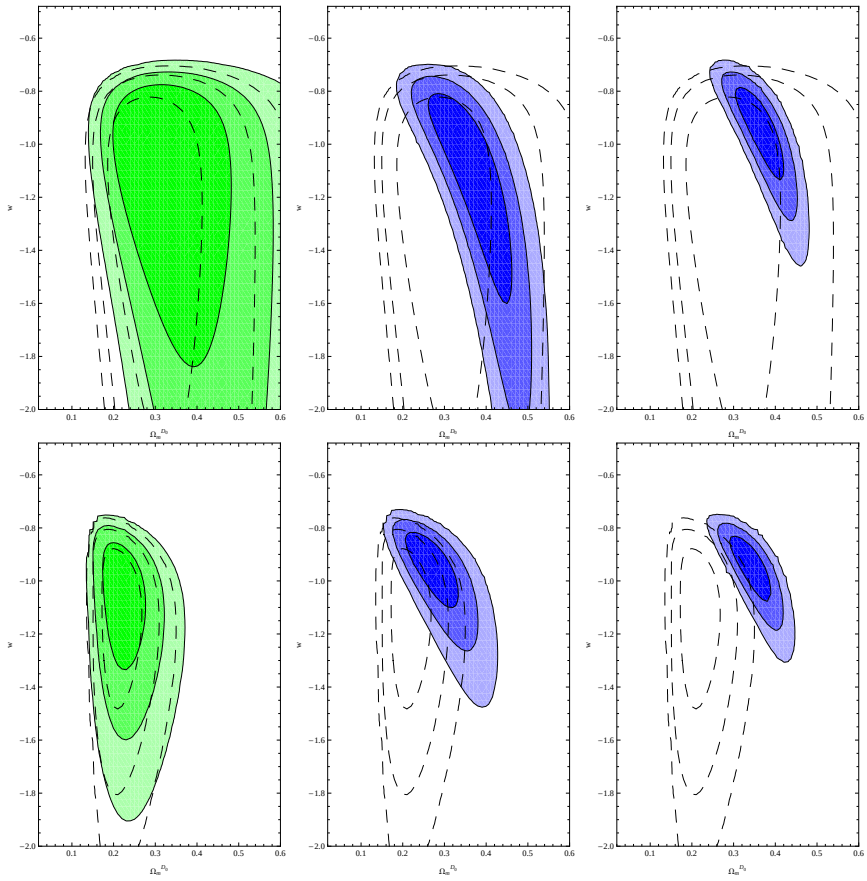

Figure 4.5: Comparison between constraints from the CMB peaks and combined ones for the backreacted Universe. Blanck contours refers to CMB data alone. Filled ellipses are joint constraints. Contours in the upper panels comes from $WMAP$-9 data,those in the lower ones comes from *Planck*. Left panels: combination with cluster data. Central panels: combination with SNLS data. Right panels: combination with Union2.1 data.

on the position of the peaks and dips of the power spectrum of the CMB change when combined with those derived from clusters or SN Ia.In the upper panels constraints are derived from $WMAP$-9 data, while those shown in the lower panles comes from *Planck*. The two panels on the left shows the deformation of the contours when clusters data are added to the likelihood analysis. Unfortunately no significant improvemenet arises. The central panels and the right ones shows the same deformation when SN Ia data are combined. SNLS data are less precise and combined constraints are wider (central panels), while the Union2.1 catalog provides narrower ellipses (right panles). We note that combined constraints overlap constraints from CMB data alone, suggesting that data sets are compatible. Our fitting procedure of $WMAP$-9 data on the power spectrum of the CMB predicts too large uncertainties and clearly the constraints are compatible with both predictions from the SNLS and Union2.1.

Using *Planck* data we are able to improve constraints coming from the analysis of the CMB spectrum. Predictions from the SNLS are still compatible with those from *Planck*, but the inconsistency hidden behind the analysis of CMB data begins to appear. In the lower right panel of figure 4.5 the 1σ regions do not overlap and the data from SN Ia and CMB seem to suggest that the model is breaking down. We are convinced that we are simply facing that approximations we used in buiding the model must be refined, since experimental uncertainties are now too small to avoid this work.

In figure 4.6 we show what happens if the method based on the CMB-shift parameters is used. Constraints from $WMAP$-9 are still better than those from *Planck*, since no home-made fitting procedure is needed for finding the data points. The use of the full covariance matrix for treating the uncertainties on the experimental data improve the final result and the ellipses corresponding to combined contraints overlap those coming from the CMB alone only at 2σ. The right panel shows clearly that the Union2.1 data provide constraints only marginally compatible.

Finally we show how the right panel of figure 4.2 is changed when backreaction is considered. We have shown that the two methods for analyzing CMB data are affected by many uncertainties. In figure 4.2 we noted that $WMAP$-9 data suggest concordance between the two methods in the standard FRW framework, since the two sets of constraints

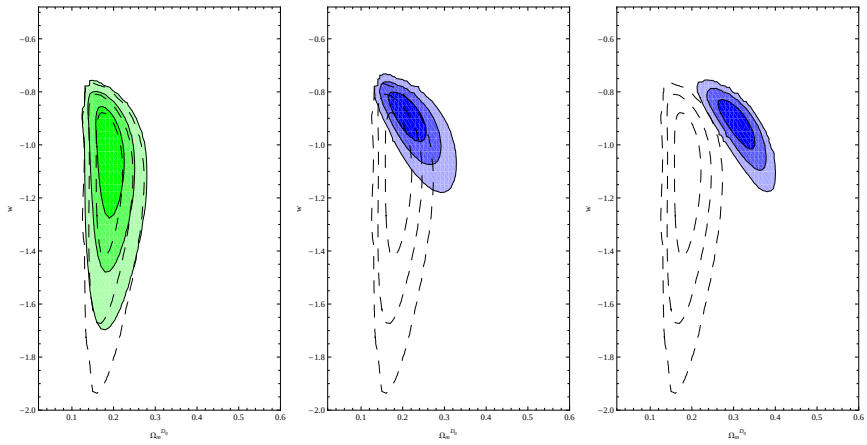

Figure 4.6: Comparison between constraints from the CMB- shift parameters and combined ones for the backreacted Universe. Blanck contours refers to CMB data alone. Filled ellipses are joint constraints. Left panel: combination with cluster data. Central panel: combination with SNLS data. Right panel: combination with Union2.1 data.

are well enveloped. This feature seems natural, since the multipole l_a is used in both procedures and common data should always give compatible conmstraints, since the likelihoods are not completely independent.

In figure 4.7 we show the superposition of constraints from $WMAP$-9 data given by the two methods, when backreaction is considered. The original envelope is destroyed, since the ellipses corresponding to predictions coming from the CMB-shift parameters are heavily distorded. The same distortion does not affect the other constraints, so, the 1σ regions do not overlap completely. We claim that this deformation is the mark of the incosistency we have described and that the figure suggests that the main core of the problem is predicting z^*. Indeed if only l_a were affected by any inconsistecy, which affects its theoretical prediction, both constraints should roughly deform likewise. The heavy deformation which affects only contours given by the shift parameters should be explained stating that also the theoretical predictions of z^* and R should in principle be corrupted. Since R implicitly depends on z^* too, we are led to guess that the evaluation of the decoupling epoch in the averaged model requires more care and better approximations.

4.5.1 $WMAP$-3 data

We have shown that the definition of the fundamental multipole l_a is affected by the boundary conditions since the relation between the size of the Universe and the redshift in the backreacted scenario changes passing through the last scattering surface. We have explained that if $a_{D_0} = a_0 = 1$ is chosen as boundary condition, then the function $a_D(z_D)$ does not take the value $(1 + z^*)^{-1}$ at the decoupling epoch z^*. In other words if we assume that after z^* the effective scale factor must follow the relation $a_D(z_D) = k(1 + z_D)^{-1}$,for a suitable constant k, we may argue that the correct value of k is set by assuming that $a_D(z_D)$ is continuous in z^*. We have also shown that the definition

$$l_a = \pi \frac{r(1/1 + z^*)}{r_s(1/1 + z^*)} \tag{4.93}$$

which corresponds to the approximation of disregarding the factor k, faces troubles when sufficently precise emasurement of the CMB are used in the likelihood analysis. This approximation simply assumes that z^* is still the

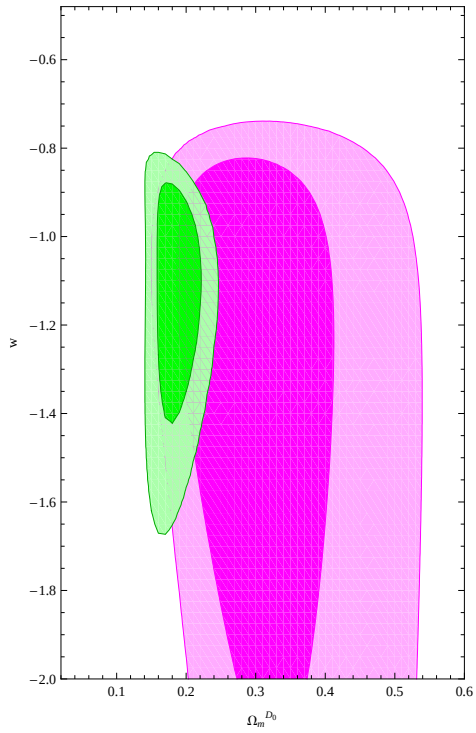

Figure 4.7: Comparison between constraints provided by the position of the CMB peaks and dips (purple fields) and those given by the CMB shift parameters (green fields) for the averaged model. Only $WMAP$-9 data were used.

correct prediction of the decoupling time, but the corresponding size of the Universe is different. Clearly we are implicitly asking that

$$a_D(z^*) - (1+z^*)^{-1} \tag{4.94}$$

is sufficently small. Our work shows that such approximation is not so good and recent data are able to point out the incosistency.

Here we are interested to show that uncertainties on the positions of the peaks and dips of the CMB anisotropy spectrum as measured by $WMAP$-3 were to large to reveal the problem. This may explain why Fig.2 of [34] shows the standard behavior when backreaction is added even if SN Ia data from the SNLS were combined with constraints coming from the analysis of $WMAP$-3 data.

In [41] the positions of the first and second peak and the first dip of the CMB are published. We perform the likelihood analysis using directly the measured values and errors as data. In figure 4.8 we show constraints in the $\Omega_m^{D_0} - w$ plane for the averaged model. We performed the marginalization on the nuisance parameter H_0 using two distinct priors. In the left panel we marginalized using our gaussian prior from the BBN, in the right panel the prior is assumed flat in the range $40 < H_0 < 100$ Km/s/Mpc.

In both cases the constraints are too wide due to the big uncertainties. Clearly the combination with constraints derived from the SNLS reproduces Fig. 2 of [34]. Small deformations may arise depending on the form of the prior on H_0.

4.5.2 Redefinition of the multipole

In order to check if the apparent incompatibility may be removed by changing the definition of the multipole we employed a different likelihood analysis of the CMB data based on the definition of the multipole

$$l_a = \pi \frac{r(a_D(z^*))}{r_s(a_D(z^*))} \tag{4.95}$$

This definition simply assumes that the correct size of the Universe at the decoupling epoch we have to employ in our computation of the multipole is given by $a_D(z^*)$, like it is suggested in [34]. Changing the size of

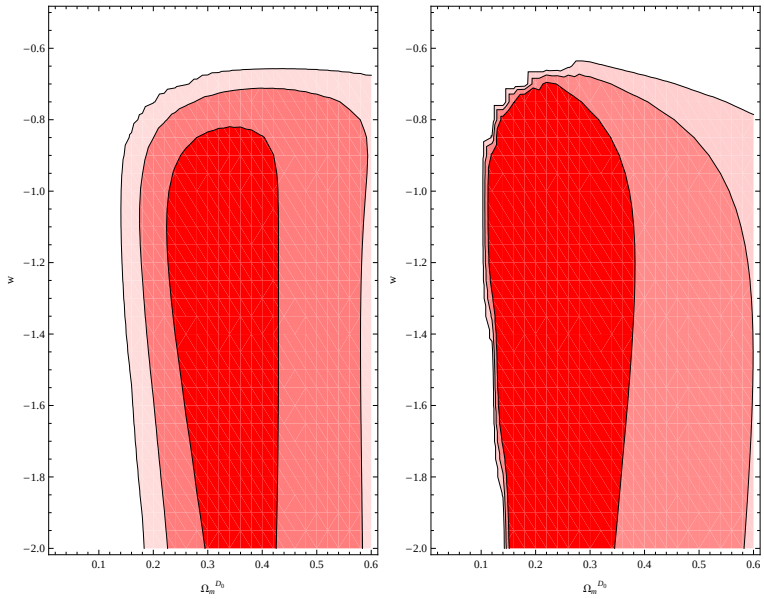

Figure 4.8: Constraints on $\Omega_m^{D_0}$ and w for the averaged model derived from $WMAP$-3 data on the position of the peaks and dips of the CMB spectrum. Only the first two peaks and the first dip were used.

the Universe at decoupling significantly changes l_a, since the sound horizon is small. We checked that we may disregard the difference in definig the comoving distance, while changing the sound horizon has significant consequences.

This can be easily shown from mathematics, since the derivative of the multipole

$$\frac{d}{da}\left[\int_a^{a_0} f(\xi)d\xi\left(\int_0^a \frac{f(\xi)}{\sqrt{1+R(\xi)}}d\xi\right)^{-1}\right] \tag{4.96}$$

is dominated by the sound horizon. We marked $f(a)$ the integrand function in the comoving distance and noted that

$$\frac{1}{\sqrt{1+R}} \sim 1 \quad a \to 0 \tag{4.97}$$

in order to simplify the structure of the derivative. Thus, taking the derivative yelds

$$\frac{dl_a}{da} \sim \frac{f(a)}{r_s(a)}\left(\frac{r(a)}{r_s(a)} - 1\right) \tag{4.98}$$

For a standard cosmological fluid $f(a) \sim (\Omega_m a + \Omega_r + \Omega_w a^{1-3w})$ and we see that for $w < 1/3$ the derivative is dominated by r/r_s^2, because $f(a)$ never vanish. Clearly r_s is small when $a \to 0$, while r is finite, which simply demonstrates that the multipole is much more affected by any variation in the sound horizon.

We analyzed $WMAP$-3 and $WMAP$-9 data assuming the definition 4.95 and we show constraints on $\Omega_m^{D_0}$ and w in figure 4.9. In the left and central panels we used data from $WMAP$-3. First we used the gaussian prior on H_0 , then we tried to employ the flat one for completeness. Contours are heavily pushed in the region of lower ws and they are clearly not compatible with constraints coming from the SNLS. We are convinced that figure 4.9 matches the incompatibility discussed in [53]. In the left panel we show that constraints from $WMAP$-9 data are not better and they are not compatible with other constraints from SN Ia if the definition 4.95 for the multipole is employed.

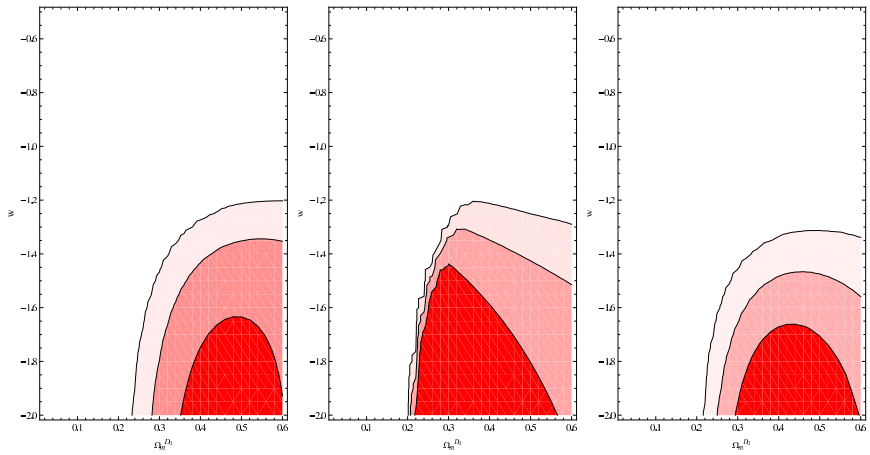

Figure 4.9: Constraints on $\Omega_m^{D_0}$ and w for the averaged model derived from $WMAP$-3 and $WMAP$-9 data on the position of the peaks and dips of the CMB spectrum. Left panel: $WMAP$-3 data, gaussian prior on H_0. Central panel: $WMAP$-3 data, flat prior on H_0. Right panel: $WMAP$-9 data, gaussian prior on H_0. The fundamental multipole l_a is defined as 4.95.

4.6 Side topics

In this section we shortly discuss some side topics which are hidden behind the likelihood analysis. These aspects played a role, since in principle the strange behavior that CMB data suggested when backreaction is considered required a more precise inspection.

We separately studied the effect of changing priors on the nuisance parameters we marginalize over and the effect on the likelihood of adding a faint peak to $WMAP$-3 data, corresponding to the position of the third peak of the CMB spectrum.

4.6.1 Shape of the priors

We studied the effect of the shape of the priors on the constraints derived from CMB data. First we focused on the case of a flat FRW spacetime. The shape of the prior on the baryon density parameter Ωbh^2does not affect contours significantly. No significant deformations of the contours arise when the BBN gaussian prior is substituted to a flat one. On the contrary the prior on H_0 has wider consequences.

In figure 4.10 we show how contours change when the H_0 takes values in wider or narrower ranges. We used $WMAP$-3 data on the position of the peaks of the CMB in order to see how much wide contours are distorded when priors on H_0 are changed. The contours computed when a gaussian prior should not change significantly, since the gaussian drops rapidly. Since the prior is centered in 72 km/s/Mpc and the corresponding dispersion is $\sigma_{H_0} = 8$ km/s/Mpc, the marginalization over any interval wider than $6\sigma_{H_0}$ centered in the central value provides the same marginalized likelihood. The lower panels of figure 4.10 shows that constraints are not affected when the integration range in H_0 is reduced from $[1, 200]$ (left panel) to $[40, 90]$ (right panel).

When we assume a flat prior the width of the marginalization interval plays a non-trivial role. Let us take $H_0 \in [a, b]$, then the flat prior is defined as

$$p(H_0) = \theta(H_0 - a) - \theta(H_0 - b) \tag{4.99}$$

where $\theta(x)$ is the Heaviside distribution. Values of H_0 outside the range $[a, b]$ are not allowed and they do not contribute to the final marginalized

likelihood. The dependence on the interval extrema is well shown in the upper panels of figure 4.10, where in the left one the range is assumed to be $[1, 200]$, while it is reduced to $[40, 90]$ while drawing the right panel.

We note the sharp cut in the lower left corner of the figure corresponding to the reduced interval $H_0 \in [40, 90]$. The motivation is clear: higher and higher values of H_0 allows lower and lower values of $\Omega_m^{D_0}$, since the coordinate distance roughly depends on the combination $(H_0\sqrt{\Omega_m^{D_0}})^{-1}$.

We decided to employ the gaussian prior in our likelihood analysis in order to reduce the effect of sharp cuts in the marginalized probability. This assumptio is reasonable because a too wide range of variability for H_0 is discouraged by current measurements of the value of the Hubble rate H_0. Consequently we employed only the gaussian prior in our study of the backreacted Universe.

4.6.2 Adding a point to $WMAP$-3

We have shown that uncertainties on $WMAP$-3 data of the positions of the peaks and dips of the CMB anisotropy spectrum are quite big and the corresponding constraints on the parameters Ω_m and w are wide. We asked ourselves how much adding a fourth data point may improve the probability contours. We studied the case of a flat FRW Universe only.

In figure the left panels of 4.11 we show constraints on $\Omega_m^{D_0}$ and w derived from the likelihood analysis of $WMAP$-3 data on the position of the first and second peak and of the first dip of the CMB power spectrum. In the upper panel we assumed a flat prior on H_0 ranging in the interval $[1, 200]$ Km/s/Mpc, in the lower ones we employed the gaussian prior. In order to draw the right panels we added an extra data point corresponding to the position of the third peak of the anisotropy spectrum. The position of the third peak has been guessed by a simple and rough fit of $WMAP$-3 measured spectrum. The corresponding error was assumed big, in order to see if adding a point may improve the likelihood analysis even if $WMAP$-3 measures of the high l part of the anisotropy spectrum are affected by huge errors. We obtained

$$l_3^{guess} = 815 \pm 10 \tag{4.100}$$

In the upper panels of figure 4.11 we assumed a flat prior on H_0, rang-

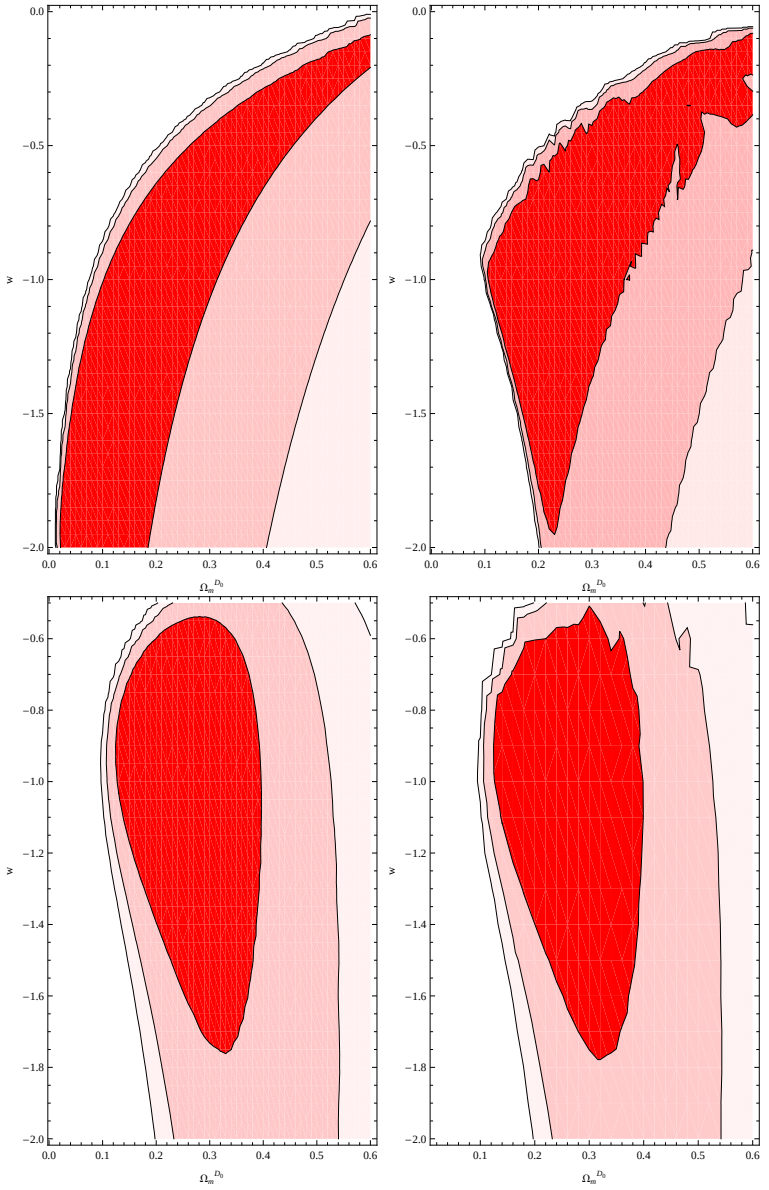

Figure 4.10: Constraints on $\Omega_m^{D_0}$ and w for a FRW Universe filled with dark Energy with a constant equation of state for different marginalization priors and different ranges of variability for H_0. In the left panles we assumed $H_0 \in [1, 200]$ KM/s/Mpc, in the right ones the interval in $H_0 \in [40, 90]$ Km/s/Mpc. In the upper panels contours are shown for a flat prior, in the lower ones the standard BBN gaussian prior is used. $WMAP$-3 data only were used.

ing in $H_0 \in [1, 200]$ Km/s/Mpc. In the lower ones we studied the same improvement when the gaussian BBN prior on H_0 is understood. In both cases we see (right panels) that the likelihood constraints got better regardless of the huge error on the guesssed point. This simple analysis suggested that $WMAP$-9 data may be used for improving the likelihood analysis based on the positions of the peaks and dips of the CMB spectrum. We knew that a fitting procedure of the rough $WMAP$-9 measured spectrum was needed, expanding the uncertainties on the positions of the peaks further, but the whole improvement would justify this approach.

4.6.3 Testing curvature

For further completeness we check the curvature prescription suggested in [34]. The average Ricci curvature is directly related to the time dependent parameter $k_D(t)$ of the template metric by the relation

$$\langle R \rangle_D = \frac{k_D(t)|\, \langle R \rangle_{D_0}\, |a_{D_0}^2}{a_D^2} \tag{4.101}$$

This equation ensures that the parameter $k_D(t)$ is not arbitrary and inherits the averaged curvature of the domain D.

In a FRW Universe the comoving distance r satisfies

$$\left(H(z) \frac{dr(z)}{dz} \right)^2 - 1 = -\Omega_{k,0} (H_0 r(z))^2 \tag{4.102}$$

which follows from the definition. It simply means that

$$\Omega_k(z) = \frac{(H_0 H(z) r'(z))^2 - 1}{H_0^4 r^2(z)} \tag{4.103}$$

does not depend on z, since it constantly takes the value of the curvature density paramater $\Omega_{k,0}$.

If we substitute the standard FRW metric with Larena's template, the effective curvature parameter $\Omega_k^D(z_D)$ is not constant, since

$$\Omega_k^D(z_D) = -k_D(t(z_D)) \tag{4.104}$$

Then we may compute the derivative with respect to the effective redshift in order to characterize an averaged Universe, since the function

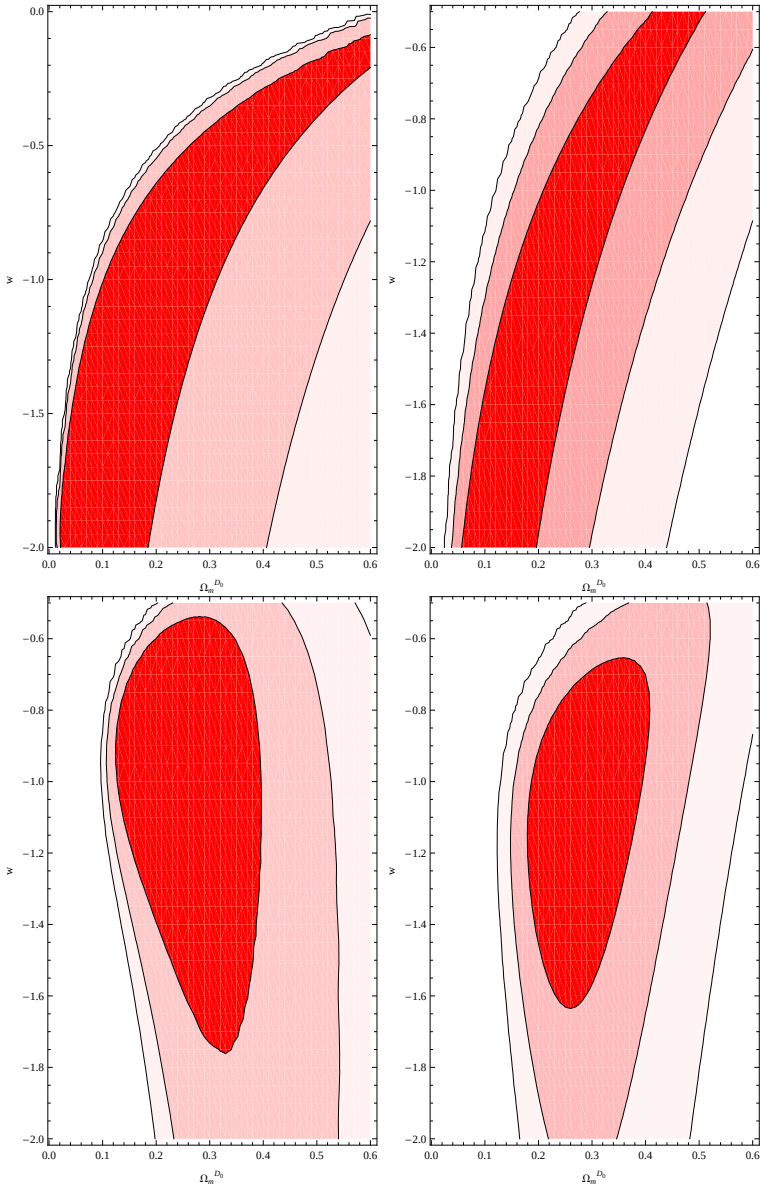

Figure 4.11: Constraints on $\Omega_m^{D_0}$ and w for a FRW Universe filled with Dark Energy with a constant equation of state: comparison between constraints derived by analyzing $WMAP$-3 data only (left panles) and those derived by adding an extra guessed point, corresponding to the third peak of the CMB spectrum (right panels), for different priors on H_0. Upper panles: flat prior in the range $H_0 \in [1, 200]$ Km/s/Mpc. Lower panels: gaussian BBN prior.

$$C_D(z_D) = -\frac{H_D(z_D)\bar{r}^3(z_D)k'_D(z_D)}{2H_{D_0}\sqrt{1-k_D(z_D)\bar{r}^2(z_D)}} \tag{4.105}$$

identically vanishes for the FRW spacetime ($k'_D = 0$). This function records the effect of the coarse-graining procedure we employed assuming the template metric: the intrinsic curvature of the bare metric is smoothed out, but *its memory is not completely lost*. Due to the local curvature related to the inhomogeneities the path of light is changed from the standard path followed by photons in the FRW spacetime and this aspect survives the coarse-graining leaving its fingerprints in the non standard relation $a_D(z_D)$ and in a non constant Ω_k^D.

Following Fig.5 of [34] we plotted the $C_D(z_D)$ function for different values of Ω_m, H_0 and w. In the top panel of figure 4.12 we show $C_D(z_D)$ when for the arbitrary values $\Omega_m^{D_0} = 0.3$, $w = -1$, $H_0 = 70$ Km/s/Mpc. Changing H_0 does not modify the curve. This may seem obvious, since H_0 simplifies in the definition of the function, but we have to remember that we the differential equation solved by the comoving distance $\bar{r}$ contains the radiation density parameter which implicitly depends on H_0.

In the central panel we show the dependence on $\Omega_m^{D_0}$. We fixed $w = -1$ and $H_0 = 70$ km/s/Mpc. The green curve corresponds to the reference value $\Omega_m^{D_0} = 0.3$. Increasing $\Omega_m^{D_0}$ to 0.4 or 0.5 enhaces the curvature (yellow and red curves respectively), while decresing $\Omega_m^{D_0}$ to 0.2 or 0.1 decreases it (blue and violet curves respectively). The black line is the most interesting. It corresponds to $\Omega_m = 0.01$ and implicitly shows that in the limit of a vacuum Universe the averaged spacetime is intrinsically curved and the curvature is not constant. This may seem strange, since no inhomogeneities should exist if the matter density in constantly null. Clearly we are facing an intrinsic aspect of the averaging procedure. We should remember that we employed two distinct averaging assumptions in building the model: on the one side we assumed Buchert's method of smoothing matter inhomogeneities on spatial domains, on the other side we postulated that some coarse-graining procedure acting on the metric exists which gives an FRW-like spacetime. This last assumption is involved here: the averaging scheme for the metric is skipped by postulating the form of the template metric, since otherwise it would be equal to solve the averaging problem, but clearly the curvature prescription, linking $k_D(t)$

to the average Ricci scalar ensures that $k_D(t)$ can be constant only if $\langle R \rangle$ scales as a_D^{-2}.This case has been disregarded since it corresponds to decoupling the scalar curvature and the backreaction, so we may simply conclude that the backreaction plays a crucial role in the coarse-graining procedure of a metric by its own right, independently of how it may be defined from the smoothing of the matter inhomogeneities. This is a pure relativistic effect and may suggest that smoothing a metric is completely uncorrelated to smoothing anything sourcing the metric itself in the Einstein equations. It is our opinion that this leads to think about the averaging problem in a purely statistical sense, where the coarse-graining scheme of the stress-energy tensor can be viewed as a sort of ergodic effect of a general averaging scheme involving only the metric.

Finally, in the bottom panel of figure 4.12 we show how $C_D(z_D)$ varies when w changes. The reference values are $\Omega_m^{D_0} = 0.3$ and $H_0 = 70$ km/s/Mpc. The yellow line corresponds to the reference value $w = -1$. Increasing w to -0.9 enhaces the curvature (red line), while lowering it to -1.1 or -1.2 reduces the curvature (green and blue lines respectively).

The panels clearly show that the template metric 3.103 describes curved slices and the curvature is enhaced at small redshifts. The curvature descreases at high redshift accordingly to the assumption that the averaged spacetime should become friedmannian at the decoupling epoch. It is interesting to note that the curvature is quite constant for high redshifts, but it does not vanish definitely. This proves that the high redshift dynamics of the smoothed solution cannot be represented by a flat FRW completely.

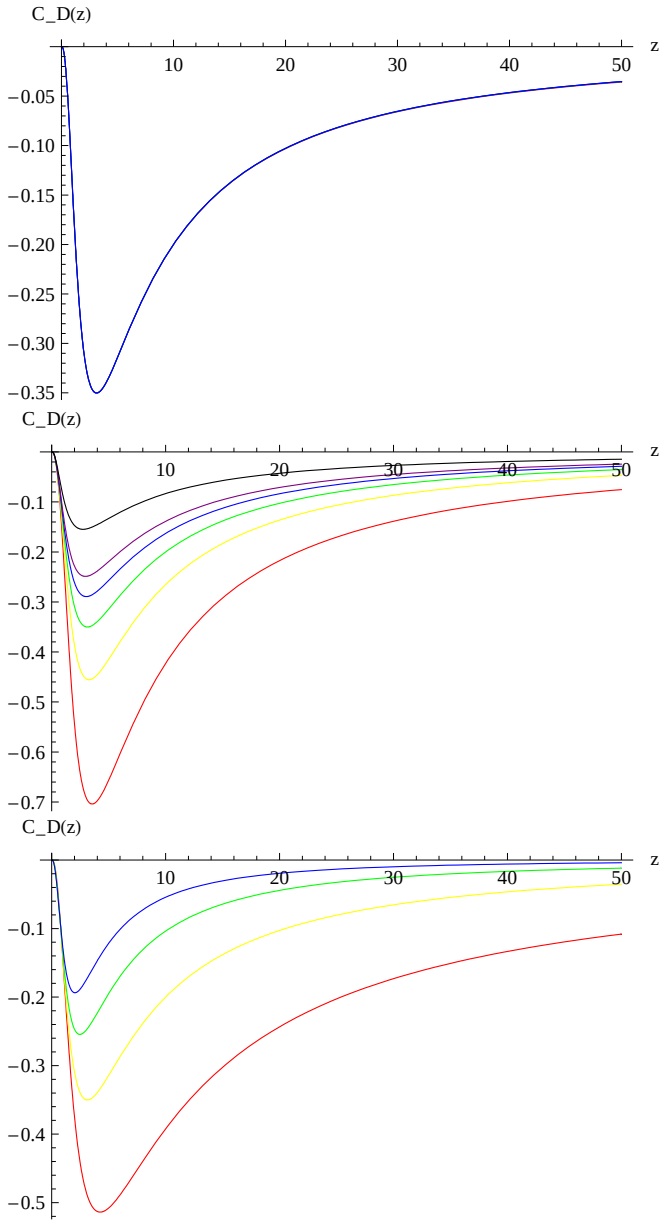

Figure 4.12: Constraints on $\Omega_m^{D_0}$ and w for a FRW Universe filled with Dark Energy with a constant equation of state. comparison between constraints derived by analyzing $WMAP$-3 data only (left panles) and those derived by adding an extra guessed point, corresponding to the third peak of the CMB spectrum (right panels), for different priors on H_0. Upper panles: flat prior in the range $H_0 \in [1, 200]$ Km/s/Mpc. Lower panels: gaussian BBN prior.

Chapter 5

Conclusions

We probed the averaged model of the Universe based on the template metric (Eq. 3.103) suggested in [34] against recent data sets. The morphon field creates a kinematical correspondence between an averaged inhomogeneous Universe based on Buchert's averaging procedure and a standard flat FRW spacetime filled with Dark Energy represented by a quintessence field of constant equation of state. The dynamical effects of the backreaction can help in distinguishing among the two models by assuming a template metric for the averaged Universe and making likelihood analysis of current data against theoretical preditions of many cosmological observables, like the luminosity distance, the angular diameter distance and the CMB anisotropy spectrum, in both models. In [34] this approach is suggested and the authors published constraints on the effective cosmological parameter $\Omega_m^{D_0}$ and the scaling index of the backreaction n by combining likelihood analysis of the set of luminosity distances of nearby SN Ia in the SNLS and constraints derived from the position of the first two peaks and the first dip of the CMB power spectrum using $WMAP$-3 data.

We upgraded their analysis employing luminosity distances of nearby supernovae in the Union2.1 catalog. Then we performed the same likelihood analysis on the set of angular diameter distances of galaxy clusters from Bonamente. We found that the Union2.1 improves the constraints due to the smaller uncertainties, while no useful information is added by clusters, since the errors are heavily affected by modelling uncertainties of the geometry of the clusters. Nevertheless we found that clusters

data confirm the behaviour that likelihood constraints follow in Fig. 2 of [34], suggesting that future surveys of galaxy clusters, based on refined modelling errors, may be useful for constraining better the cosmological parameters and may help in distinguish between an effective solution of the Einstein field equation and the standard homogeneous and isotropic FRW.

We also upgraded the likelihood analysis based on data from the CMB. We separately employed two methods, based on different observables. First we followed the path suggested in [34], performing a likelihood analysis of the positions of the first three peaks and the first dip of the anisotropy spectrum of the CMB. We discovered that adding a point corresponding to the third peak to $WMAP$-3 data may improve the likelihood constraints regardless of the big uncertainty on the extra point, which was derived by a rough fitting procedure of the $WMAP$-3, high l, spectrum. We decided to apply the fitting procedure to $WMAP$-9 and *Planck* data separately, extracting two sets of data corresponding to the position of the first three peaks and the first dip of the CMB spectrum. Then we followed the method based on the direct measurement of the CMB-shift parameters provided by $WMAP$-9. We found that the last method was better than the others since the full covariance matrix has been used in the likelihood. *Planck* data are sufficently precise to give good results, but the fitting procedure we used for extracting the positions of the peaks overestimated teh uncertainties: we hope that in the near future the *Planck* collaboration will extract the positions of many peaks and dips from the extrimely precise high l CMB spectrum following better fitting procedures.

Likelihood analysis based on CMB data work well for the FRW spacetime, provinding good constraints. Adding the backreaction we face a distortion of the constraints that suggested a behavior opposite to that predicted in [34]. We studied how the refinement of statistical and systematic errors in recent years changed constraints derived from $WMAP$-3 data enhacing the distortion effect. The method based on the CMB-shift parameters employed on $WMAP$-9 data shows that the constraints only marginally overlap those given by the SNLS and the overlap reduces further when Union2.1 data are used. Following the inconsistency that are argued in [53], we tried to explain the bad behavior the ellipses show when backreaction is added in terms of incosistencies hidden behind the non

trivial relation between the effective scale factor and the effective redshift before and after the recombination epoch. We claimed that an incosistency seems to arise due to the standard boundary conditions ($a_0 = a_{D_0} = 1$) usually assumed for both the FRW spacetime and the backreacted model. We tried to demonstrate that the approximation suggested in [34] of a friedmannian evolution for any domain D in the backreacted Universe up to the recombination epoch is fairly not well posed. This led us to suggest that the correspondence between an averaged model and a standard flat FRW filled with Dark Energy shoud be formulated for suitably boundary conditions today. We noted that in standard cosmology fixing the recombination epoch means fixing the size of the Universe and we suggested that the main role is played by the latter, since it has a thermodynamical meaning related to the actual temperature of the CMB. Finally we argued that the incosistency should affect the likelihood analysis because the effective scale factor $a_D(z_D)$ cannot follow the solution $a(z)$ which takes exactly the value $(1 + z^*)^{-1}$ at the recombination epoch z^*.

We tried to explain the incosistency from prime principles looking at the basic definitions of statistical mechanincs underlying the concept of temperature. We found that the scaling $T \sim a^{-1}$ holds only for the standard FRW as a consequence of the scaling properties of the canonical partition function, but some care is required. The generalization of the basic definitions to the model based on the template metric meets difficulties in averaging fundamental equations involving the bare metric and in applying the definitions themselves, since they implicitly assume that the volume of the statistical ensemble is constant. We argue that a full treatment of the problem from prime principles is far beyond the scope of this thesis, so we simply assumed as an approximation that a small error is introduced by the incosistency in checking the model against data.

Current data sets told us that SN Ia and clusters provide compatible predictions and a denser Universe is expected if the backreaction is considered. Current CMB data, on the other hand, clearly told us that the incosistency related to how we treat the CMB physics in order to avoid the complication of rewriting all the microphysics of the photon-baryon fluid on a spacetime described by the template metric cannot be disregarded anymore. Distortions induced by this approach to the CMB physics are now compatible with the experimental errors and predictions based on cur-

rent data are completely affected by them, destroying any predictivity. We are not able to understand if CMB data are truly in contraddictions with other data sets or the modelling approximations are too weak. Clearly the dynamical effects of the backreaction enter deeply the structure of the lightcone and current approximations seem to fail.

We suggest that in the near future surveys of SN Ia or SZ clusters may be helpful in constraining models based on backreaction and, in general, models based on any assumption of coarse-graining the spacetime geometry which involve a template metric. CMB data are powerful and precise, but much more care is needed and a full theoretical approach should be developed in order to deal with many technicalities, like understanding the deep meaning of breaking the standard relation between the size of the Universe and the redshift (this has longstanding consequences on observational cosmology) or writing the physics of the CMB on a template underlying geometry, which requires to study the coarse-graining procedure related to the fundamental physics involved in the photon-baryon fluid.

We do not want to infer anymore about the backreaction scheme based on Buchert's approach. The backreaction problem is complicated and very widely debated on its theoretical basis. In our opinion this work was not aimed to confirm or rejects Buchert's approach to the averaging problem. We are convinced that too many theoretical aspects are currently debated that assumptions must be made *a priori* in order to define the background for checking a model against data. Currently, despite of the huge literature on the theoretical aspects of backreaction, comparison with data are lacking. In upgrading the original idea of [34] we encountered many difficulties which primarly arise from the theoretical framework of backreaction. We decided to go on pointing out the weakness of our scheme because we believe that in the last years cosmological observations improved drastically and we should start to check hypothesis relying on backreaction against data, even if many theoretical aspects are difficult or maybe unclear. The wide debate on the backreaction requires to address the problem from the side of observations too, because no theoretical model may be completely accepted or disregarded without making comparison with experimental data. We hope that in the near future new chances for testing backreaction may take place going beyond our simple approach.

Appendix A: Marginalization

Here we give a proof of the marginalization procedure under quite general assumptions. Let us consider a likelihood depending on a D-dimensional random variable x and a D-dimensional parameter p. Proofs are given in literature under the assumption of a 1-dimensional parameter $p = \lambda v$, where v is a given fixed vector (see [39, 40, 36, 37] for example). Here we try to generalize the proof to a D-dimensional marginalization. The theoretical predition of x is $x_T - p$. Let us consider a likelihood function given by

$$L(x|p) = \frac{\exp\left[-\frac{1}{2}(x - x_T - p)^t A^{-1}(x - x_T - p)\right]}{(2\pi)^{\frac{D}{2}}\sqrt{\det(A)}} \tag{5.1}$$

where A is the covariance matrix of the random variable x. It is well know that the likelihood gives the probability $P(x|p)$ of x given a fixed value of the parameter p.

If we are interested in computing the absolute probability $P(x)$ of the random variable x, we can immediately use the completeness relation

$$P(x) = \int_E P(x|p)P(p)dp \tag{5.2}$$

that requires to know the absolute probability $P(p)$ of the parameter, usually called *the prior* and the domain E of p. Here the term *probability* must be substituted with *probability density function* in the case of a continuous random variable. At the same time the integrals are meant as discrete series if the random variable is discrete.

We are left with the computation of the integral

$$P(x) = L_M = \int_E \frac{\exp\left[-\frac{1}{2}(x - x_T - p)^t A^{-1}(x - x_T - p)\right]}{(2\pi)^{\frac{D}{2}}\sqrt{\det(A)}} P(p) d^D p \quad (5.3)$$

where L_M stands for the marginalized likelihood.

To compute the integral we need to make assumptions on the functional form of the *prior*. We can suppose that the *prior* is simple, allowing for an analytic calculation. For example a gaussian prior

$$P(p) = \frac{1}{(2\pi)^{\frac{D}{2}}\sqrt{\det(C)}} e^{-\frac{p^t C^{-1} p}{2}} \quad (5.4)$$

is common.

The marginalized likelihood then becomes

$$L_M(x) = \int \frac{\exp[-\frac{(x-x_T-p)^t A^{-1}(x-x_T-p)}{2} - \frac{p^t C^{-1} p}{2}]}{(2\pi)^D \sqrt{\det(A)\det(C)}} d^D p \quad (5.5)$$

We expand the exponent such that

$$(x - x_T - p)^t A^{-1}(x - x_T - p) = (x - x_T)^t A^{-1}(x - x_T) - (x - x_T)^t A^{-1} p - p^t A^{-1}(x - x_T) + p^t A^{-1} p \quad (5.6)$$

which shows that the integral over p is gaussian. Such integrals can be handled by remembering the general formula

$$\int e^{-\frac{y^\dagger M^{-1} y}{2} + b^\dagger y} dy = (2\pi)^{\frac{D}{2}} \sqrt{\det(M)} e^{\frac{b^\dagger M b}{2}} \quad (5.7)$$

and identifying

$$y = p \qquad b = A^{-1}(x - x_T) \qquad M^{-1} = A^{-1} + C^{-1} \quad (5.8)$$

The integration is easy and provides

$$L_M(x) = \frac{\exp[-\frac{(x-x_T)^t A^{-1}(x-x_T)}{2}]}{(2\pi)^{\frac{D}{2}}\sqrt{\det(A)\det(C)\det(A^{-1}+C^{-1})}} \exp[\frac{(x-x_T)^t A^{-1}[A^{-1}+C^{-1}]^{-1}A^{-1}(x-x_T)}{2}] \tag{5.9}$$

The determinant can be simplified by using the Sylvester formula

$$\det(A)\det(C)\det(A^{-1}+C^{-1}) = \det(A)\det(CA^{-1}+1) = \det(A)\det(A^{-1}C+1) = \det(A+C) \tag{5.10}$$

which gives

$$L_M(x) = \frac{\exp[-\frac{(x-x_T)^t A^{-1}(x-x_T)}{2}]}{(2\pi)^{\frac{D}{2}}\sqrt{\det(A+C)}} \exp[\frac{(x-x_T)^t A^{-1}[A^{-1}+C^{-1}]^{-1}A^{-1}(x-x_T)}{2}] \tag{5.11}$$

The inverse matrix $(A^{-1}+C^{-1})^{-1}$ can be expressed as an infinite sum

$$(A^{-1}+C^{-1})^{-1} = A - AC^{-1}A + AC^{-1}AC^{-1}A - ... = \sum_{n=0}^{+\infty} A(-C^{-1}A)^n \tag{5.12}$$

Substituting into the integral gives

$$A^{-1}(A^{-1}+C^{-1})A^{-1} = \sum_{n=0}^{+\infty}(-C^{-1}A)^n A^{-1} = A^{-1}\sum_{n=0}^{+\infty}(-AC^{-1})^n = A^{-1} - \sum_{n=0}^{+\infty} C^{-1}(-AC^{-1})^n \tag{5.13}$$

and the likelihood becomes

$$L_M(x) = \frac{\exp[-\frac{(x-x_T)^t A^{-1}(x-x_T)}{2}]}{(2\pi)^{\frac{D}{2}}\sqrt{\det(A+C)}} \exp[\frac{(x-x_T)^t(A^{-1} - \sum_{n=0}^{+\infty} C^{-1}(-AC^{-1})^n)(x-x_T)}{2}] \tag{5.14}$$

The matrix at the exponent can be computed explicitly:

$$A^{-1} - A^{-1} + \sum_{n=0}^{+\infty} C^{-1}(-AC^{-1})^n = (A+C)^{-1} \tag{5.15}$$

by applying the expansion in Eq. 5.12 for the inverse of a square matrix.

This simply gives the final marginalized likelihood

$$L_M(x) = \frac{1}{(2\pi)^{\frac{D}{2}}\sqrt{\det(A+C)}} \exp\left[-\frac{1}{2}(x-x_T)^t(A+C)^{-1}(x-x_T)\right] \tag{5.16}$$

Now we prove that the same results follows by taking the maximum of the probability $P(x|p)P(p)$ with respect to the parameter p and substituting it into the expression of the likelihood, under some approximations. We will derive the approximations by comparing the procedures and we will show that they are equivalent when the prior on p is uniform.

Let us take the derivative of

$$L(x,p) = P(x|p)P(p) = \frac{\exp[-\frac{(x-x_T-p)^t A^{-1}(x-x_T-p)}{2} - \frac{p^t C^{-1} p}{2}]}{(2\pi)^D\sqrt{\det(A)\det(C)}} \tag{5.17}$$

with respect to the i-th component of p. Equating the derivative to zero gives the following equations:

$$2A^{-1}_{ij}p_j + 2C^{-1}_{ij}p_j = 2A^{-1}_{ij}(x-x_T)_j \tag{5.18}$$

where summation over repeated indexes is understood. The prevoius set of equations is solved in matrix notation

$$p_{min} = (1 + AC^{-1})^{-1}(x - x_T) \tag{5.19}$$

We expand the inverse matrix as follows

$$p_{min} = (1 - AC^{-1} + AC^{-1}AC^{-1} + ...)(x - x_T) = \sum_{n=0}^{+\infty}(-AC^{-1})^n(x - x_T) \tag{5.20}$$

and substitute into the likelihood:

$$L(x,p) \approx \exp\left[-\frac{(x-x_T)^t[(1-\sum_{n=0}^{+\infty}(-C^{-1}A)^n)A^{-1}(1-\sum_{m=0}^{+\infty}(-AC^{-1})^m)](x-x_T)}{2} + \right.$$
$$\left. - \frac{(x-x_T)^t\sum_{n=0}^{+\infty}(-C^{-1}A)^nC^{-1}\sum_{m=0}^{+\infty}(-AC^{-1})^m(x-x_T)}{2}\right] \tag{5.21}$$

We can focus on the two matrix multiplications in the exponent. The former gives

$$[1 - \sum_{n=0}^{+\infty}(-C^{-1}A)^n]A^{-1}[1 - \sum_{m=0}^{+\infty}(-AC^{-1})^m] = A^{-1} - A^{-1}\sum_{n=0}^{+\infty}(-AC^{-1})^n +$$
$$- \sum_{m=0}^{+\infty}(-C^{-1}A)^mA^{-1} + \sum_{n=0}^{+\infty}\sum_{m=0}^{+\infty}(-)^{n+m}(C^{-1}A)^nA^{-1}(AC^{-1})^m \tag{5.22}$$

while the latter is

$$\sum_{n=0}^{+\infty}(-C^{-1}A)^nC^{-1}\sum_{m=0}^{+\infty}(-AC^{-1})^m = \sum_{n=0}^{+\infty}\sum_{m=0}^{+\infty}(-)^{n+m}(C^{-1}A)^nC^{-1}(AC^{-1})^m \tag{5.23}$$

We expand the double sum in Eq. 5.22 and we find

$$\sum_{n=0}^{+\infty}\sum_{m=0}^{+\infty}(-)^{n+m}(C^{-1}A)^n A^{-1}(AC^{-1})^m = A^{-1} - 2C^{-1} + A^{-1}\sum_{m=2}^{+\infty}(-AC^{-1})^m + C^{-1}\sum_{m=1}^{+\infty}(-)^{1+m}(AC^{-1})^m + \sum_{n=2}^{+\infty}(-C^{-1}A)^n A^{-1} + \sum_{n=2}^{+\infty}\sum_{m=1}^{+\infty}(-)^{n+m}(C^{-1}A)^n A^{-1}(AC^{-1})^m. \quad (5.24)$$

Summing Eq. 5.22 and Eq. 5.23 we see that many terms cancel out and the matrix in the exponent can be written as a sum of two contributions E_1 and E_2, defined as

$$E_1 = C^{-1}\textstyle\sum_{m=1}^{+\infty}(-)^{1+m}(AC^{-1})^m + \sum_{m,n}^{+\infty}(-)^{n+m}(C^{-1}A)^n A^{-1}(AC^{-1})^m \quad (5.25)$$

$$E_2 = \textstyle\sum_{n=0}^{+\infty}\sum_{m=0}^{+\infty}(-)^{n+m}(C^{-1}A)^n C^{-1}(AC^{-1})^m \quad (5.26)$$

By expanding the sum, we can have a look at the structure of the two contributions:

$$E_1 \approx C^{-1}AC^{-1} - 2C^{-1}AC^{-1}AC^{-1} + 3C^{-1}AC^{-1}AC^{-1}AC^{-1} - ... \quad (5.27)$$

$$E_2 \approx C^{-1} - 2C^{-1}AC^{-1} + 3C^{-1}AC^{-1}AC^{-1} - ... \quad (5.28)$$

It is clear that for each term $C^1(AC^{-1})^n,\ n > 0$ the first contribution is $(-)^{n+1}n$ while the second is $(-)^n(n+1)$. Summing the two terms provides

$$E_1 + E_2 = C^{-1} - C^{-1}AC^{-1} + C^{-1}AC^{-1}AC^{-1} - ... = \sum_{n=0}^{+\infty} C^{-1}(-AC^{-1})^n = (A+C)^{-1} \quad (5.29)$$

The corresponding likelihood follows

$$L(x,p)|_{p=p_m in} = \frac{1}{(2\pi)^D\sqrt{\det(AC)}}e^{-\frac{(x-x_T)^t(A+C)^{-1}(x-x_T)}{2}} \quad (5.30)$$

We can compare this expression with the marginalized likelihood 5.16, and we find that the two expressions disagree only in the normalization constant. Indeed the exact marginalization procedure directly provides the correct normalization constant, while the substituition $p = \bar{p}$ gives a different constant. Let us assume that the matrix A is *small* in some mathematical sense. We simply suppose that the matrices A and C are simultaneously diagonalizable, which is not always true, but simplify our further argument. under this assumption we can write

$$\det A = \prod_i \sigma_i^2 \qquad \det C = \prod_i \lambda_i^2 \tag{5.31}$$

where $\{\sigma_I^2\}$ are the eigenvalues of A and $\{\lambda_i^2\}$ are those of C. We can state that the matrix A is *small* with respect to C if $\lambda_i >> \sigma_i$. This statement could seem quite arbitrary, but it simply has an immediate meaning in terms of probability. Indeed if the eigenvalues of C are much bigger than those of A, the gaussian associated to the prior is wider than the Gaussian associated to the bare likelihood L. The geometrical interpretation is obvious if we suppose tha the two gaussians take their maxima at the same point: the gaussian with covariance C completely embeds the gaussian with covariance A. Moreover, if $\lambda_i >> \sigma_i$, the bigger gaussian is quite constant on the variability range of the smaller one, mimicking a constant prior. This easily prove that the two procedures are similar if the prior of the parameter p is constant.

So, we are able to rougly estimate the error in the normalization constant caused by the substitution in Eq.5.20. The direct computation gives

$$\frac{\det(A+C)}{\det(AC)} = \frac{\prod_i(\sigma_i^2+\lambda_i^2)}{\prod_i \sigma_i^2 \prod_j \lambda_j^2} \tag{5.32}$$

since we have assumed that A and C are diagonal in a common basis. The calculation requires little boring algebra and provides

$$\frac{\det(A+C)}{\det(AC)} = \sum_{i=0}^{D}\prod_{j=0}^{k}\frac{1}{\sigma_j^2}\frac{1}{\lambda_{D-j}^2} \approx \frac{1}{\det(A)}\left[1+\sum_{i=1}^{D}\frac{\sigma_i^2}{\lambda_i^2}\right] \tag{5.33}$$

up to first order in σ^2/λ^2.

This proves that the error in the marginalization constant is finite under our assumption and it could be forgot by a simple rescaling of the likelihood after the substitution 5.20.

Appendix B:Fitting procedure

Here we discuss the home-made fitting procedure we employed for finding the position of the peaks and dips of the CMB anisotropy spectrum. We applied the same scheme to $WMAP$-9 row data and to the combined TT-power spectrum measured by *Planck*.

$WMAP$-9 data are listed giving the values of $l(l+1)C_l/(2\pi)$ for each value of the multipole l in a wide range from $l = 2$ up to $l = 1200$ and the corresponding statistical error.

We arbitrarly divided the range $l \in [2, 1200]$ into wide subsets corresponding to a rough estimation of the extension of each peak or dip. After we have fixed the range, we modelled $WMAP$-9 spectrum with three-parameters curves. The first peak is modelled with a gaussian, the other two peaks are modelled with parabolas. The first dip is modelled with a parabola too. The fitting procedure involves only parabolas, since, only for the first peak, we fit the logarithm of the spectrum. This simply reduce the gaussian fit down to a standard parabolic fit. Then we generally use

$$p(x) = ax^2 + bx + c \tag{5.34}$$

as the template curve. Given the value of the parameters from the fitting parabola, we estimate the position of the corresponding peak (or dip) assuming that it is well approximated by the position of the vertex

$$v = -\frac{b}{2a} \tag{5.35}$$

For $WMAP$-9 data we assumed as fitting intervals:

- First peak: $l \in [50, 350]$
- First dip: $l \in [300, 550]$
- Second peak: $l \in [400, 700]$
- Third peak:$l \in [650, 950]$

The choice of the intervals is completely arbitrary. We decided to overlap the intervals correspondiong to different peaks since the spectrum should be continuous. The overlap does not ensure continuity, but we checked that always an intesection exists between the fitting parabolas in the overlapping regions of neighbour ranges.

In order to achieve a statistical sample of the position of the vertex, we storage the value of l corresponding to the vertex of the fitting parabola, then we randomly move the measured $WMAP$-9 spectrum by adding a different random number to each point and we refit with the same template curve. The range in l is held fixed and the random numbers are gaussianly distributed with null mean and variance corresponding to the square of the statistical error associated to the data point. The refitting procedure is achieved at least 10^5 times in order to obtain a statistical sample. The final position of the n-th peak (or dip) is computed taking the mean of the sample and the corresponding error is estimated as the squareroot of the sample variance. In other terms the position of each vertex is treated as a random variable $V^{(n)}$ and the discrete set

$$S = \{v_i^{(n)}\}_{i=1}^{N} \tag{5.36}$$

is assumed to be a fair sample of the final distribution of $V^{(n)}$. The position of the n-th peak is then

$$l^{(n)} = E[V] \pm \sqrt{Var[V]} \tag{5.37}$$

where the *expected value* $E[V]$ of the full random variable is estimated by the sample mean

$$\bar{v} = \sum_{i=1}^{N} \frac{v_i}{N} \tag{5.38}$$

and the error by the standard deviation

$$\sigma = \sqrt{\frac{1}{N-1}\sum_{i=1}^{N}(v_i - \bar{v})^2} \tag{5.39}$$

We checked that while increasing the number of iterations of the fitting procedure N, the vertexes distribute following a gaussian, ensuring that the main uncertainties in evaluating the position of the peak are truly statistical. Our results are achieved taking $N = 10^5$ for each vertex.

Since the fixed range in l is quite arbitrary we tried to estimate the error we introduced by fixing the fitting range in a statistical way. This simply accounts for the uncertainty we faced in estimating where we a peak begins and ends. We held the data point fixed and let the extrema of the fitting range fluctuate randomly. We assumed that each extremum can fluctuate with a gaussian distribution with null mean and σ corresponding to the 10% of the width of the interval. Again we note that this choice is arbitrary, but we are convinced that the uncertainty should increase for wider peaks and decrease for narrower ones, since sharp structures are more easily modelled. Again we storage the position of the vertex of the fitting parabola and then we refit after the extrema of the fitting range are changed. We estimate the error on the position of each peak as the standard deviation of the corresponding sample, which contains again 10^5 realizations.

We noticed that the uncertainty on the position of each peak introduced by fixing the fitting range is significant only for the first peak and the first dip because it is of the same order of magnitude of the statistical uncertainty predicted by the fitting procedure holding the extrema fixed. Then we decided to add this contribution to the final error on the first peak and on the first dip in quadrature, assuming that they were uncorrelated.

In figure 5.1 we show the histograms of the values in the set S for each peak and for the first dip. For each histogram the corresponding gaussian is superimposed in order to visualize easily the coincidence. The gaussians correponding to the first peak and to the first dip are a little bit wider since their variance is enhaced by the contribution coming from having held fixed the fitting ranges.

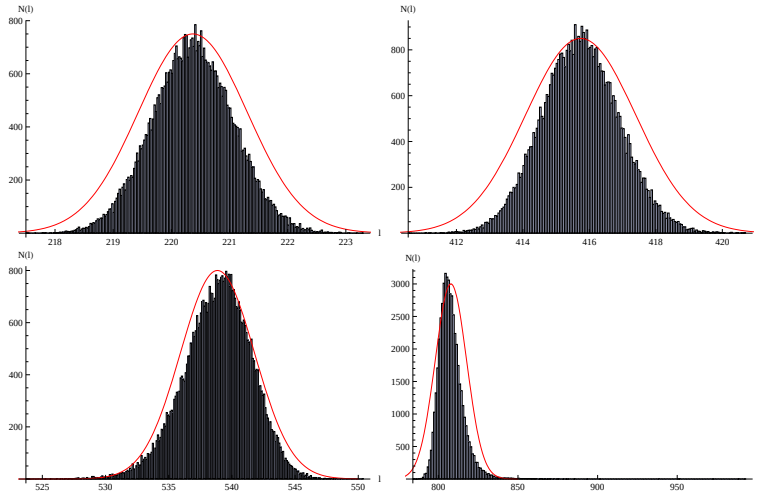

Figure 5.1: Fitting procedure of $WMAP$-9 data: distribution of the estimator of the position of the peaks and dips. Upper left: first peak. Upper right: first dip. Lower left: second peak. Lower right: third peak

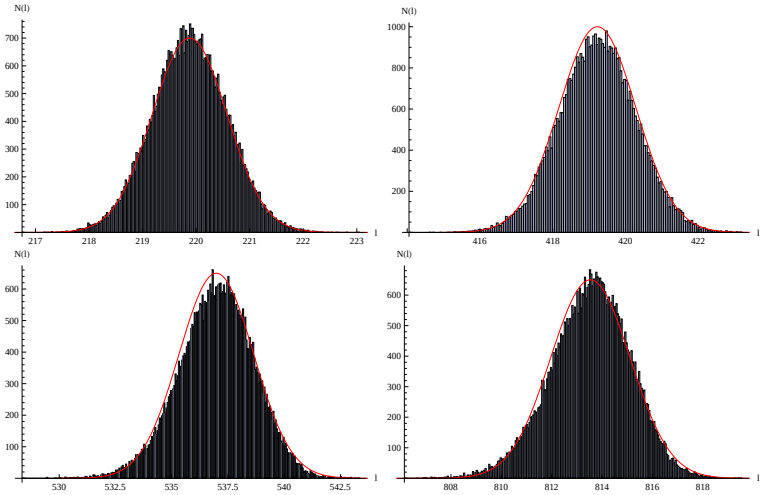

Figure 5.2: Fitting procedure of *Planck* data: distribution of the estimator of the position of the peaks and dips. Upper left: first peak. Upper right: first dip. Lower left: second peak. Lower right: third peak.

We applied the same procedure to *Planck* data. The values of the combined TT-power spectrum are given only for a few specific reference values of the multipole l. The statistical uncertainty is drastically reduced due to the combining procedure employed by *Planck*. We assumed the same ranges we used for fitting $WMAP$-9 data, but no error is computed for leaving the extrema of any range free to fluctuate, since the reference values of l are too separated.

In figure 5.2 we show the histograms corresponding to the set of predicted values of the position of each vertex of the fitting parabolas and the corresponding gaussian.

A comparison between figure 5.1 and 5.2 shows that the set of positions of the third peak is rather better if *Planck* data are used. The predicted positions of the third peak derived from $WMAP$-9 data distribute quite asymmetrically. On the other hand the set derived from *Planck* data shows a more symmertic distribution. We may simply argue that uncertainties on $WMAP$-9 raw data increase drastically for $l > 700$ and the prediction of the position of the third peak may be biased towards lower values of l,

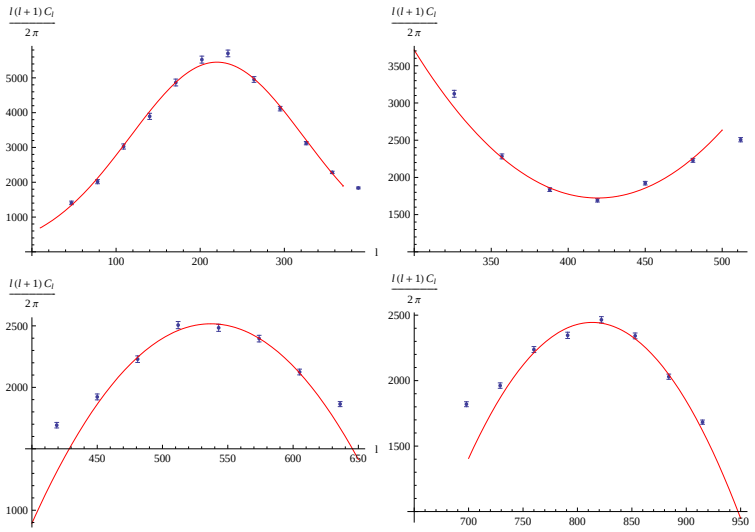

Figure 5.3: Fitting procedure of *Planck* data: superposition of raw data and fitting curves. Upper left: first peak. Upper right: first dip. Lower left: second peak. Lower right: third peak.

corresponding to lower errors.

For completeness in figures 5.3 and 5.4 we show the superposition of the fitting parabolas and the measured spectra.

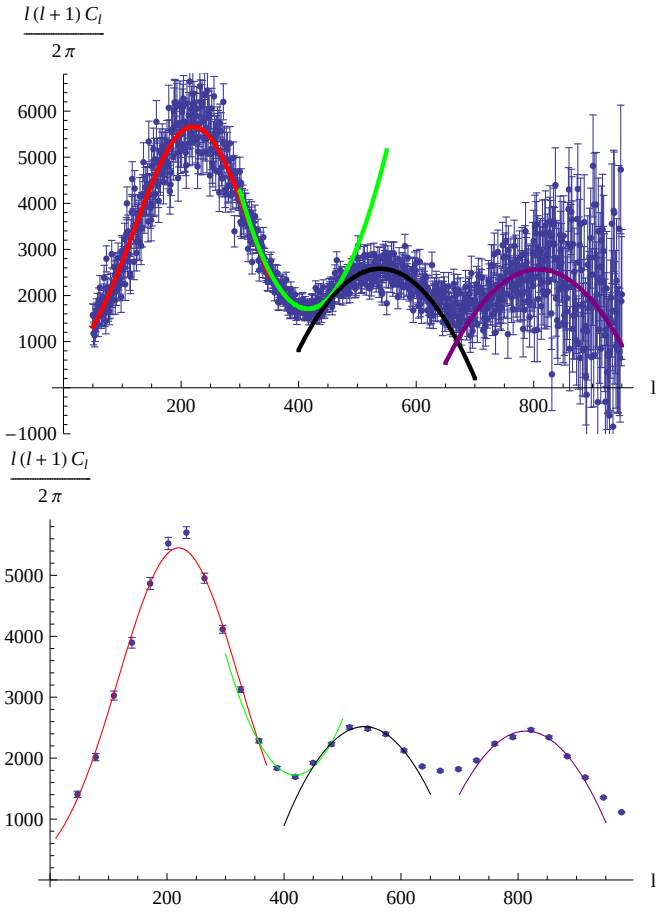

Figure 5.4: Fitting procedure of CMB data: superposition of raw data and fitting curves. Upper panel: full $WMAP$-9 data Lower panel: full *Planck* data

Bibliography

[1] A. G. Riess *et al.* [Supernova Search Team Collaboration], Astron. J. **116** (1998) 1009 [astro-ph/9805201].

[2] S. Perlmutter *et al.* [Supernova Cosmology Project Collaboration], Astrophys. J. **517** (1999) 565 [astro-ph/9812133].

[3] U. Seljak *et al.* [SDSS Collaboration], Phys. Rev. D **71** (2005) 103515 [astro-ph/0407372].

[4] A. G. Riess *et al.* [Supernova Search Team Collaboration], Astrophys. J. **607** (2004) 665 [astro-ph/0402512].

[5] M. Kowalski *et al.* [Supernova Cosmology Project Collaboration], Astrophys. J. **686** (2008) 749 [arXiv:0804.4142 [astro-ph]].

[6] R. Amanullah, C. Lidman, D. Rubin, G. Aldering, P. Astier, K. Barbary, M. S. Burns and A. Conley *et al.*, Astrophys. J. **716** (2010) 712 [arXiv:1004.1711 [astro-ph.CO]].

[7] N. Suzuki, D. Rubin, C. Lidman, G. Aldering, R. Amanullah, K. Barbary, L. F. Barrientos and J. Botyanszki *et al.*, Astrophys. J. **746** (2012) 85 [arXiv:1105.3470 [astro-ph.CO]].

[8] B. Leibundgut, Ann. Rev. Astron. Astrophys. **39**, 67 (2001).

[9] P. Astier *et al.* [SNLS Collaboration], Astron. Astrophys. **447** (2006) 31 [astro-ph/0510447].

[10] G. Folatelli, M. M. Phillips, C. R. Burns, C. Contreras, M. Hamuy, W. L. Freedman, S. E. Persson and M. Stritzinger *et al.*, Astron. J. **139** (2010) 120 [arXiv:0910.3317 [astro-ph.CO]].

[11] E. J. Copeland, M. Sami and S. Tsujikawa, Int. J. Mod. Phys. D **15** (2006) 1753 [hep-th/0603057].

[12] J. Frieman, M. Turner and D. Huterer, Ann. Rev. Astron. Astrophys. **46** (2008) 385 [arXiv:0803.0982 [astro-ph]].

[13] M. Li, X. -D. Li, S. Wang and Y. Wang, Commun. Theor. Phys. **56** (2011) 525 [arXiv:1103.5870 [astro-ph.CO]].

[14] R. L. Arnowitt, S. Deser and C. W. Misner, gr-qc/0405109.

[15] Y. .B. Zeldovich, V. G. Kurt and R. A. Sunyaev, J. Exp. Theor. Phys. **28** (1969) 146 [Zh. Eksp. Teor. Fiz. **55** (1968) 278].

[16] R. A. Sunyaev and Y. .B. Zeldovich, Astrophys. Space Sci. **7** (1970) 3.

[17] R. A. Sunyaev and Y. .B. Zeldovich, Astrophys. Space Sci. **7** (1970) 20.

[18] A. Cavaliere and R. Fusco-Femiano, Astron. Astrophys. **49** (1976) 137.

[19] M. Birkinshaw, Phys. Rept. **310** (1999) 97 [astro-ph/9808050].

[20] J. J. Mohr, B. Mathiesen and A. E. Evrard, Astrophys. J. **517** (1999) 627 [astro-ph/9901281].

[21] S. J. Laroque, UMI-31-81369.

[22] E. D. Reese, J. E. Carlstrom, M. Joy, J. J. Mohr, L. Grego and W. L. Holzapfel, Astrophys. J. **581** (2002) 53 [astro-ph/0205350].

[23] S. LaRoque, M. Bonamente, J. Carlstrom, M. Joy, D. Nagai, E. Reese and K. Dawson, Astrophys. J. **652** (2006) 917 [astro-ph/0604039].

[24] M. Bonamente, M. K. Joy, S. J. La Roque, J. E. Carlstrom, E. D. Reese and K. S. Dawson, [astro-ph/0512349].

[25] E. De Filippis, M. Sereno, M. W. Bautz and G. Longo, Astrophys. J. **625** (2005) 108 [astro-ph/0502153].

[26] T. Buchert and J. Ehlers, Astron. Astrophys. **320** (1997) 1 [astro-ph/9510056].

[27] T. Buchert, M. Kerscher and C. Sicka, Phys. Rev. D **62** (2000) 043525 [arXiv:astro-ph/9912347].

[28] T. Buchert, Gen. Rel. Grav. **32** (2000) 105 [gr-qc/9906015].

[29] T. Buchert and M. Carfora, gr-qc/0101070.

[30] T. Buchert, Gen. Rel. Grav. **33** (2001) 1381 [gr-qc/0102049].

[31] T. Buchert and M. Carfora, Class. Quant. Grav. **19** (2002) 6109 [gr-qc/0210037].

[32] T. Buchert, Gen. Rel. Grav. **40** (2008) 467 [arXiv:0707.2153 [gr-qc]].

[33] J. Larena, T. Buchert and J. -M. Alimi, astro-ph/0612774.

[34] J. Larena, J. –M. Alimi, T. Buchert, M. Kunz and P. -S. Corasaniti, Phys. Rev. D **79** (2009) 083011 [arXiv:0808.1161 [astro-ph]].

[35] M. Carfora and T. Buchert, arXiv:0801.0553 [math-ph].

[36] S. L. Bridle, R. Crittenden, A. Melchiorri, M. P. Hobson, R. Kneissl and A. N. Lasenby, Mon. Not. Roy. Astron. Soc. **335** (2002) 1193 [astro-ph/0112114].

[37] O. Elgaroy and T. Multamaki, JCAP **0609** (2006) 002 [astro-ph/0603053].

[38] O. Elgaroy and T. Multamaki, Astron. Astrophys. **471** (2007) 65 [astro-ph/0702343 [ASTRO-PH]].

[39] R. Lazkoz and E. Majerotto, JCAP **0707** (2007) 015 [arXiv:0704.2606 [astro-ph]].

[40] I. Sendra, R. Lazkoz and N. Benitez, arXiv:1105.4943 [astro-ph.CO].

[41] G. Hinshaw *et al.* [WMAP Collaboration], Astrophys. J. Suppl. **170** (2007) 288 [astro-ph/0603451].

[42] E. Komatsu *et al.* [WMAP Collaboration], Astrophys. J. Suppl. **180** (2009) 330 [arXiv:0803.0547 [astro-ph]].

[43] G. Hinshaw *et al.* [WMAP Collaboration], arXiv:1212.5226 [astro-ph.CO].

[44] P. A. R. Ade *et al.* [Planck Collaboration], arXiv:1303.5076 [astro-ph.CO].

[45] M. Doran and M. Lilley, Mon. Not. Roy. Astron. Soc. **330** (2002) 965 [astro-ph/0104486].

[46] R. Durrer, B. Novosyadlyj and S. Apunevych, Astrophys. J. **583** (2003) 33 [astro-ph/0111594].

[47] W. Hu and N. Sugiyama, Astrophys. J. **471** (1996) 542 [astro-ph/9510117].

[48] Y. Wang and P. Mukherjee, Phys. Rev. D **76** (2007) 103533 [astro-ph/0703780].

[49] S. Nesseris, A. De Felice and S. Tsujikawa, Phys. Rev. D **82** (2010) 124054 [arXiv:1010.0407 [astro-ph.CO]].

[50] G. Efstathiou and J. R. Bond, Mon. Not. Roy. Astron. Soc. **304** (1999) 75 [astro-ph/9807103].

[51] P. S. Corasaniti and A. Melchiorri, Phys. Rev. D **77** (2008) 103507 [arXiv:0711.4119 [astro-ph]].

[52] T. Clifton, P. G. Ferreira and J. Zuntz, JCAP **0907** (2009) 029 [arXiv:0902.1313 [astro-ph.CO]].

[53] E. Rosenthal and E. E. Flanagan, arXiv:0809.2107 [gr-qc].

[54] P. A. R. Ade *et al.* [Planck Collaboration], arXiv:1303.5082 [astro-ph.CO].

[55] D. A. Dicus, D. N. Page and V. L. Teplitz, Phys. Rev. D **26** (1982) 1306.

[56] G. Mangano, G. Miele, S. Pastor and M. Peloso, Phys. Lett. B **534** (2002) 8 [astro-ph/0111408].

[57] D. W. Hogg, astro-ph/9905116.

[58] J. A. Peacock, Cambridge, UK: Univ. Pr. (1999) 682 p

[59] S. M. Carroll, gr-qc/9712019.

[60] R. M. Wald, Chicago, Usa: Univ. Pr. (1984) 491p

[61] G. F. R. Ellis, Gen. Rel. Grav. **41** (2009) 581 [Proc. Int. Sch. Phys. Fermi **47** (1971) 104].

[62] J. Kristian and R. K. Sachs, Astrophys. J. **143** (1966) 379 [Gen. Rel. Grav. **43** (2011) 337].

[63] S. Weinberg " Gravitation and Cosmology (John Wiley)"

[64] C. Wetterich, Nucl. Phys. B **302** (1988) 668.

[65] A. A. Penzias and R. W. Wilson, Astrophys. J. **142** (1965) 419.

[66] D. J. Fixsen, Astrophys. J. **707** (2009) 916 [arXiv:0911.1955 [astro-ph.CO]].

[67] G. Arnison *et al.* [UA1 Collaboration], Phys. Lett. B **129** (1983) 273.

[68] S. Weinberg, Phys. Rev. D **13** (1976) 974.

[69] S. Weinberg, Phys. Rev. D **19** (1979) 1277.

[70] P. W. Higgs, Phys. Rev. Lett. **13** (1964) 508.

[71] S. Dodelson, Amsterdam, Netherlands: Academic Pr. (2003) 440 p

[72] M. E. Peskin and D. V. Schroeder, Reading, USA: Addison-Wesley (1995) 842 p

[73] D. J. Fixsen, E. S. Cheng, J. M. Gales, J. C. Mather, R. A. Shafer and E. L. Wright, Astrophys. J. **473** (1996) 576 [astro-ph/9605054].

[74] G. Ellis, R. Poltis, J. -P. Uzan and A. Weltman, Phys. Rev. D **87** (2013) 103530 [arXiv:1301.1312 [astro-ph.CO]].

[75] Y. Rephaeli, Ann. Rev. Astron. Astrophys. **33** (1995) 541.

[76] R. Zalaletdinov, gr-qc/0701116.

[77] S. Rasanen, JCAP **0402** (2004) 003 [astro-ph/0311257].

[78] E. W. Kolb, S. Matarrese and A. Riotto, New J. Phys. **8** (2006) 322 [astro-ph/0506534].

[79] A. Paranjape and T. P. Singh, Gen. Rel. Grav. **40** (2008) 139 [astro-ph/0609481].

[80] Y. Chen and B. Ratra, Astron. Astrophys. **543** (2012) A104 [arXiv:1105.5660 [astro-ph.CO]].

Aknowledgments

...ovvero i ringraziamenti. Ho giá scritto questa frase una volta, in una precedente occasione, proprio come *incipit* dei ringraziamenti al termine di un altro testo. Era la mia Tesi di Laurea *Heavy/Light mesons in marginally deformed Gauge Theories*. Da quell'istante sembrano passati pochi attimi. Poi é stato tutto rapidissimo: laurea, lode, applausi, tutto il meglio che si possa desiderare.

Se penso al lavoro, allo studio, allora sembrano passati secoli. Ho studiato ancora mille cose da quel tempo e come canta un testo tanto caro *I did what I have to do....* Insomma la vita é andata avanti ed oggi scrivo qui con diversa consapevolezza. Mi rendo conto che l'ultimo punto che metteró oggi segna l'ultimo limite di essere studente, coronato da questo Dottorato. Se é pur vero che non si smette mai di imparare, la formalitá ha comunque il suo peso.

Per questo, cosa comunque agli uomini, sento il bisogno di dare un perché a questi anni ed a questo studio. Ero bambino e dovevo andare a scuola. Una sera mio padre mi disse *Non studiare per fare contento me o la mamma, non studiare per i voti o i professori... studia per te stesso, perché cosí sarai un uomo libero.* Qui, alla fine, posso dire che aveva ragione. Ho assolto a quel mandato ogni giorno cercando il massimo. E se é vero che ho mille difetti e mille limiti, so che questo compito, che finisce simbolicamente oggi, l'ho concluso come desiderava lui.

Voglio dire grazie al Prof. Luigi Guzzo, che per noi é Gigi, per avermi accolto in un momento difficile. Non diró degli innumerevoli consigli profusi nel corso del Dottorato, perché se ne é perso il conto.

Abbraccio Elisabetta per il lavoro che ha svolto, anche a congrua distanza, in questo Dottorato e per il coraggio.

Infine voglio porgere un saluto a tutti coloro che hanno lavorato con me in questi anni all'Osservatorio. Hanno stoicamente sopportato i miei *journal clubs*, i miei conti, la Relativitá Generale ed il mio bislacco modo di vedere la fisica. Auguro a tutti loro un futuro professionale di prima grandezza. Comunque un saluto in particolare lo rivolgo a Davide per lo scambio di opinioni non solo scientifiche.

Ma alla fine di tutto questa Tesi é dedicata ad una sola persona, a mia madre. Con il suo silenzioso e costante lavoro, lungo una vita intera, lei non sa quanto abbia contribuito a tutto questo.